

การโคลนยีนและศึกษาคุณลักษณะของยีนโฮโมเจนไทเซตไฟฟิวทรานสเฟอเรสจากอัญชันและมะหาด



นางสาวธनिया วัฒนคุปต์

จุฬาลงกรณ์มหาวิทยาลัย

CHULALONGKORN UNIVERSITY

บทคัดย่อและแฟ้มข้อมูลฉบับเต็มของวิทยานิพนธ์ตั้งแต่ปีการศึกษา 2554 ที่ให้บริการในคลังปัญญาจุฬาฯ (CUIR)

เป็นแฟ้มข้อมูลของนิสิตเจ้าของวิทยานิพนธ์ ที่ส่งผ่านทางบัณฑิตวิทยาลัย

The abstract and full text of theses from the academic year 2011 in Chulalongkorn University Intellectual Repository (CUIR) are the thesis authors' files submitted through the University Graduate School.

วิทยานิพนธ์นี้เป็นส่วนหนึ่งของการศึกษาตามหลักสูตรปริญญาวิทยาศาสตรดุษฎีบัณฑิต

สาขาวิชาชีวเวชเคมี ภาควิชาชีวเคมีและจุลชีววิทยา

คณะเภสัชศาสตร์ จุฬาลงกรณ์มหาวิทยาลัย

ปีการศึกษา 2557

ลิขสิทธิ์ของจุฬาลงกรณ์มหาวิทยาลัย

CLOWING AND CHARACTERIZATION OF HOMOGENTISATE PHYTYLTRANSFERASE GENES
FROM *CLITORIA TERNATEA* AND *ARTOCARPUS LAKOOCHA*

Miss Thaniya Wunnakup



A Dissertation Submitted in Partial Fulfillment of the Requirements
for the Degree of Doctor of Philosophy Program in Biomedical Chemistry

Department of Biochemistry and Microbiology

Faculty of Pharmaceutical Sciences

Chulalongkorn University

Academic Year 2014

Copyright of Chulalongkorn University

Thesis Title	CLONING AND CHARACTERIZATION OF HOMOGENISATE PHYTYLTRANSFERASE GENES FROM <i>CLITORIA TERNATEA</i> AND <i>ARTOCARPUS LAKOOCHA</i>
By	Miss Thaniya Wunnakup
Field of Study	Biomedical Chemistry
Thesis Advisor	Associate Professor Wanchai De-eknamkul, Ph.D.

Accepted by the Faculty of Pharmaceutical Sciences, Chulalongkorn
University in Partial Fulfillment of the Requirements for the Doctoral Degree

.....Dean of the Faculty of Pharmaceutical Sciences
(Assistant Professor Rungpetch Sakulbumrungsil, Ph.D.)

THESIS COMMITTEE

.....Chairman
(Associate Professor Maneewan Suksomtip, Ph.D.)

.....Thesis Advisor
(Associate Professor Wanchai De-eknamkul, Ph.D.)

.....Examiner
(Assistant Professor Boonsri Ongpipattanakul, Ph.D.)

.....Examiner
(Associate Professor Duangdeun Meksuriyen, Ph.D.)

.....External Examiner
(Associate Professor Worapan Sitthithaworn, Ph.D.)

5276954933 : MAJOR BIOMEDICINAL CHEMISTRY

KEYWORDS: HOMOGENITISATE PHYTYLTRANSFERASE / CLITORIA TERNATEA / ARTOCARPUS LAKOOCHA / α -TOCOPHEROL

THANIYA WUNNAKUP: CLONING AND CHARACTERIZATION OF HOMOGENITISATE PHYTYLTRANSFERASE GENES FROM *CLITORIA TERNATEA* AND *ARTOCARPUS LAKOOCHA*.
ADVISOR: ASSOC. PROF. WANCHAI DE-EKNAMKUL, Ph.D., 94 pp.

Prenylated aromatic compounds are secondary metabolites found to be distributed in various plant families. The group of key enzymes catalyzing the prenylation reaction to produce these prenylated aromatic compounds is called aromatic prenyltransferases (PTases). Each of these enzymes transfers a prenyl group in different lengths (C5, C10, C15 or C20) to an aromatic substrate at a specific carbon position to form a prenylated aromatic product. In this study, two genes encoding similar homogentisate phytyltransferases (HPT), a member of aromatic PTases were isolated from *Clitoria ternatea* L. (*clt*) and *Artocarpus lakoocha* Rox. (*alc2*). The full-length cDNAs of *clt* and *alc2* were 1,495 and 1,625 bp in size, containing 1,224 bp and 1,233 bp ORF, respectively. The *clt* and *alc2* genes encoded CLT and ALRC2 proteins of 407 and 410 amino acids with predicted MWs of 45.58 and 45.59 kDa, respectively. Both proteins contained important characteristics of aromatic PTase structures, including a signal transit peptide at N-terminal, Asp-rich regions of substrate binding site (NQXXDXXXD and KDXXDXD), and nine trans-membrane α -helices. According to the results from phylogenetic analysis, both were closely related to the HPT family members. The functional study of *clt* and *alc2* was then carried out in tomato by transient expression using agroinfiltration method, and evaluated by RT-PCR. For their enzyme activities, these were indirectly evaluated by detection of the accumulation of the intermediate 2,3-dimethyl-5-phytyl-1,4-benzoquinone (DMPBQ) and the pathway product α -tocopherol by TLC and GC-MS. The results revealed that the isolated *clt* and *alc2* could enhance the α -tocopherol accumulation in tomato leaves after 3 days agroinfiltration by 2.4 + 0.38 and 1.4 + 0.05 fold higher than control. Taken together, both genes were possibly functioned as HPT enzyme.

Department: Biochemistry and Microbiology Student's Signature

Field of Study: Biomedical Chemistry Advisor's Signature

Academic Year: 2014

ACKNOWLEDGEMENTS

I would like to express deepest gratitude to my advisor, Assoc. Prof. Wanchai De-Eknamkul for his advice and encouragement that lead me to finish my doctoral research. His comments helped me to establish overall direction of the research and reach my goal. I thank him for gave me the opportunity and freedom to explore on my own.

I am grateful Asst. Prof. Sorkanok Vimolmangkang and Dr. Worrawat Promden for suggestion with direction, technical support and teaching me how to do research that helped me sort out the detail of my work.

I thank my colleagues of our laboratory for sharing idea and become a good friend.

I also thankful to all staffs of my department (Biochemistry and microbiology, Faculty of pharmaceutical sciences) for kind advice and help in information management and always ready to help with smile.

I acknowledge the 90th Anniversary of Chulalongkorn University Fund for providing scholarships for chemicals and faculty of pharmaceutical sciences for supporting.

Finally, none of this would have been possible without the love, patience and understanding of my family. They never complain and tell me to focus on my study. I fell so lucky to have them to be my parents.

CONTENTS

	Page
THAI ABSTRACT	iv
ENGLISH ABSTRACT	v
ACKNOWLEDGEMENTS	vi
CONTENTS	vii
List of Tables	xi
List of Figures.....	xii
CHAPTER I Introduction	1
CHAPTER II Literature review.....	3
2.1 Plant prenylated aromatic compounds.....	3
2.1.1 Prenylated flavonoids.....	3
2.1.2 Prenylated xanthenes	5
2.1.3 Prenylated quinones.....	6
2.2 Plant aromatic prenyltransferase	7
2.2.1 Aromatic prenyltransferase in prenylated flavonoid biosynthesis.....	8
2.2.2 Aromatic prenyltransferase in prenylated quinone biosynthesis.....	11
2.3 Characterize and function of aromatic PTases	14
2.4 <i>Artocarpus lakoocha</i> Rox.....	17
2.4.1 Plant description.....	17
2.4.2 Chemical constituents and biological activities of <i>A. lakoocha</i>	18
2.5 <i>Clitoria ternatea</i> L.	19
2.5.1 Plant description.....	19
2.5.2 Chemical constituents and biological activities in <i>C. ternatea</i>	20

CHAPTER III Material and Methods	21
3.1 Plant materials	21
3.2 Bacterial Strains	21
3.3 Plasmids	22
3.4 Total RNA extraction	22
3.5 Synthesis cDNA	23
3.6 Determination of core sequences encoding PTases	23
3.7 Determination of full length gene by rapid amplification of cDNA ends (RACE)	25
3.8 Determination of full length gene for prenyltransferases genes	29
3.9 Cloning of gene in pGEM®-T Easy Vector for sequencing	30
3.10 Bioinformatics analysis	31
3.11 Alkaline lysis method for plasmid extraction (Sambrook, et al., 1989)	32
3.12 Presto™ Mini Plasmid Kit for plasmid extraction	32
3.13 Preparation of competent <i>E. coli</i> cells	33
3.14 Transformation by heat-shock	33
3.15 Construction of expression vector	34
3.15.1 pENTR™ /D-TOPO® vector	34
3.15.2 Binary vector	36
3.16 Preparation of competent <i>Agrobacterium</i> cells	36
3.17 Transformation of <i>A. tumefaciens</i> by electroporation	37
3.18 <i>Agrobacterium</i> infiltration into tomato leaves	37
3.19 Gene expression analysis	38

	Page
3.19.1 RT-PCR	38
3.20 Extraction of recombinant protein from tomato leaves.....	39
3.21 Protein analysis.....	40
3.21.1 Sodium Dodecyl Sulfate Polyacrylamide Gel Electrophoresis (SDS- PAGE) 40	
3.21.2 Western blot.....	40
3.22 Tocopherol extraction	41
3.23 Chlorophyll analysis	41
3.24 Tocopherol analysis	42
3.24.1 Thin Layer Chromatography (TLC)	42
3.24.2 Gas Chromatography-Mass Spectrophotometer (GC-MS).....	42
CHAPTER IV Results	44
4.1 Total RNA extraction	44
4.2 Isolation of core sequences from degenerate primers.....	44
4.3 Full length genes from RACE PCR	45
4.4 Cloning of full length genes	51
4.5 <i>In silico</i> protein identification and characterization.....	51
4.6 Phylogenetic analysis.....	59
4.7 Construction of plant expression vectors.....	62
4.8 Gene expression of <i>ctl</i> and <i>alrc2</i> overexpressed in tomato leaves	64
4.9 Recombinant protein expression in tomato leaves	67
4.10 Determination of tocopherol content in agroinfiltrated tomato leaves	68
4.11 Determination of total chlorophyll content in agroinfiltrated tomato leaves	68

	Page
CHAPTER V Discussion	76
CHAPTER VI Conclusion	83
REFERENCES	84
VITA.....	94



List of Tables

	Pages
Table 1 Aspartate rich regions of plant aromatic PTases.....	16
Table 2 Specific primers the determination of PTase core sequence.....	24
Table 3 The expected size PCR products of each pair of primers.....	24
Table 4 PCR thermal cycling condition for amplification of the core sequence.....	25
Table 5 The specific primers for RACE PCR technique.....	28
Table 6 The components of RACE PCR reaction.....	28
Table 7 RACE PCR thermal cycling condition.....	29
Table 8 The specific primers of full length gene.....	30
Table 9 PCR thermal cycling condition of full length gene.....	30
Table 10 The components of ligation reaction for pGEM®-T Easy Vector.....	31
Table 11 PCR thermal cycling condition of gene expression analysis.....	39
Table 12 Summary of computed pI and MW of the deduced proteins.....	53
Table 13 List of transmembrane domains of ALRC2 and CTL.....	54
Table 14 Sequence data analysis by TargetP.....	55
Table 15 Sequence data analysis by WoLF PSORT and Protcomp.....	56

List of Figures

	Pages
Figure 1 The example of plant prenylated flavonoids.....	4
Figure 2 The example of plant prenylated xanthoness.....	6
Figure 3 The example of plant prenylated quinones.....	7
Figure 4 The example of plant flavonoid prenylated prenyltransferases activity.....	10
Figure 5 The activity of p-hydroxybenzoate geranyltransferase (PGT) in shikonin biosynthesis.	11
Figure 6 Biosynthesis of tocopherol, tocotrienol and plastoquinone in plants.....	13
Figure 7 Phylogenetic relationship of aromatic prenyltransferases.	14
Figure 8 Leaves of <i>Artocarpus lakoocha</i> Rox.....	17
Figure 9 The secondary metabolites from <i>A. lakoocha</i>	19
Figure 10 Plant and flower of <i>Clitoria ternatea</i> L.	20
Figure 11 The strategies for RACE PCR.	27
Figure 12 The strategies for construction of expression vector.....	35
Figure 13 The alignment of western blot setup.	41
Figure 14 Agarose gel of the total RNA isolated from <i>C. ternatea</i> L. (A) and <i>A. lakoocha</i> Rox (B).....	44
Figure 15 Agarose gel of the partial gene sequences from <i>C. ternatea</i> L. (A) and <i>A. lakoocha</i> Rox (B) amplified by multiple pairs of the degenerate primers.....	45
Figure 16 Isolation of full length cDNA of <i>ctl</i> and <i>alrc2</i> by RACE PCR. The nested RACE-PCR products (5' and 3' fragments) from <i>C. ternatea</i> (A) and <i>A. lakoocha</i> (B) are shown on 1% agarose gel, M: 1 kb DNA marker..	47
Figure 17 Agarose gels of <i>ctl</i> and <i>alrc2</i> coding sequence.....	48
Figure 18 The full length cDNA of <i>ctl</i> gene and its translated protein.....	49

Figure 19 The full length cDNA of <i>alrc2</i> gene and its translated protein.....	50
Figure 20 Verification of gene insertion to pGemT vector by restriction enzyme digestion are shown on 1% agarose gel against 1 kb DNA marker (M).....	51
Figure 21 PSI-blast search of the putative proteins CTL and ALRC2.	52
Figure 22 TMHMM analysis of ALRC2 and CTL protein sequences..	55
Figure 23 Multiple alignment of prenyltransferases family in plants.	57
Figure 24 The graphical image of transmembrane prediction by SignalP, C-, S-, and Y-score cleavage site were predicted to be at position of maximal Y score (A) CTL and (B) ALRC2.....	58
Figure 25 The phylogenetic tree of putative protein sequences of CTL and ALRC2 and related prenyltransferase proteins in plants.	60
Figure 26 Phylogenetic trees for conserved amino acid sequences (the aspartate rich regions) of prenyltransferase family.....	61
Figure 27 The construction of the entry vector (pENTR TM /D-TOPO [®] harboring the <i>ctl</i> and <i>alrc2</i> genes were analyzed on 1% agarose gel against 1 kb DNA marker (M).....	63
Figure 28 The construction of the destination vector.....	64
Figure 29 Tomato leaves after infiltration of the recombinant expression vectors via <i>A. tumefaciens</i> -mediated transformation.....	66
Figure 30 RT-PCR expression analysis of <i>ctl</i> and <i>alrc2</i> in the agroinfiltrated tomato leaves at 1 – 9 dpa..	67
Figure 31 Detection of the recombinant proteins by western blots analysis.....	68
Figure 32 The standard curve of α -tocopherol.....	69
Figure 33 The α -tocopherol and total chlorophyll contents in pGWB6:: <i>alrc2</i> and pGWB6:: <i>ctl</i> agroinfiltrated leaves.....	70
Figure 34 TLC patterns of tomato leaves expressing <i>alrc2</i> and <i>ctl</i> extracts.....	71

Figure 35 GC-MS chromatogram of infiltrated leaves in 3 dpa of pGWB6:: <i>ctl</i> showed the increase of metabolites.....	73
Figure 36 GC-MS analysis of the chemical profiles of phytol and fatty acids comparing between the transient expression of <i>ctl</i> (A) and <i>alrc2</i> (B) and α -tocopherol together with intermediates (MPBQ, DMPBQ) involved in the biosynthetic pathway of <i>ctl</i> (C) and <i>alrc2</i> (D) in tomato leaves at 1, 3, 6 and 9 dpa compare with control (empty vector: pGWB6)..	74
Figure 37 Mass spectra of silylated (A) α -tocopherol (12.955 min), (B) MPBQ (7.923 min) and (C) DMPBQ (8.203 min) from infiltrated leaves.	75



CHAPTER I

Introduction

The aromatic prenyltransferases (PTases) are a group of enzymes involved in the catalysis of prenylation reaction by transferring an isoprenoid unit to an aromatic molecule. In plants, aromatic PTases are involved in the biosynthesis of prenylated flavonoids and lipoquinones, including ubiquinones, menaquinones, and plastoquinones. Tocopherol, well known as vitamin E, is a branch of lipoquinone biosynthesis. It has been found in photosynthetic organisms such as plants and algae. Vitamin E is a highly potent antioxidant that protects and stabilize plant membrane against photo-oxidative damage or lipid peroxidation (Falk and Munne-Bosch, 2010). Moreover, it is important to plant by controlling lipid oxidation during the stages of seed germination, early seedling, and stress condition (biotic and abiotic stress) (Abbasi et al. 2007; Sattler et al. 2006). It has been shown that tocopherol disturbs lipid peroxidation chain reaction by donation proton from hydroxyl group of tocochromanol ring to polyunsaturated fatty acid (PUFA) peroxy radical (Asensi-Fabado and Munné-Bosch, 2010).

Vitamin E has been divided into two groups, tocopherols and tocotrienols which differ from each other in the degree of saturation of their hydrophobic phytyl side chain. Each group has four derivatives, including α -, β -, γ - and δ - forms by which they differ in methyl group number and position on the hydrophilic chromanol head group (DellaPenna and Mène-Saffrané, 2011). Tocopherol biosynthesis starts with the condensation of the aromatic head group precursor, homogentisate (HGA), and the phytyl tail precursor, phytyl diphosphate (PDP). HGA is derived from *p*-hydroxyphenylpyruvate (HPP) by the action of 4-hydroxyphenylpyruvate dioxygenase (HPPPD) whereas PDP is derived from the reduction of geranylgeranyl diphosphate

(GGDP) from the isoprenoid pathway (Vranová, et al., 2013). The condensation reaction of HGA and PDP is catalyzed by homogentisate phytyltransferase (HPT or VTE2), the key enzyme in the first step of tocopherol biosynthesis, to produce 2-methyl-6-phytylbenzoquinol (MPBQ). MPBQ is then methylated to yield 2,3-dimethyl-5-phytylbenzoquinol (DMPBQ) by the enzyme MPBQ methyltransferase (VET3). Subsequently, the second ring of γ -tocopherol is formed by tocopherol cyclase (TC or VTE1), and finally, α -tocopherol is formed by γ -tocopherol methyltransferase (γ TMT or VTE4) (DellaPenna and Pogson, 2006).

So far, overexpression of HPT has been reported in *Arabidopsis* (Collakova and DellaPenna, 2003a), *Synechocystis* sp. PCC 6803 (Savidge, et al., 2002), apple (Seo, et al., 2011), and lettuce (Ren, et al., 2011), which usually cause the increase of α -tocopherol accumulation. HPT has therefore been considered as the enzyme catalyzing the rate-limiting step of the pathway.

In this study, *Artocarpus lakoocha* Rox and *Clitoria ternatea* L. known respectively as Mahaad and Un-Chann in Thai name were used as potential sources for isolating aromatic PTase genes and enzymes. Both plants are abundant of the secondary metabolites such as flavonoids, stilbenes, and their derivative compounds which have high potential of biological activities, such as antimicrobial, anticancer, antioxidant and anti-tyrosinase activities (Likhitwitayawuid, et al., 2005; Mukherjee, et al., 2008; Sritularak, et al., 2010; Swain, et al., 2012a; Swain, et al., 2012b). The main objective of this study is to discover novel aromatic PTase genes from these plants. Methods of molecular biology were used to obtain full-length aromatic PTase genes, followed by expressing the genes in a suitable system. The expressed enzymes were then determined for their activities.

CHAPTER II

Literature review

2.1 Plant prenylated aromatic compounds

Prenylated aromatic compounds are a group of secondary metabolites that have been found ubiquitously in plant kingdom, particularly the family of Leguminosae, Moraceae, Umbelliferae, and Rutaceae (Botta, et al., 2009; Botta, et al., 2005; Epifano, et al., 2007). Diversity of compound structures is due to various precursors and prenyl side chain in prenylated aromatic biosynthesis. . According to the structure, these compounds can be classified into three types which are prenylated flavonoids, prenylated xanthone, and prenylated quinone.

2.1.1 Prenylated flavonoids

Prenylated flavonoids (Figure 1) are a group of secondary metabolites found in plants and bacteria and their structures contain prenyl moieties on the flavonoid nucleus. Generally, these compounds have been found in many prenylated derivative forms after binding to flavonoids such as flavones, flavonols, flavanones, flavanonols, isoflavones, isoflavanones, isoflavans, and chalcones. An example of prenylated flavanone, Sophoraflavanone G (**1**), was isolated from root of *Sophora flavescens* and showed antibacterial activity and inhibitory activity against cyclooxygenase 1 (COX1), 5-lipoxygenase (5-LOX), and tyrosinase (Cha, et al., 2007; Kim, et al., 2002; Son, et al., 2003; Tashiro, et al., 2001). Papyriflavonol A (**2**) is a prenylated flavonol isolated from 6 *Broussonetia papyrifera* root that exhibited anti-tyrosinase and anti-5-lipoxygenase (5-LOX) activities (Lee, et al., 2004; Son, et al., 2001; Zheng, et al., 2008). Artelastin (**3**) was extracted from wood bark of *Artocarpus elasticus* and showed broad range inhibitory activities of reactive oxygen species

(ROS) and nitric oxide (NO) production, lymphocyte proliferation, and DNA replication in MCF-7 human breast cancer cell line (Cerqueira, et al., 2008; Cerqueira, et al., 2003; Pedro, et al., 2005). Kuwanon G (**4**) is a prenylated derivative of isoflavone has been isolated from root bark of *Morus alba*. This compound has biological activities as antibacterial agent against oral pathogens and nitric oxide production inhibitor (Cheon, et al., 2000; Park, et al., 2003). Ganconin Q (**5**), 6-prenylapigenin (**6**), and 8-prenylapigenin (**7**) are prenylated flavones have been extracted from genus *Dorstenia* and it has been reported that they showed cytotoxic activity and inhibited cancer cell proliferations (Kuete, et al., 2011; Wang, et al., 2006).

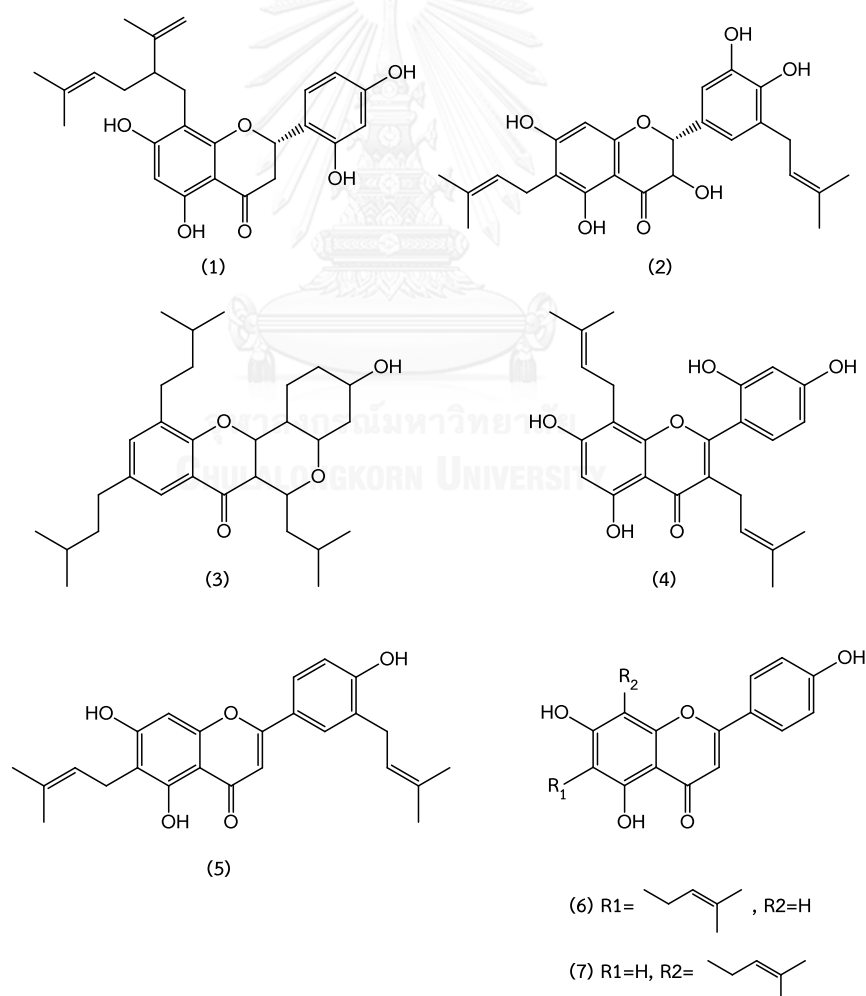


Figure 1 The example of plant prenylated flavonoids.

2.1.2 Prenylated xanthenes

Prenylated xanthenes are a group of xanthenes that having prenyl moieties attached to different positions of xanthone structure. The prenylated xanthenes were found in ethanol extract from leaves of *Garcinia griffithii* pericarb consisting of garcinones C (**8**), garcinones D (**9**), garcinones E (**10**), gartanin (**11**), xanthone I (**12**), and γ - mangostin (**13**), and also Rubraxanthone (**14**) (Figure 2). They showed cytotoxicity against human cancer cells (Chen, 2002; Xu, et al., 2014) and inhibitory effects on platelet-activating factor (PAF) (Alkadi K. A. A, et al., 2013; Jantan, et al., 2002).



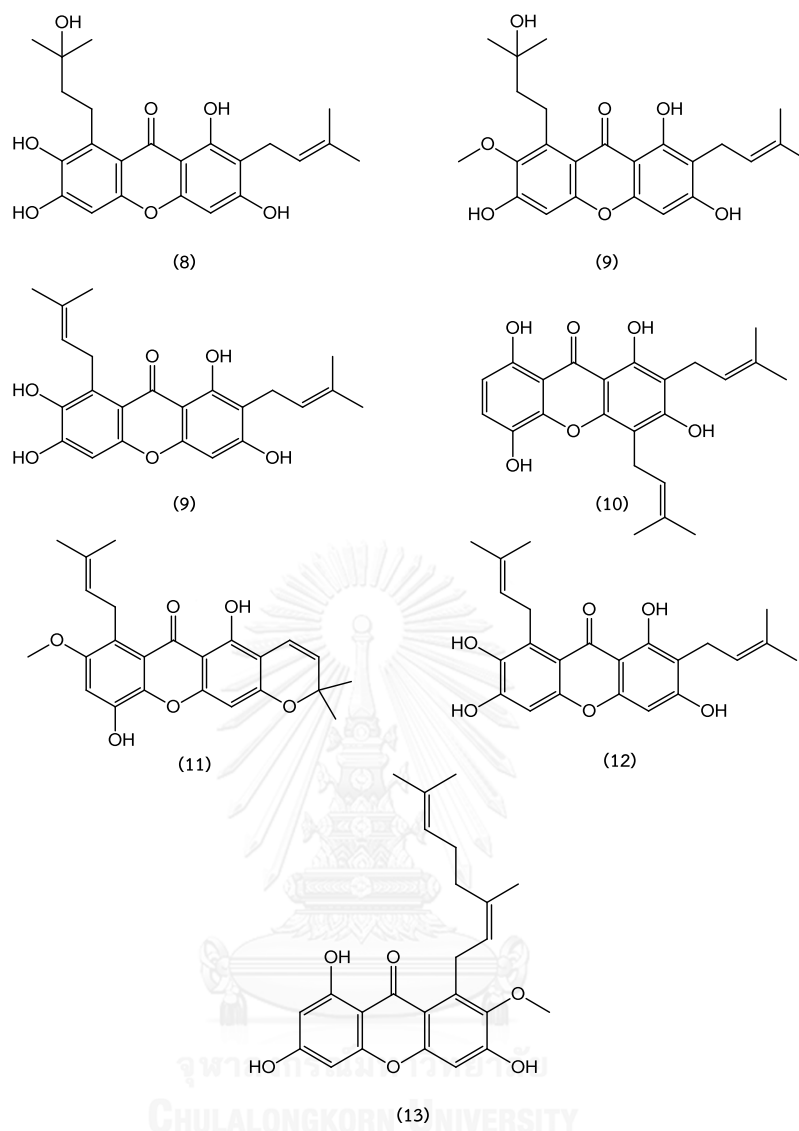


Figure 2 The example of plant prenylated xanthenes.

2.1.3 Prenylated quinones

In higher plants, prenylated quinones (Figure 3) are a group of aromatic compounds consisting of prenyl moieties attached to an aromatic ring e.g. 4-hydroxybenzoate (4-HB) and homogentisate (HGA). The phyloquinone (vitamin K1) (14), plastoquinone (15), ubiquinone (16) and tocochromanol (tocopherol (17) and tocotrienol (18)) belong to lipoquinones that are important for electron transport system in photosynthetic organelle (Biggins and Mathis, 1988; Nowicka and Kruk,

2010; Pshybytko, et al., 2008). The tocopherols (α -, γ -, β - and δ - form) have inhibitory activity against cancer cells by upregulating the mRNA and protein expressions of cleaved-caspase 3, peroxisome proliferator activated receptor γ (PPAR- γ), and nuclear factor (erythroid-derived 2)-like 2 (Nrf2) and also decreasing the gene expression of interleukin 8 (IL-8) (Smolarek, et al., 2013; Soo, et al., 2004; Stone, et al., 2004; Zingg, et al., 2013).

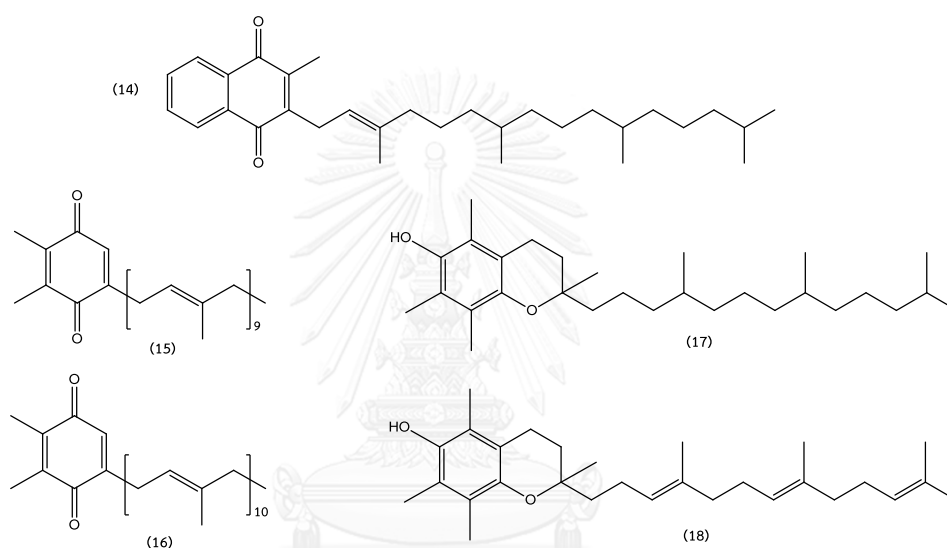


Figure 3 The example of plant prenylated quinones.

2.2 Plant aromatic prenyltransferase

The aromatic prenyltransferases (PTases) are groups of catalytic enzymes involved in prenylation reaction by transferring an isoprenoid molecule in form of allylic isoprenyl diphosphate such as dimethylallyl pyrophosphate (DMAPP), isopentyl pyrophosphate (IPP), geranylgeranyl pyrophosphate (GGPP) or phytol pyrophosphate (PDP) to an aromatic molecule that contributed significantly to structure diversity of prenylated aromatic compounds. In plant kingdom, the aromatic PTase usually belongs to UbiA superfamily of membrane bound enzymes that accept various aromatic compounds as a substrate leading to two groups of

compounds including prenylated flavonoids and prenylated quinones. Recently, several studies of aromatic PTase in terms of molecular biology and enzyme activity were successfully investigated.

2.2.1 Aromatic prenyltransferase in prenylated flavonoid biosynthesis

In prenylated flavonoid biosynthesis, flavonoid and prenyl groups are precursors of flavonoid PTases. The flavonoid core structure arises mainly from shikimate pathway via cinnamoyl-CoA and chain extension using three molecules of malonyl-CoA to produce initially polyketide and change to chalcone scaffold forming a flavonoid core structure, naringenin, by chalconesynthase. The prenyl units can come from two pathways: mevalonate (MVA) and methylerythritol phosphate (MEP) pathway. These pathways occur in different organelles in plant. The MVA pathway has been found in cytosol or mitochondria while the MEP pathway occurs in chloroplast. All identified flavonoid PTases from plants utilized DMAPP rather than IPP to connect with flavonoid core structure and Mg^{2+} or other cation are required in catalytic reaction. Despite numerous prenylated flavonoids were found in plant, six flavonoid PTases of UbiA superfamily have currently been identified and characterized. The naringenin 8-dimethylallyltransferase (SfN8DT) has been isolated from *Sophora flavescens* suspension cells and it transferred DMAPP to C-8 position of naringenin to produce 8-dimethylallyl naringenin (Sasaki, et al., 2009). Hence, isoflavone PTase (SfG6DT) and chalcone PTase (SfiLDT) have been isolated from *S. flavescens* which corresponding to prenylation of the genistein at 6 position and isoliquiritigenin to produce dimethylallyl genistein and dimethylallyl isoliquiritigenin, respectively (Sasaki, et al., 2011). LaPT1 was identified from white lupin (*Lupinus albus*). This enzyme prenylated the genistin and 2'-hydroxygenistin with DMAPP at C-3' position to produce isowighteone and licoisoflavone, respectively (Shen, et al., 2012). The biosynthetic pathway of these prenylated flavonoids was shown in figure

4. The glycinol-4-dimethylallyltransferase (G4DT) has been isolated from soybean (*Glycine max*) and its function was to produce 4-dimethylallylglycinol which is an intermediate in glyciolin I biosynthesis (Akashi, et al., 2009a). MalDT and CtDT are flavonoid PTase identified from *Morus alba* and *Cudrania tricuspidata* (Wang, et al., 2014). These enzymes can accommodate a broad range of substrates, for example, isoliquiritigenin, dihydroxychalcone, butein, genistein, and hydroxygenistein for prenylation reaction to produce 3'-dimethylallylisoliquiritigenin, 3'-dimethylallyl-2,4-dihydroxychalcone, 3'-dimethylallyl-2,4,2',4'-tetrahydroxychalcone, 3'-dimethylallylbutein, 6'-dimethylallylgenistein, 6'-dimethylallyl-2'-hydroxygenistein, respectively. The Figure 4 showed the plant flavonoid PTases activity. Recently, PT1 which is an enzyme involved in bitter acid biosynthetic pathway was characterized in hop (*Humulus lupulus*). This enzyme catalyzed prenylation by transferring DMAPP to naringenin chalcone to obtain desmethylxanthohumol (Li, et al., 2015).

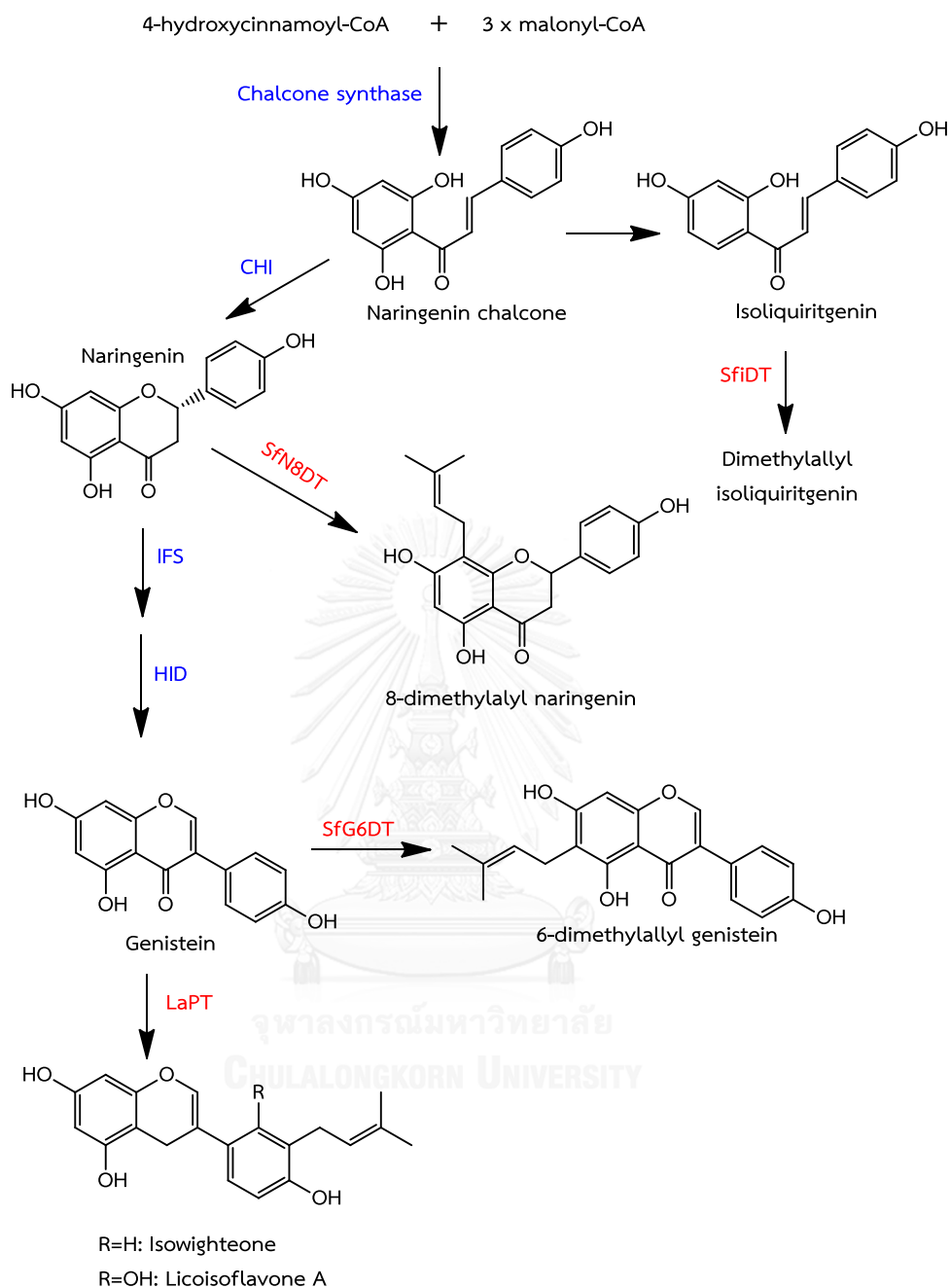


Figure 4 The example of plant flavonoid prenylated prenyltransferases activity. CHI: chalcone isomerase; IFS: 2-hydroxyisoflavanone synthase and HID: 2-hydroxyisoflavanone dehydratase. SfN8DT: naringenin 8-dimethylallyltransferase, SfG6DT: genistein 6-dimethylallyltransferase, SfiLDT: isoliquiritigenin dimethylallyltransferase.

2.2.2 Aromatic prenyltransferase in prenylated quinone biosynthesis

In plants, the prenyl, quinone, or lipoquinone serve as electron transporters in photosystem I and II (PSI and PSII) and protect against lipid oxidation. The biosynthesis of these compounds is started from hybridization of aromatic head group and prenyl side chain by aromatic PTase. The aromatic head group and prenyl side chain are derived from shikimate pathway and MVA or MEP pathway, respectively. The *p*-hydroxybenzoate polyprenyltransferase (PPT) catalyzes prenylation reaction in critical step of ubiquinone biosynthesis by connecting *p*-hydroxybenzoate (PHB) with polyprenyl side chain to form C-C bond to generate polyprenyl PHB (Ohara, et al., 2006). In addition, the PPT is involved in naphthoquinone and shikonin biosynthesis. The *p*-hydroxybenzoate geranyltransferase (PGT) showed substrate specificity with geranyl diphosphate (GPP) to produce geranyl PHB as an intermediate in the pathway as shown in Figure 5 (Ohara, et al., 2009; Yazaki, et al., 2002).

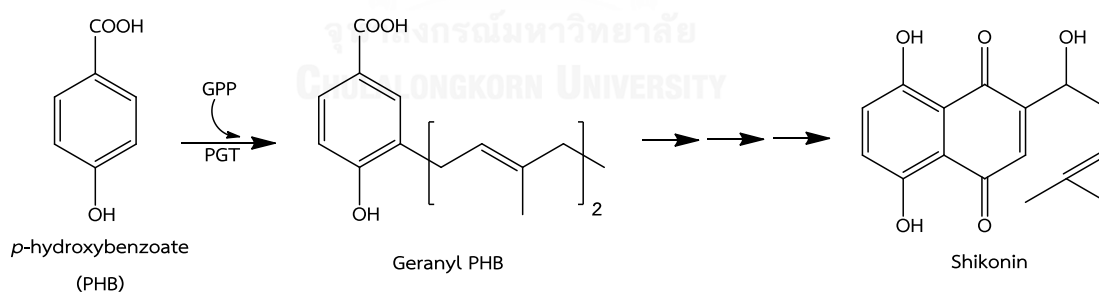


Figure 5 The activity of *p*-hydroxybenzoate geranyltransferase (PGT) in shikonin biosynthesis.

Homogentisate phytyltransferase (HPT/VTE2) is another group of aromatic quinone PTase involved in the rate limiting step of tocopherol biosynthesis in plant.

Biosynthesis of tocopherol, tocotrienol and plastoquinone in plants was illustrated in Figure 7. It is first started from homogentisic acid (HGA) that is synthesized from p-hydroxyphenyl pyruvate by 4-hydroxyphenylpyruvate diogenase (HPPD), followed by the addition of phytyl pyrophosphate (PDP) or geranylgeranyl pyrophosphate (GGPP) or solanesyl pyrophosphate to HGA by HPT/VTE2 or homogentisate geranylgeranyltransferase (HGGT) or homogentisate solanesyl transferase (HST) for the production of key intermediates in the biosynthesis of tocopherol, tocotrienol and plastoquinone, respectively. To produce α -tocopherol, HPT/VTE2 prenylates HGA with PDP to produce the first intermediate of 2-methyl-6-phytyl-1,4-benzoquinone (MPBQ), then methylation reaction of MPBQ catalyzes by MPBQ methyltransferase (MPBQ MT/VTE3) to yield 2,3-dimethyl-5-phytyl-1,4-benzoquinone (DMPBQ). The DMPBQ is cyclized by tocopherol cyclase (TC/VTE1) to produce γ -tocopherol and subsequently γ -tocopherol is methylated by γ -tocopherol methyltransferase (γ -TMT/VTE4) to yield α -tocopherol. For the production of tocotrienol, HGGT utilizes HGA as prenyl acceptor and transfers prenyl group from GGPP to HGA resulting in formation of the first intermediate which is 2-methyl-6-geranylgeranyl-1,4-benzoquinone (MGGBQ). Hence, methylation of MGGBQ by VTE3 yields 2,3-dimethyl-5-phytyl-1,4-geranylgeranyl benzoquinone (DMGGBQ) and VTE1 cyclizes DMGGBQ to form γ -tocotrienol and then methylation of γ -tocotrienol finally yield α -tocotrienol. In plastoquinone biosynthesis pathway, HST catalyzes prenylation reaction by transferring solanesyl diphosphate (a prenyl group) to HGA to form 2-methyl-6-solanesyl-1,4-benzoquinol (MSBQ) intermediate. The biosynthesis of tocopherol, tocotrienol and plastoquinone occur in chloroplast and HPT, HGGT and HST are embedded in chloroplast membrane. Under oxidative stress conditions induced by high light, drought or infection, these compounds are increasingly produced to protect cell membrane from free radical or reactive oxygen species (ROS) (Sharma, et al., 2012).

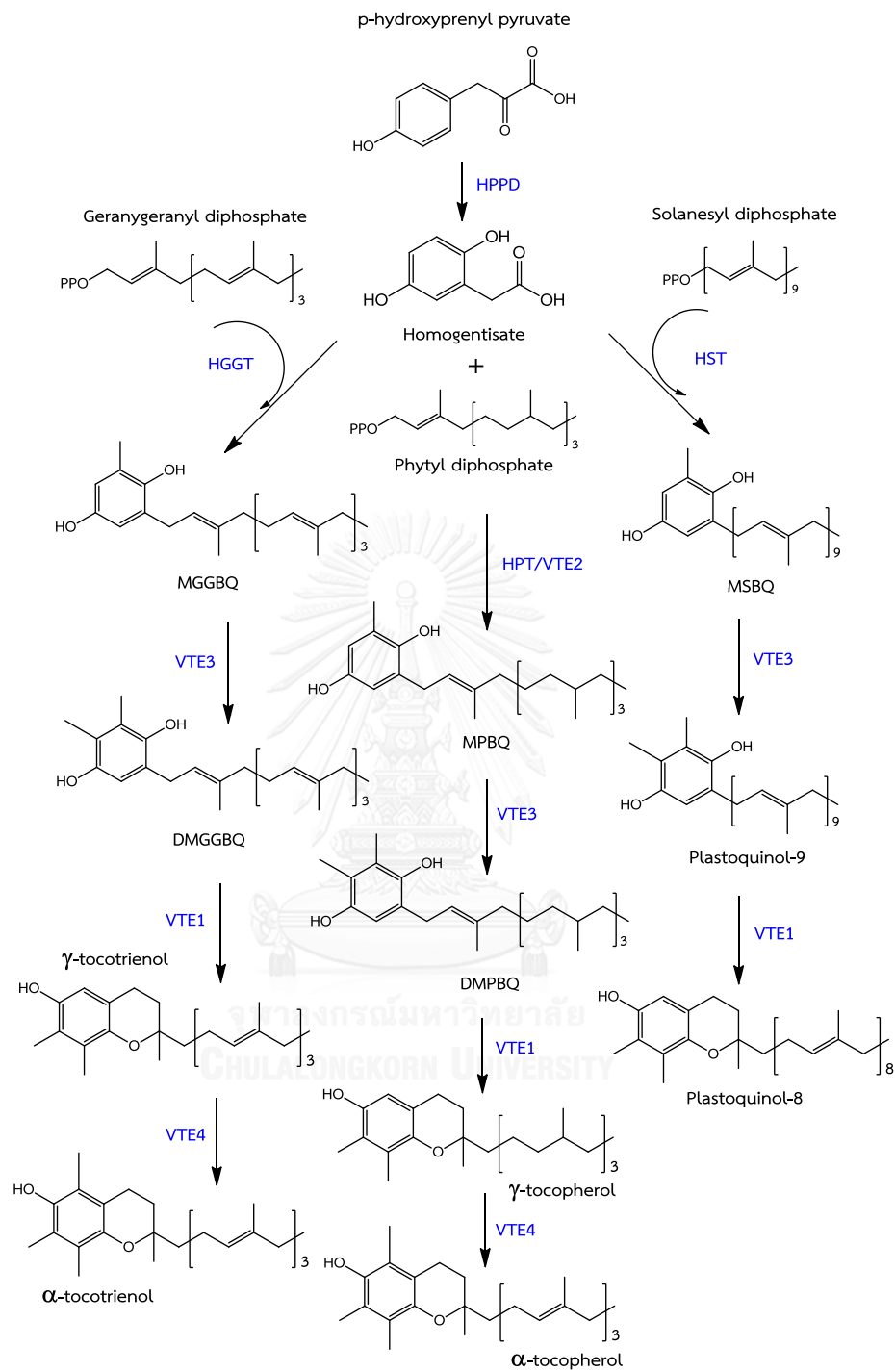


Figure 6 Biosynthesis of tocopherol, tocotrienol and plastoquinone in plants.

2.3 Characterize and function of aromatic PTases

The HPT, HGGT and HST are a group of enzymes that transfer different forms of prenyl group to HGA. Although these enzymes catalyze prenylation reaction and their structures are very similar (transmembrane α -helix), their amino sequences are not quite different. The phylogenetic analysis showed the amino acid sequences of flavonoid PTases shared sequence similarity with HPT. It is implied that the flavonoid PTases may evolve from HPT (Figure 7).

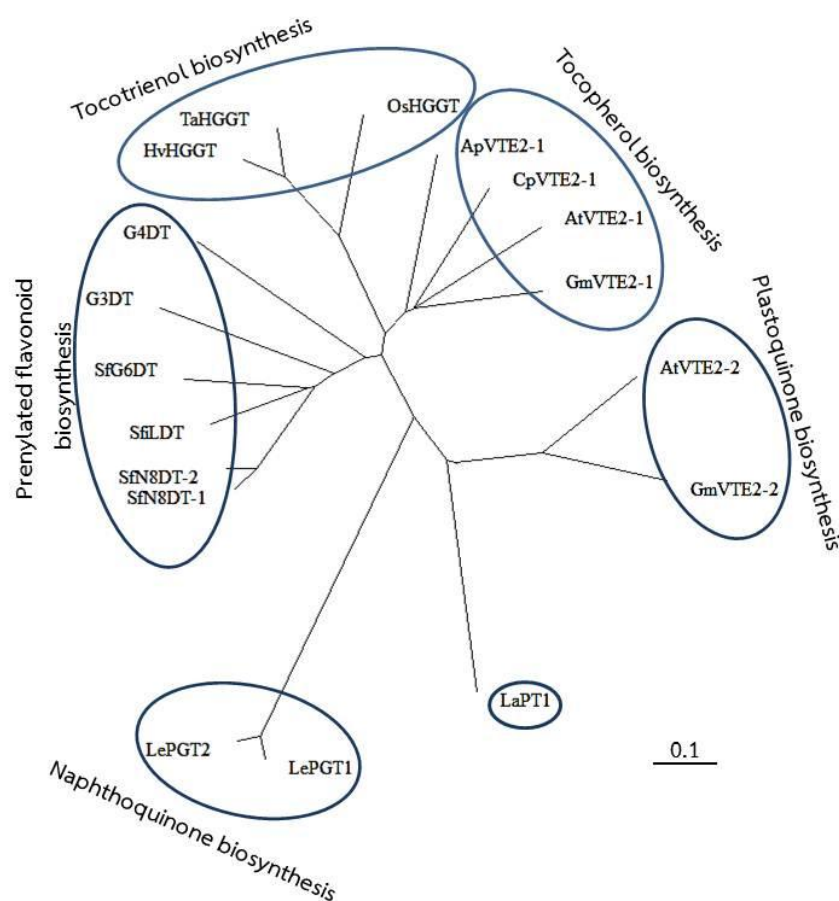


Figure 7 Phylogenetic relationship of aromatic prenyltransferases. A rooted phylogram was generated using a ClustalW alignment. Ap, *Allium porrum*; At, *Arabidopsis thaliana*; Cp, *Cuphea pulcherrima*; Gm, *Glycine max*; Hv, *Hordeum vulgare*; Os, *Oryza sativa*; Ta, *Triticum aestivum*.

Aromatic PTases in plant are membrane-bound proteins of UbiA superfamily localized in plastid membrane. They contains two aspartate-rich regions for binding of the prenyl diphosphate substrate via chelating Mg^{2+} ion required for enzyme activity (Table 1) (Huang, et al., 2014). In *E. coli*, the UbiA protein catalyzes cleavage of pyrophosphate from polyprenyl diphosphate and transfer prenyl chain to PHB (Ashby, et al., 1992). Generally, identified aromatic PTases have 7 – 9 transmembrane α -helixes and N-signal transit peptide to localize at chloroplast membrane. Expression of flavonoid PTase proteins was successfully done in yeasts such as strain W303-1A- Δ coq2 (Sasaki, et al., 2009) and strain YPH499 (Wang, et al., 2014). It has been found that PTases activity from Leguminosae expressed in yeast microsomal fractions preferred DMAPP as prenyl substrate while PTase activity from Moraceae can use DMAPP and GPP in prenylation. The enzyme assay required Mg^{2+} for catalyzing reaction with the optimal pH of 7 -10. Functional study of aromatic PTase can be tested in plant system. The overexpression of aromatic PTases has been reported in several plant systems such as *Arabidopsis* (Mene-Saffrane, et al., 2010), tobacco (Harish, et al., 2013a), tomato and lettuce (Lee, et al., 2007). Overexpression of *SfN8DT* gene encoding naringenin 8-dimethylallyltransferase in *Arabidopsis* showed the accumulation of 8-prenylated kaempferol which was not detected in *in vitro* enzyme assay (Sasaki, et al., 2008).

The PPT enzyme involve in ubiquinone biosynthesis are located in the inner membrane of mitochondria but LePG1 that member of PPT involved in naphthoquinone biosynthesis is localized to the endoplasmic reticulum (Ohara, et al., 2010; Ohara, et al., 2006; Okada, et al., 2004). In addition, the HPT and HST catalyzing the prenylation in tocopherol biosynthesis and plastoquinone, respectively are located at the plasmid (Block, et al., 2013; Hunter and Cahoon, 2007). Same as flavonoid PTases, the study of PPT protein expression was done in yeast stain W303-

1A- Δ coq2 and tobacco and the protein activity was detected from microsomal fraction (Ashby, et al., 1992; Ohara, et al., 2006; Okada, et al., 2004) while LePG1 expression was performed in insect cell (sf9 cell) system.

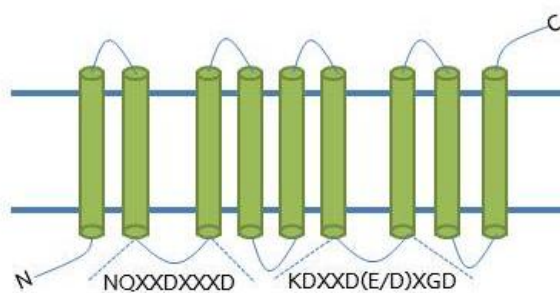


Table 1 Aspartate rich regions of plant aromatic PTases.

Protein	Motif I	Motif II	Protein	Motif I	Motif II
ApVTE2-1	NQLFDIEID	KDIPDIDGD	OsHGGT	NQLYDIQID	KDIPDIDGD
AtVTE2-1	NQLSDVEID	KDIPDIEGD	TaHGGT	NQLYDIQID	KDIPDVDGD
CpVTE2-1	NQLSDIDID	KDIPDIEGD	SfN8DT-1	NQLCDIEID	KDIPDMEGD
GmVTE2-1	NQLSDVEID	KDIPDIEGD	SfN8DT-2	NQLCDIEID	KDIPDMEGD
TaVTE2-1	NQLFDIEID	KDIPDIEGD	G4DT	NQLYDLEID	KDIPDVEGD
MdVTE2-1	NQLSDIDID	KDIPDIDGD	SfILD	NELCDVELD	KDIPDIEGD
GmVTE2-2	NQIYDISID	KDLPDVEGD	SfG6DT	NQLCDIEID	DIPDTEGD
AtVTE2-2	NQIYDIGID	KDLPDVEGD	G3DT	NQLCDLEID	KDIPDMEGD
LaPT1	NQIFDMDID	KDLSDINGD	MaIDT	NQIYDADID	KDLTDMEGD
HvHGGT	NQLYDIQID	KDIPDVDGD	LePGT1	NDYFDRNFD	YAHQDKVDD

2.4 *Artocarpus lakoocha* Rox

2.4.1 Plant description

Artocarpus lakoocha Rox or known in Thai as Mahaad (Figure 8) is a deciduous plant belonging to Moraceae family. It is widely distributed in South and South-east Asia such as India, Nepal, Malaysia, and Thailand. *A. lakoocha* is a tree that can reach to 15 – 18 m in height and its elliptical pointed leaf is 10 – 25 cm long. Its fruits are yellow at maturity and changed to reddish brown later and its seeds have thin white seed coat and sticky latex.



Figure 8 Leaves of *Artocarpus lakoocha* Rox

2.4.2 Chemical constituents and biological activities of *A. lakoocha*

A. lakoocha is a plentiful source of secondary metabolites, especially a group of flavonoids, stilbenes, and their derivative compounds. In phytochemical studies, artocarpin (**19**), norartocarpin (**20**), cycloartocarpin (**21**), resorcinol (**22**), and oxyresveratrol (**23**) has been found in the heartwood of *A. lakoocha* (Tunsaringkarn, et al., 2007) and prenylated 2-arybenzofurans consist of artolakoochol (**24**), 4-hydroxyartolakoochol (**25**) and cyclo-artolakoochol (**26**) (Sritularak, et al., 2010) as well as prenylated stilbene (lakoochin A (**27**) and lakoochin B (**28**)) were found in the root (Puntumchai, et al., 2004). Moreover, the *A. lakoocha* callus culture produces prenylated flavones and stilbenes (Maneechai, et al., 2012) (Figure 9).

Several biological activities have been reported from the extracts of *A. lakoocha*. The crude extracted from heartwood showed antityrosinase activity by inhibiting melanin production, antimicrobial, antibiofilm activity from oral pathogen and *Candida*. The leave extracted has been found activity against inflammatory, analgesic and CNS depressant (Nesa, et al., 2015). The root extract showed antiherpetic and anticancer activities (Arung, et al., 2006; Dej-adisai, et al., 2014; Shimizu, et al., 2002).

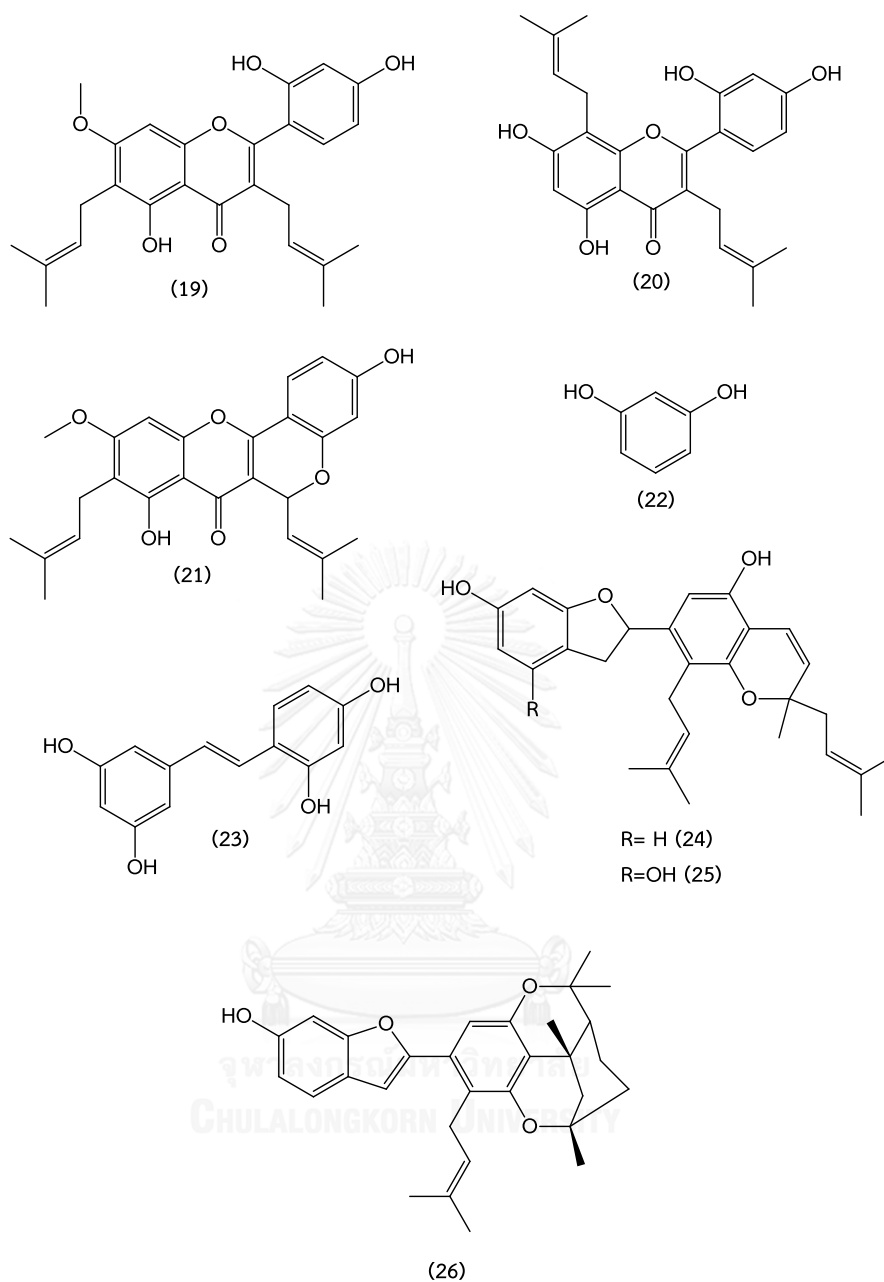


Figure 9 The secondary metabolites from *A. lakoocha*.

2.5 *Clitoria ternatea* L.

2.5.1 Plant description

Clitoria ternatea L. or Un-chann in Thai name is climbing plant belonging to Fabaceae family. It is distributed in India, Philippines, and other tropical Asian

countries. The plant leaf is imparipinnate with five to seven leaflets, 6 - 13 cm long and ovate. The seeds are yellowish-brown or blackish in color and oval in shape. Its flower color is blue or white (Figure 10).



Figure 10 Plant and flower of *Clitoria ternatea* L.

2.5.2 Chemical constituents and biological activities in *C. ternatea*

C. ternatea is a medicinal plant which has many biologically active compounds. The taraxerol and taraxerone were isolated from root. A number of anthocyanins and flavonoids were separated from flower. Leaves contain essential oils and flavone glycosides. *C. ternatea* has been screened for biological activities. It has an effect on learning and memory enhancing by which it increased acetylcholine content (Rai, et al., 2002). It also showed antidepressant, anti-inflammatory, anticancer, and anti-platelet aggregation (Devi, et al., 2003; Jacob and Latha, 2012; Jain, et al., 2003; Kelemu, et al., 2004; Nithianantham, et al., 2011).

CHAPTER III

Material and Methods

3.1 Plant materials

The calli of *Artocarpus lakoocha* Rox. were induced on WPM medium containing 1 mg L⁻¹ of 2,4-dichlorophenoxyacetic acid (2,4-D) and 1 mgL⁻¹ benzyladenine (BA) with 2% sucrose. According to Maneechai, all cultures were grown at 25 °C in the dark (17 days) to induce the production of secondary metabolites (Maneechai, et al., 2012).

The *Clitoria ternatea* L. leaves were collected from planting area of department of biochemistry and microbiology, faculty of pharmaceutical sciences, Chulalongkorn University.

3.2 Bacterial Strains

Escherichia coli

Stains	Genotype
DH5 α (Invitrogen)	F ⁻ , Lambda ⁻ , <i>recA1</i> , <i>endA1</i> ⁻ , <i>hsdR17</i> (rK ⁻ , mK ⁺), (<i>lacZYA-argF</i>), <i>supE44</i> , U169, Φ 80 <i>dlacZ</i> Δ M15, <i>thi-1</i> , <i>gyrA96</i> , <i>relA1</i>
One shot TOP10 (Invitrogen)	F _j , <i>mcrA</i> Δ (<i>mrr-hsdRMS-mcrBC</i>) Φ 80 <i>lacZ</i> M15 Δ <i>lacX74</i> <i>deoR</i> <i>recA1</i> <i>araD</i> 139 Δ (<i>ara leu</i>)7697 <i>galU</i> <i>galK</i> <i>rpsL</i> (Str ^R) <i>endA1</i> <i>nupG</i>

Agrobacterium tumefaciens

Strain GV3101 (Kan^R) carrying the helper plasmid pj19

3.3 Plasmids

pGEM [®] -T Easy Vector (Promega)	Cloning vector, Amp ^R
pENTR [™] /D-TOPO [®] (Invitrogen)	Entry vector, Kan ^R
pGWB6	Binary vector, Kan ^R , GFP

3.4 Total RNA extraction

Total RNAs were purified from plants using the RNeasy Plant Mini Kit (Qiagen), according to the supplier's recommendations. One hundred milligram of plant samples were ground in liquid N₂ with mortar and pestle then homogenized with 450 µl RLT buffer and incubated at 56 °C for 2 – 3 min. The homogenized lysate was transferred into QIAshredder spin column and centrifuged at 13,000 rpm for 2 min. The flow-through was transferred to new tube. After the flow-through was mixed by pipetted with 250 µl of ethanol, that transferred to RNeasy spin column and centrifuged at 12,000 rpm for 15 sec. The RNA was washed with 700 µl RW1 buffer in column and centrifuged in the same condition. The RNA was cleaned again with 500 µl RPE buffer and centrifuged in the same condition for twice times. The RNA was dried by centrifuged at 12,000 rpm for 2 min prior to elute with 50 µl of RNase-free water. Total RNA was treated with DNase I, RNase-free DNase (Fermentas). The following components were added to reaction, 1 ug of total RNA, 1X reaction buffer with CaCl₂, 1 U of DNase I, RNase-free DNase and DEPC water up to 10 µl. After the reaction was incubated at 37 °C for 30 min, the 1 µl of 50 mM EDTA was added for inactivation reaction and incubated at 65 °C for 10 min. RNA concentration was calculated following the formula $C (\mu\text{g}/\mu\text{l}) = \text{OD}_{260\text{nm}} \times 40 \times \text{dilution factor}$. The ratio of the readings at 260 nm and 280 nm (A₂₆₀ /A₂₈₀) ranged from 1.8 to 2.1, indicates

that the purity of RNA. The concentration of RNA was checked by using spectrophotometer.

3.5 Synthesis cDNA

The cDNAs were then prepared using the RevertAid™ H Minus Reverse Transcriptase (Thermo scientific™) in the presence of RiboLock™ RNase Inhibitor (Thermo scientific). The reaction mixture containing 1 ug of total RNA, 5 µg of oligo (dT)18 and DEPC water up to 12.5 µl, was incubated at 65 °C for 5 min. Then the reaction was mixed with 1X reaction buffer, 0.5 µl RiboLock™ RNase Inhibitor, 1 mM dNTP mix (10 mM for each) and 200 U RevertAid™ H Minus Reverse Transcriptase, and incubated at 42 °C for 60 min. The reaction was terminated by heating at 70 °C for 10 min.

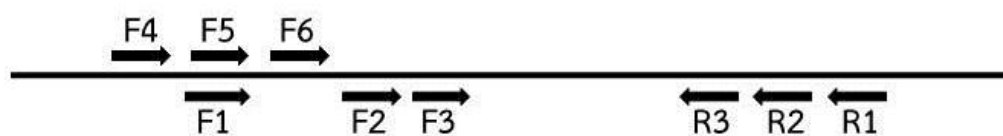
3.6 Determination of core sequences encoding PTases

The primers used in this study (Table 2) were designed based on the conserved regions of the aromatic PTases genes by multiple alignments using ClustalW (Chenna, et al., 2003; Larkin, et al., 2007). These primers were designed as degenerated primers using IUPAC codes to establish the ambiguous nucleotide (Wei, et al., 2003). The position and size of primers were shown in Table 3. The PCR of partial gene was performed with 1 µl cDNA in 50 µl reaction mixture consist of 1X High Fidelity PCR buffer, 2 mM MgSO₄, 0.2 mM dNTP each, 0.2 µM of forward and reverse degenerate primers (Table 2) and 1U Platinum® Taq DNA polymerase High Fidelity. The reaction was subjected to thermal cycling according to the following PCR program in Table 4.

Table 2 Specific primers the determination of PTase core sequence.

primer name	Sequence (5'--> 3')
Prenyl-F1	AATCAR <u>H</u> TRTNYGAYVTHGAAATAGACAA
Prenyl-F2	G <u>D</u> TTGTHGGTTC <u>D</u> TGGCCRTTRYTKT
Prenyl-F3	TYRAT <u>D</u> TRCCNYT <u>D</u> TTGAGATGGAA
Prenyl-F4	GGH <u>D</u> TGAATCARYTRTNTGA
Prenyl-F5	TTGAAATW <u>G</u> ACAAGRTHAABAARCC
Prenyl-F6	CTCCA <u>H</u> T <u>D</u> GCATCTGGRRAAT
Prenyl-R1	AGCTTCCADATAAACATRTARAANG
Prenyl-R2	ATTTCAA <u>W</u> AGNGHWAYACAARTCCA
Prenyl-R3	CCTTCNAYRTCDGGDATATCCTT

Table 3 The expected size PCR products of each pair of primers.



Primer	F1R1	F1R2	F1R3	F2R1	F2R2	F2R3	F3R1	F3R2	F3R3
Expected Size PCR product (bp)	674	502	418	544	372	283	479	309	224
Primer	F4R1	F4R2	F4R3	F5R1	F5R2	F5R3	F6R1	F6R2	F6R3
Expected Size PCR product (bp)	692	520	437	669	497	414	640	468	414

Table 4 PCR thermal cycling condition for amplification of the core sequence.

Step	Temperature	Time	Number of cycles
Initial denaturation	95 °C	3 min	1
Denaturation	95 °C	30 sec	
Annealing	48 °C	40 sec	35
Extension	72 °C	1 min	
Finale extension	72 °C	5 min	1
Cold	4 °C	infinity	

3.7 Determination of full length gene by rapid amplification of cDNA ends (RACE)

The 5' and 3' end were done by using a 5'-RACE and 3'-RACE system for rapid amplification of cDNA ends, (Invitrogen, USA) according to the manufacturer's instructions (Figure 11). In 5'-RACE end, five microgram of total RNA was removed contaminate by treated with calf intestinal phosphatase (CIP) in the reaction mixture (10 µl) containing 1X CIP buffer, 40 U RneaseOut™, 10 U CIP. After incubated at 50 °C for 1 hour, the mRNA was extracted with 100 µl phenol:chloroform and centrifuged at 13,000 rpm for 5 min. The supernatant was transferred into new tube, and then mixed with 2 µl mussel glycogen, 10 µl 3 M sodium acetate, pH 5.2. The mixture was added 220 µl of 95% ethanol and mixed by vortex and then incubated at -20 °C for 10 minutes. The RNA was precipitated by centrifugation at 13,000 rpm at 4 °C for 20

min. The supernatant was discarded and RNA pellet was washed with 500 μ l of 70% ethanol. After centrifuged, the supernatant was removed and the pellet was dry for 2 min prior resuspended in 7 μ l DEPC water.

The dephosphorylated RNA was removed 5' cap by tobacco acid pyrophosphatase (TAP) in the reaction mixture containing 1X TAP buffer, 40 U RneaseOut[™] and 0.5 U TAP followed by incubated at 37 °C for 1 hour. The recapped RNA was extracted and precipitated same as previous condition. The dephosphorylated and recapped RNA was ligated with the GeneRacer[™] RNA oligo to 5'-end using T4 RNA ligase. The ligation reaction started by incubation RNA with 0.25 μ g GeneRacer[™] RNA oligo at 65 °C for 5 min and 1X ligase buffer, 1 μ l of 10 mM ATP, 40 U RneaseOut[™] and 5 U T4 RNA ligase were added into the mixture. After incubated at 37 °C for 1 hour, RNA was extracted and precipitated again.

The first stand of cDNA was amplified using ligated RNA as a template and the GeneRacer[™] Oligo dT as primer. The reaction mixture (20 μ l) containing 1.25 mM dNTP, 1X RT buffer, 15 U Cloned AMV RT and 40 U RneaseOut[™] followed by incubated at 45 °C for 1 hour. The reaction was inactivated by heat at 85 °C for 15 min. For investigation full length at 5' and 3' end, the PCR was performed using primers were provided with the kit and gene specific primers (GSP) were designed using the partial gene sequence (Table 5). The RACE PCR reaction was performed follow in Table 6 and thermal cycling according to the following PCR program in Table 7.

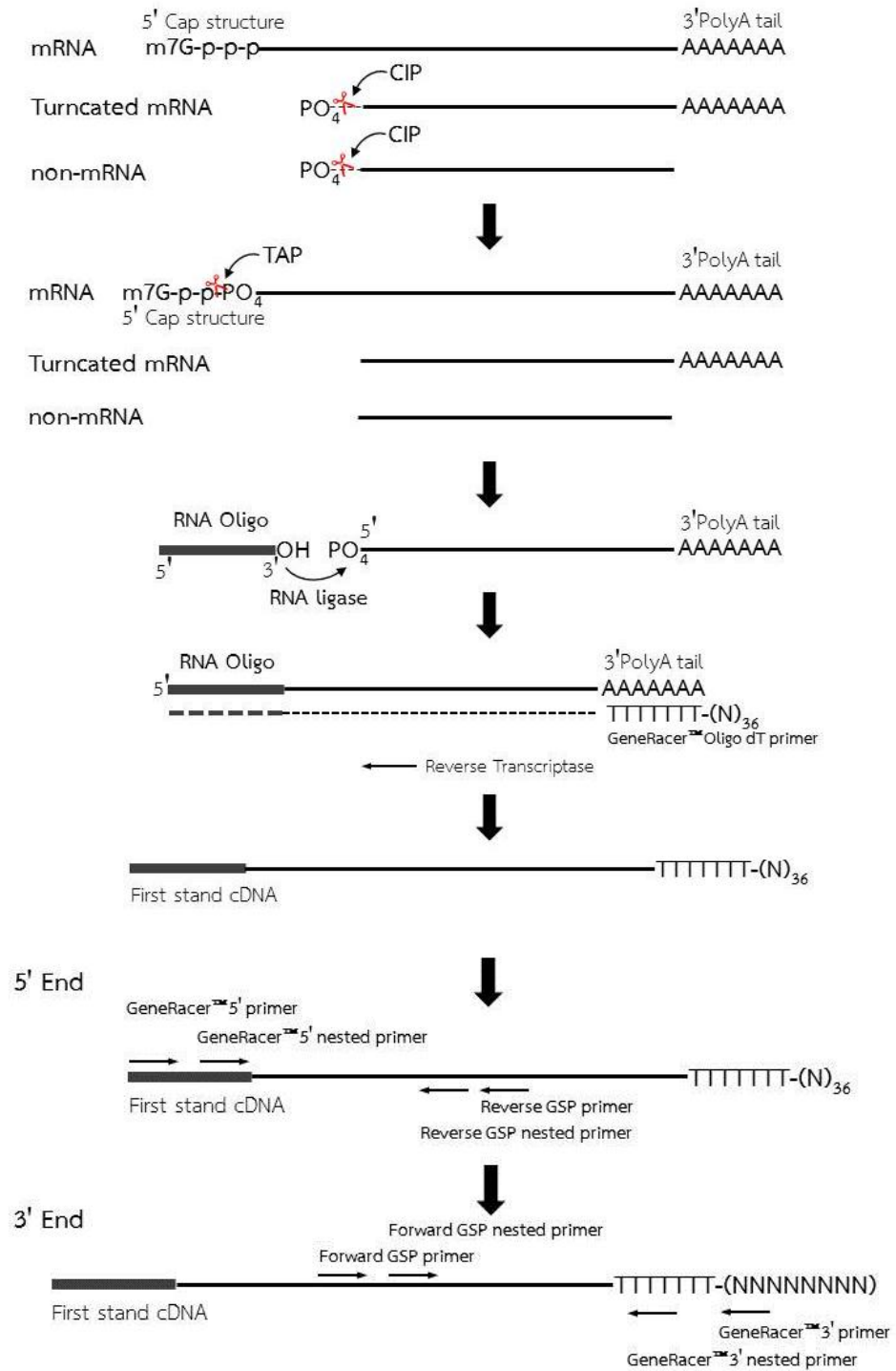


Figure 11 The strategies for RACE PCR.

Table 5 The specific primers for RACE PCR technique.

Primer name	Sequence (5'--> 3')
5' RACE	
CTin-R ^{**}	TGTACACATGGGTCTGCATGTGCAGGAAA
CTout-R [*]	GAGAAGAAGCTCATAAATGCAGTAGCAAAA
ALRin-R ^{**}	GACACCCGCTCGAATCGGAGCCTGGA
ALRout-R [*]	TAAAGAGGGCAGCAACCACAGCCTCCAG
3' RACE	
RACEin-F ^{**}	TTTCCTGCACATGCAGACCCATGTGTACAA
RACEout-F [*]	AGTTTTGTACTAGGAACTGCTTATTCAAT

* Primer for first RACE PCR and ** Primer for second RACE PCR

Table 6 The components of RACE PCR reaction.

First PCR		Second PCR	
Reagents		Reagents	
10 µM GeneRacer™ 5' or 3' primer	4.5 µl	10 µM GeneRacer™ 5' or 3' Nested primer	1 µl
10 µM Reverse or Forward GSP primer	1.5 µl	10 µM Reverse or Forward Nested GSP primer	1 µl
cDNA	1 µl	First PCR (dil 10X)	1 µl
10X High Fidelity PCR buffer	5 µl	10X High Fidelity PCR buffer	5 µl
dNTP Solution (10 mM each)	1.5 µl	dNTP Solution (10 mM each)	1 µl
Platinum [®] Taq DNA polymerase High Fidelity (5U/µl)	0.5 µl	Platinum [®] Taq DNA polymerase High Fidelity (5U/µl)	0.5 µl
50 mM MgSO ₄	1 µl	50 mM MgSO ₄	1 µl
water	35 µl	water	39.5 µl

Table 7 RACE PCR thermal cycling condition.

Step	Temperature	Time	Number of cycles
First PCR			
Initial denaturation	94 °C	2 min	1
Denaturation	94 °C	30 sec	5
Annealing	72 °C	30 sec	
Denaturation	94 °C	30 sec	5
Annealing	70 °C	30 sec	
Denaturation	94 °C	30 sec	25
Annealing	60 °C	30 sec	
Extension	68 °C	1 min	
Finale extension	68 °C	10 min	1
Step	Temperature	Time	Number of cycles
Second PCR			
Initial denaturation	94 °C	2 min	1
Denaturation	94 °C	30 sec	25
Annealing	60 °C	30 sec	
Extension	68 °C	1 min	1
Finale extension	68 °C	10 min	

3.8 Determination of full length gene for prenyltransferases genes

In order to confirmed the sequence of genes that obtained from RACE PCR. The sequence of contigs at 5' and 3' ends were aligned with partial gene and observed start codon at 5'-end and stop codon at 3'-end. Then the primers were designed from sequence of start codon and stop codon as showed in Table 8 and

also PCR reactions were performed in reaction mixture containing 1 μ l cDNA, 1X High Fidelity PCR buffer, 2 mM MgSO₄, 0.2 mM dNTP, 0.4 μ M of forward and reverse primer and 1 U Platinum[®] Taq DNA polymerase High Fidelity. The reaction was subjected to thermal cycling according to the following PCR program in Table 9.

Table 8 The specific primers of full length gene.

Primer name	Sequence (5'--> 3')
CTFull-Fw	ATGGATTCCGGTGCTCTATGGATCTT
CTFull-Rv	TCATCTAACATAAGGGAGGAGCAGGT
ALRFull-Fw	ATGGATTCTTTTCTTCTGGGTTCATTGAA
ALRFull-Rv	TCACCTAACGAACGGTATAAGTAGATACT

Table 9 PCR thermal cycling condition of full length gene.

Step	Temperature	Time	Number of cycles
Initial denaturation	94 °C	2 min	1
Denaturation	94 °C	30 sec	
Annealing	60 °C	30 sec	30
Extension	68 °C	1.30 min	
Finale extension	68 °C	10 min	1

3.9 Cloning of gene in pGEM[®]-T Easy Vector for sequencing

The PCR products from every process were ligated into pGEM[®]-T easy vector for checked the sequence. The cloning was carried out by set up a ligation reaction following in Table 10 and incubation overnight at 4 °C. The ligation product was

transformed into *E. coli* DH5 α competent cell and screening by blue-white colonies selection on LB agar containing 50 $\mu\text{g ml}^{-1}$ ampicillin, 40 $\mu\text{g ml}^{-1}$ x-gal and 0.1 mM IPTG. A group of white colonies were picked and grown overnight in 5 ml LB broth containing 50 $\mu\text{g ml}^{-1}$ ampicillin. The mixture was incubated overnight at 37 $^{\circ}\text{C}$ with shaking at 250 rpm. These white colonies were confirmed the insert gene by extraction plasmid using alkaline lysis method and restriction digestion analysis. In addition to sequencing, the plasmid was extracted with PrestoTM Mini Plasmid Kit (GeneAid) and sequencing by universal primer in pGEM[®]-T easy vector (M13 Forward: 5' GTAAAACGACGGCCAGT 3' and M13 reverse: 5' GCGGATAACAATTTACACAGG 3').

Table 10 The components of ligation reaction for pGEM[®]-T Easy Vector.

Reaction Component	Standard reaction
pGEM [®] -T Easy Vector (50ng)	1 μl
PCR product [*]	x μl
2X Rapid Ligation Buffer	5 μl
T4 DNA Ligase	1 μl
Nuclease-free water	up to 10 μl

* Insert:Vector Molar Ratios = 1:1 - 3:1

3.10 Bioinformatics analysis

The sequences were compared with nucleotide and protein sequence in NCBI (<http://www.ncbi.nlm.nih.gov>) database using tblastx tool. Molecular mass and pI value was calculated by ExPASy Proteomic tools (http://web.expasy.org/compute_pi/). Protein localization and signal peptide were predicted by TargetP v1.1 (<http://www.cbs.dtu.dk/services/TargetP/>), SignalP v4.1 (<http://www.cbs.dtu.dk/services/SignalP/>), WoLF and PSORT

(http://www.genscript.com/psort/wolf_psort.html) and Protcomp 9.0 (<http://www.softberry.com/berry.phtml?topic=protcomppl>). The phylogenetic tree was carried out with MEGA6 program (Tamura, et al., 2013) based on the distance algorithmic neighbor-joining method. The transmembrane (TM) domains were predicted by TMHMM program (<http://www.cbs.dtu.dk>).

3.11 Alkaline lysis method for plasmid extraction (Sambrook, et al., 1989)

The overnight grown *E. coli* culture was collected by centrifugation at 12,000 rpm for 1 min. The obtained pellet was resuspended with 200 μ l of the alkaline lysis solution I (25 mM Tris-HCl pH 8, 10 mM EDTA pH 7 and 50 mM glucose). Adding 200 μ l of alkaline lysis solution II (0.2 N NaOH, 1 % SDS) for lysis cells and mixed by inversion and incubation for 2 min at room temperature. The mixture was renatured by adding 300 μ l solution III (3 M potassium acetate, 11.5 % glacial acetic acid) and remove a contaminate by centrifugation at 13,000 rpm for 5 min at 4 $^{\circ}$ C. The supernatant was obtained and mixed with isopropanol. After incubation for 30 min at -20 $^{\circ}$ C, the pellet was obtained by centrifugation at 13,000 rpm for 10 min at 4 $^{\circ}$ C and wash pellet with 70% ethanol (twice). After remove alcohol, the pellet was resuspended with 50 μ l nuclease-free water and keep at -20 $^{\circ}$ C.

3.12 PrestoTM Mini Plasmid Kit for plasmid extraction

The extraction plasmid for sequencing was done by PrestoTM Mini Plasmid Kit (GeneAid). After harvested the overnight grown *E. coli* cells, the pellet cells were resuspended with 200 μ l PD1 buffer. The cell mixture was lysis with 200 μ l PD2 buffer and neutralized in 300 μ l PD3 buffer. The cell lysate was transferred to PD column and centrifuged at 13,000 rpm for 30 sec. The plasmid was washed two times with 400 μ l W1 buffer and 600 μ l washing buffer, respectively. After dry by

centrifugation at 13,000 rpm for 2 min, plasmid was eluted with 30 – 45 μ l nuclease-free water.

3.13 Preparation of competent *E. coli* cells

Bacterial strain *E. coli* DH5 α was used as a host cells for all intermediate cloning constructs. Competent cells of *E. coli* were prepared modified from Nakata's protocol (Nakata, et al., 1997). *E. coli* from glycerol stock was streaked on LB agar plate and incubated at 37 $^{\circ}$ C for overnight. Single colony from the plate was transferred to 5 ml LB broth for overnight. The culture was subculture to grown at 37 $^{\circ}$ C with vigorous shaking (250 rpm) until OD₆₀₀ = 0.3 - 0.5. The culture was transferred to centrifuge tubes under sterile condition and incubated on ice for 30 min. The culture was centrifuged at 3,500 rpm at 4 $^{\circ}$ C for 10 min. The pellet was gently washed twice time with 20 ml and 10 ml of pre-chilled 100 mM CaCl₂ followed by centrifugation using same conditions. The new pellet was dissolved with 2 ml pre-chilled 100 mM CaCl₂ and 15 % glycerol with gentle swirling on ice for 30 min. Dissolved competent cells were aliquoted (100 μ l) into eppendorf tubes and incubated in ice for 5 min and then frozen in liquid nitrogen before storing at -80 $^{\circ}$ C.

3.14 Transformation by heat-shock

Transformation into *E. coli* were performed according to previous protocol (Sambrook, et al., 1989). The 100 μ l competent cells were thawed on ice and 2-5 μ l plasmid DNA (up to 100 ng) or 3 – 5 μ l ligation products was mixed gently and incubated on ice for 30 minutes. The cells were then incubated at 42 $^{\circ}$ C for 30 - 45 sec and placed on ice for 2 min. 500 μ l of LB broth were added and gently mixed by inverting the tube. The transformation was achieved by shaking (200 rpm) for 1 hour at 37 $^{\circ}$ C. Selection to appropriate antibiotic was conducted by spreading 100 μ l of

the transformed competent cells onto LB plate containing antibiotic. After overnight incubation at 37 °C, resistant colonies were observed on next day.

3.15 Construction of expression vector

3.15.1 pENTR[™]/D-TOPO[®] vector

The full-length genes from *A. lakoocha* and *C. ternatea* were amplified by *alrc2*-pENTR Fw: 5'-CACCATGGATTCTTTTCTTCTG-3', *alrc2*-pENTR Rv: 5'-TCACCTAACGAACGGTATAAG-3', *clt*-pENTR Fw: 5'-CACCATGGATTCCGGTGCTCTATGGATCT-3' and *clt*-pENTR Rv: 5'-TCATCTAACATAAGGGAGGAGCAG-3' (Fig12: I and II). The full-length gene was clone into pENTR[™]/D-TOPO[®] vector (Invitrogen, USA) by following the manufacturer's protocol (Figure 12: III and IV). The components of cloning reaction consist of 5 µg fresh PCR product, 1 µl salt solution, 1 µl pENTR/D-TOPO vector and water to final volume 6 µl. The reaction was incubated at room temperature for 5 minutes. The pENTR-*alrc2* and pENTR-*clt* plasmid (Entry clone) constructs were individually transformed into Oneshot[®] TOP10 competent cells. Successful cloning of genes was confirmed by PCR, restriction digestion and sequencing.

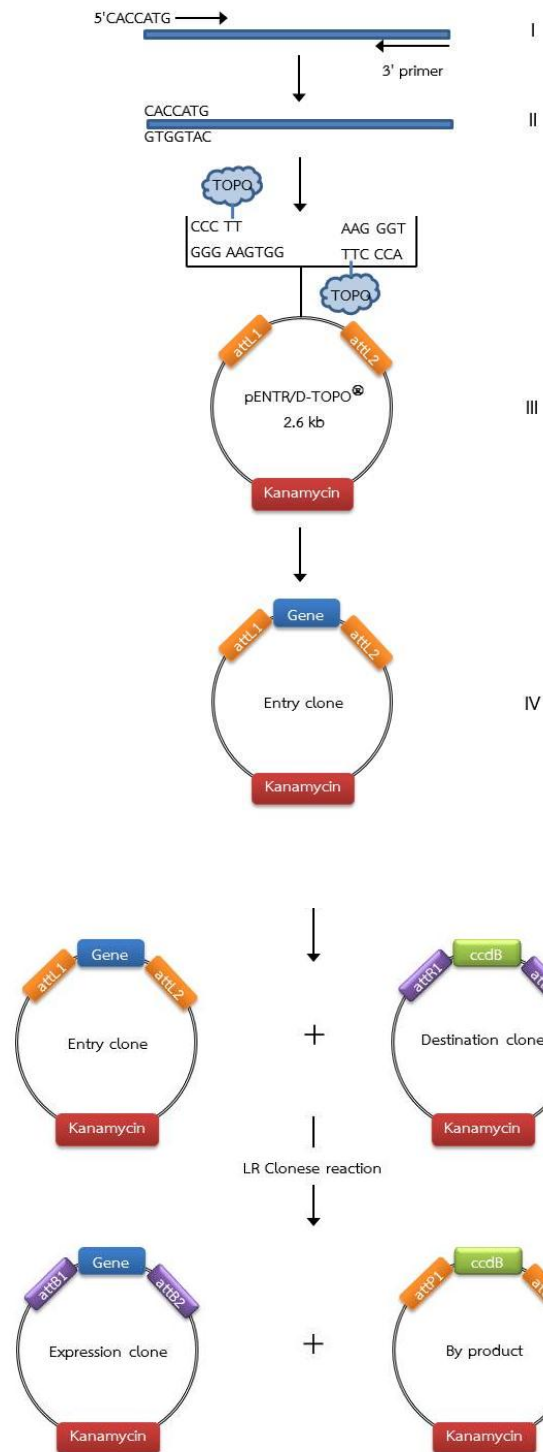


Figure 12 The strategies for construction of expression vector.

3.15.2 Binary vector

In order to construction of plant expression vector was be done by Gateway[®] Technology (Invitrogen, USA) following the manufacturer's protocol. The entry vector allowed recombining the desired sequences into the destination vector (pGWB6) by LR recombination events using Gateway[®] LR CLonase enzyme kit (Invitrogen, USA). The LR reactions were carried out by added 100 – 300 ng μl^{-1} entry clone with the gene of interest, 150 ng μl^{-1} destination vector, 2 μl 5X LR Clonase reaction buffer and TE buffer, pH8 to make volume to 8 μl . Start reaction by added 2 μl LR Clonase enzyme mix and mixed reaction mixture by vortex for 2 sec (two times). After incubated the reaction mixture at room temperature for 1 hour, one microliter of protease K was added into reaction and incubated at 37 °C for 10 min for stop enzyme activity. The ligation reaction was transformed into E. coli and checked correction by PCR.

3.16 Preparation of competent *Agrobacterium* cells

The preparation of competent cells were performed according to previous protocol (Lin, 1995). *A. tumefaciens* GV3101 cells were streaked on YEB agar plates containing antibiotics (25 $\mu\text{g ml}^{-1}$ Rifampicin) and incubated at 28 °C for 2 days. A single colony was inoculated in 10 ml of LB medium containing antibiotic and incubated at 28 °C for overnight with shaking (200 rpm). A fresh overnight culture was inoculated in 50 ml of LB medium containing antibiotic until OD_{600} is 0.6 was reached. The cells were chilled on ice for 15 min and spin down by centrifugation at 5,000 $\times g$ for 10 min at 4 °C. The culture medium was discarded and pellet was washed in 25 ml and 10 ml of cold water and followed by centrifugation in the same condition. The pellet was resuspended in 2 -5 ml of cold water containing 10 % (v/v)

glycerol. 50 μl aliquots of the suspension were dispensed into prechilled eppendorf tubes, frozen immediately in liquid nitrogen and stored at $-80\text{ }^{\circ}\text{C}$.

3.17 Transformation of *A. tumefaciens* by electroporation

The transformation of *A. tumefaciens* by electroporation was performed according to previous protocol (Lin, 1995). The 50 μl competent cells *A. tumefaciens* GV3101 were thawed on ice and mixed with 1-2 μl of DNA sample (10 – 50 ng). The mixture was transferred into pre-chilled electroporation cuvette and then placed the cuvette in the holder. The electroporation was performed at 2.5 kV, 200 Ω and 25 μF . Immediately 500 μl of SOC medium was added and whole mixture was transferred into new sterile eppendorf and incubated at $28\text{ }^{\circ}\text{C}$ for 2 hours. One hundred microliters of culture was spread on YEB agar containing $25\text{ }\mu\text{g ml}^{-1}$ rifampicin and $50\text{ }\mu\text{g ml}^{-1}$ kanamycin and incubated at $28\text{ }^{\circ}\text{C}$ for 2 days. Then successful cloning was check by colony PCR.

3.18 Agrobacterium infiltration into tomato leaves

The transient expression was performed modified previous described protocol (Mangano, et al., 2014). Overnight-grown Agrobacterium cultures in YEB medium ($50\text{ }\mu\text{g mL}^{-1}$ kanamycin and $25\text{ }\mu\text{g mL}^{-1}$ rifampicin) carrying expression vector an optical density (OD_{600}) of 1 were pelleted by centrifugation at 3000 $\times g$ for 5 min. The pellets were resuspended in induction solution (10 mM 2-N-morpholinoethanesulfonic acid (MES) pH 5.5, 10 mM MgCl_2 , and 200 μM acetosyringone). After 2 h incubations at room temperature with shaking at 50 rpm, Agrobacterium cultures carrying each expression vector were collected by centrifugation in the same condition. The pellets were washed with infiltration buffer (10 mM 2-N-morpholinoethanesulfonic acid (MES) pH 5.5 and 10 mM MgCl_2) two times and resuspended in

infiltration buffer until OD_{600} is 0.5. The mature leaves of 5–8 weeks old tomato plants (*Lycopersicon esculentum* Mill.) were co-infiltrated using a 5 mL syringe without a needle from underneath of the leaves. Harvested leaf materials at 1, 3, 6 and 9 day post agroinfiltration (dpa) and stored at -20°C until further use.

3.19 Gene expression analysis

3.19.1 RT-PCR

RNA was extracted from the infiltration tomato leaves (100 mg) at different dpi using RNeasy Plant Mini Kit (Qiagen). The first stand cDNA was synthesized by RevertAid™ H Minus Reverse Transcriptase (Thermo scientific) with 1 μg total RNA and 5 μg oligo dT. PCR was performed using specific primers ALR1_Fw: 5'-ATGGATTCTTTTCTTCTGGGTTTCATTGAAAGG-3', ALR250_Rv: 5'-GTCTTTTGTGGTCCATGGTAAAATGTAG-3', CT34_Fw: 5'-GCCTCTTCACTAACCACTGGTGCC-3' and CT494_Rv: 5'-TAAATATTCATAAACAGGGCAGCAACC-3' also using β -tubulin as a house keeping gene (TUB_Fw: 5'-TGAGCACCAAGGAAGTTGATGA-3' and TUB_Rv: 5'-CCATTCCTTACCTGTGTACCA-3'). The PCR reactions were conducted in final volume in 25 μl using 0.6 μl first stand cDNA, 1X One *Taq* standard reaction buffer, 0.2 mM dNTP mix, 0.2 μM each specific primers, 0.625 U One *Taq*[®] DNA polymerase (NEB) and water. Cycling conditions were following in Table 11.

Table 11 PCR thermal cycling condition of gene expression analysis.

Step	Temperature	Time	Number of cycles
Initial denaturation	94 °C	2 min	1
Denaturation	94 °C	30 sec	
Annealing	50 °C	40 sec	30
Extension	68 °C	40 sec	
Finale extention	68 °C	1 min	1

3.20 Extraction of recombinant protein from tomato leaves

The total proteins were obtained from modified previous described protocol (Liu, et al., 2007). Total proteins were prepared from 1 g of infiltration leaves. It was ground into powder with liquid nitrogen and resuspended in extraction buffer, pH 7.8 (50 mM Tris-HCl, pH 7.8, 150 mM NaCl, 1mM PMSF, 0.5 mM DTT, 0.5% TritonX-100 and 10% glycerol). After stirred at 4 °C for 30 min, the homogenize was centrifuged at 12,000 xg for 15 min (4 °C). The supernatant was collected and measured protein concentration using Bradford method.

3.21 Protein analysis

3.21.1 Sodium Dodecyl Sulfate Polyacrylamide Gel Electrophoresis (SDS-PAGE)

One hundred microgram of total proteins from infiltration leaves were mixed with 2X loading dye and boiled in boiling water for 5 min to denatured protein then cooled down protein on ices for 2 min. Twenty microliters of denatured protein were loaded into 10% polyacrylamide gel against PageRuler[™] plus pre-stained protein marker (Thermo Scientific[™]). The SDS-PAGE was running at 110 V for 1.20 hour.

3.21.2 Western blot

After separated protein on SDS-PAGE, proteins were transferred to PVDF membrane. The PVDF was soaked in methanol for 1 minute and equilibrated in transfer buffer, pH 8.3 (25 mM Tris-HCl, 190 mM Glycine and 20% methanol) for 10 min before transfer protein also gel was equilibrated in transfer buffer, pH 8.3 for 10 min. The proteins were transfer to PVDF membrane by electroblotting apparatus (BioRad) was assembled followed as Figure 13 and transferred at constant current of 100 V for 1.30 hour (4 °C). After transferred, the blot was rinsed in water and blocked with blocking buffer (5% skim milk in TBST buffer, pH 7.5) at room temperature for 1 hour with gentle agitates. Then blotted membrane was washed with TBST buffer, pH 7.5 (20 mM Tris-HCl, 150 mM NaCl and 0.1% Tween 20) for 5 min for tree times and incubated with 1:2000 in dilution buffer (1% skim milk in TBST buffer, pH 7.5) of anti-GFP antibody conjugated HRP (Thermo Scientific[™]) for 2 hours with gentle agitate. After washed with TBST buffer, pH 7.5 for 5 min for tree times, the blot was treated with chemiluminescent HRP substrate (Luminata[™] Crescendo, Merck) and captured the chemiluminescent signal by CCD camera (Gel Doc[™] XR, Bio-Rad)

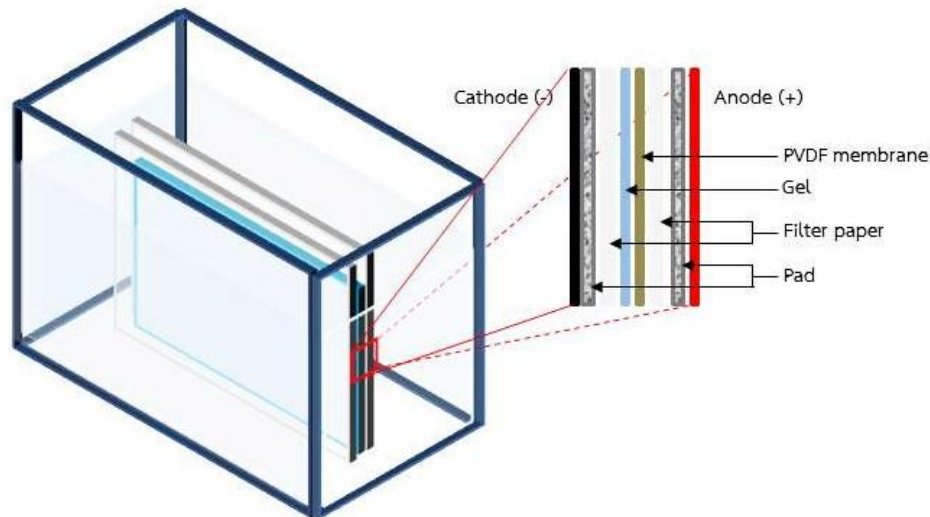


Figure 13 The alignment of western blot setup.

3.22 Tocopherol extraction

α -Tocopherol was extracted from agroinfiltration tomato leaves according to the protocol described previously (Wilmoth, 2002). One gram of leaves was grounded in liquid N_2 . Leaves powder was resuspended with 0.5 mM EDTA containing 20 mg ascorbic acid (pH 3.1) and mixed with vortex. After added 2 ml 100 mM SDS, the extract was incubated on ices for 6 min. And then 5 ml cooled-ethanol and 3 ml of hexane containing 0.2 % BHT (w/w) were added to an extracted. The extracted was mixed with vortex for 6 min and centrifuged for 3 min at 1,200 xg at 18 $^{\circ}C$. The upper organic phase was kept. After evaporated to dryness under N_2 gas, an extracted was redissolved in 300 μl hexane containing 0.2 % BHT (w/w).

3.23 Chlorophyll analysis

Chlorophylls content from transient tomato leaves were determined according to method validated previously (Lima, et al., 2014), based on the molar

coefficient of chlorophyll in acetone:hexane (4:6 v/v). The samples were measured total chlorophyll at 663 and 645 nm and converted to chlorophyll (mg/100 ml) following equations:

$$\text{Total chlorophylls} = \text{Chlorophyll a} + \text{Chlorophyll b}$$

$$\text{Chlorophyll a} = 0.999(A_{663\text{nm}}) - 0.0989(A_{645\text{nm}}) \quad (1)$$

$$\text{Chlorophyll b} = -0.328(A_{663\text{nm}}) + 1.77(A_{645\text{nm}}) \quad (2)$$

3.24 Tocopherol analysis

3.24.1 Thin Layer Chromatography (TLC)

The tocopherols were analyzed by TLC technique. Five microliters of each extracted and α -tocopherol standard was loaded on TLC plate using Limonat IV (CAMAG). After TLC plate was developed with chloroform/cyclohexane (11:9) (Pyka, et al., 2011), the tocopherol was detected by scanned at 292 nm with TLC scanner 3 (CAMAG). Visualization and documentation of TLC was done under 254 nm after derivatized by iodine vapor. For quantitative analysis α -tocopherol, the various concentration of α -tocopherol standard was prepared by dissolved in 95% ethanol and spotted on TLC in range 0.05 – 1 μg . The calibration curve was calculated using relationship between peak area (AU) and concentration of α -tocopherol standard.

3.24.2 Gas Chromatography-Mass Spectrophotometer (GC-MS)

Eighty microliters of leaves extracted were evaporated in nitrogen gas stream and resuspended with 40 μl pyridine. Then the extracted was derivatized by silylation (Kobayashi and DellaPenna, 2008), added 100 μl BSTFA + 1% TMCS (Fluka) and incubated at 50 $^{\circ}\text{C}$ for 45 min. GC-MS was performed on an Agilent 7890B GC system with Agilent 7000C GC/MS Triple Quad mass detector using an HP5 column

(30 m x 0.25 mm, 0.25 μm) and the oven temperature was programmed from initial 150 $^{\circ}\text{C}$ for 1 min to 260 $^{\circ}\text{C}$ at a rate of 25 $^{\circ}\text{C min}^{-1}$ and up to 300 $^{\circ}\text{C}$ (20 min hold) at a rate of 5 $^{\circ}\text{C min}^{-1}$. Flow rate was 1.2 ml min^{-1} . The injection volume was 0.5 μl , split ratio 10:1 with MS detection in electron ionization mode at 70 eV. Full-scan spectra were recorded over a mass range of 33–650.



CHAPTER IV

Results

4.1 Total RNA extraction

Young leaves of *C. ternatea* L. and calli of *A. lakoocha* Rox. were used for RNA sources. Total RNAs were extracted by RNeasy Plant Mini Kit (Qiagen). The quality and concentration of all total RNA samples were determined on agarose gel as shown in Figure 14, and UV absorption at wavelength of 260 nm, respectively. The concentration of the total RNA was 320 and 225 $\mu\text{g ml}^{-1}$ from *C. ternatea* L. and *A. lakoocha* Rox., respectively.

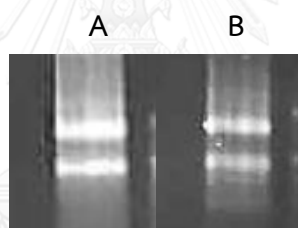


Figure 14 Agarose gel of the total RNA isolated from *C. ternatea* L. (A) and *A. lakoocha* Rox (B).

4.2 Isolation of core sequences from degenerate primers

Partial gene sequences were performed by PCR technique using the cDNA synthesized from RT-PCR as a template with multiple pairs of the degenerate primers. The results are showed in Figure 15. The pairs of degenerate primers F2R1, F2R3, F6R1 and F6R3 were able to amplify partial gene sequences from cDNA of *C.*

ternatea while the partial gene sequences from *A. lakoocha* were amplified by F2R1, F3R1 and F6R1.

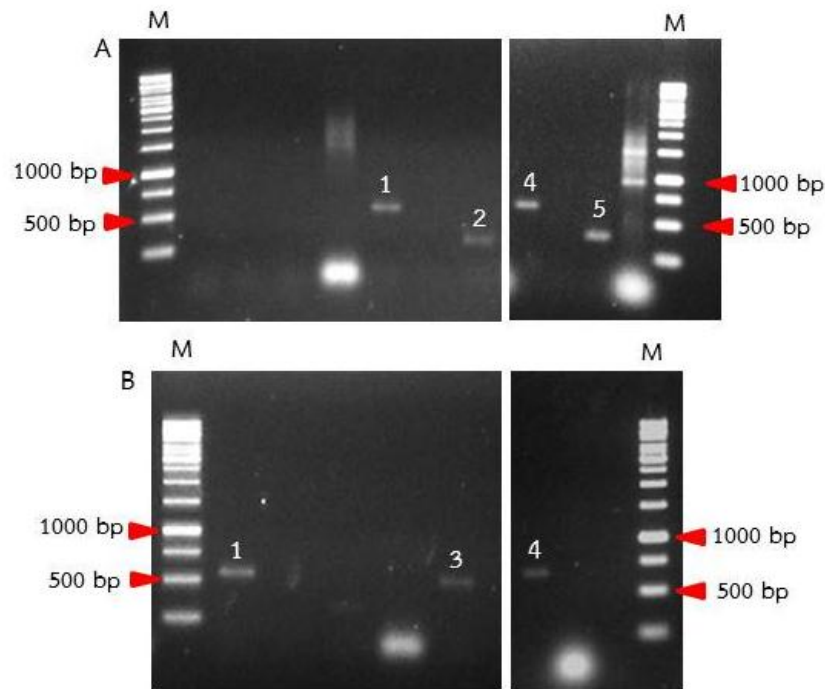


Figure 15 Agarose gel of the partial gene sequences from *C. ternatea* L. (A) and *A. lakoocha* Rox (B) amplified by multiple pairs of the degenerate primers. M: 1 kb DNA marker, Band number 1, 2, 3, 4, and 5 represented the partial gene sequences from sets of primers including F2R1 (544 bp), F2R3 (283 bp), F3R1 (479 bp), F6R1 (640 bp), and F6R3 (414 bp), respectively.

4.3 Full length genes from RACE PCR

Based on partial gene sequences of *C. ternatea* obtained from F6R1 primer pair, the new set of primers were designed overlapping the region between upstream and downstream of 5'-end (CTin_R, CTout_R, ALRin_R and ALRout_R) and 3'-end (RACEin_F and RACEout_F). The contig of 5'-RACE PCR was obtained from *C. ternatea* (1000 bp) and *A. lakoocha* (500 bp). In 3'-RACE PCR, the contig was obtained from *C.*

ternatea (700 bp) and *A. lakoocha* (900 bp) as showed in Figure 16. Then all contigs from both ends were aligned with the isolated partial gene sequence and the putative full-length cDNAs were recovered. The open reading frame (ORF) was determined from the start codon of ATG to the stop codon of TAA by ClonManager 9.0. To retrieve the full coding sequence cDNAs, the primers covering the whole coding sequence were designed from start and stop codons and amplified by PCR.

The full length cDNA of *ctl* gene, 1,495 bp, contained 122 bp at 5' untranslated region and 149 bp of 3' untranslated region with a poly (A) tail. The *ctl* showed open reading frame (ORF) of 1,224 bp (Figure 17A) encoding a putative polypeptide of 407 amino acids residues (Figure 18). For *alrc2* gene sequence retrieved by RACE, the 1,625 bp full length cDNA of *alrc2* gene was obtained and it contained 134 bp and 210 bp of 5' untranslated region and 3' untranslated region with a poly A tail, respectively. The *alrc2* showed open reading frame of 1,233 bp (Figure 17B) encoding a putative polypeptide of 410 amino acids residues (Figure 19).

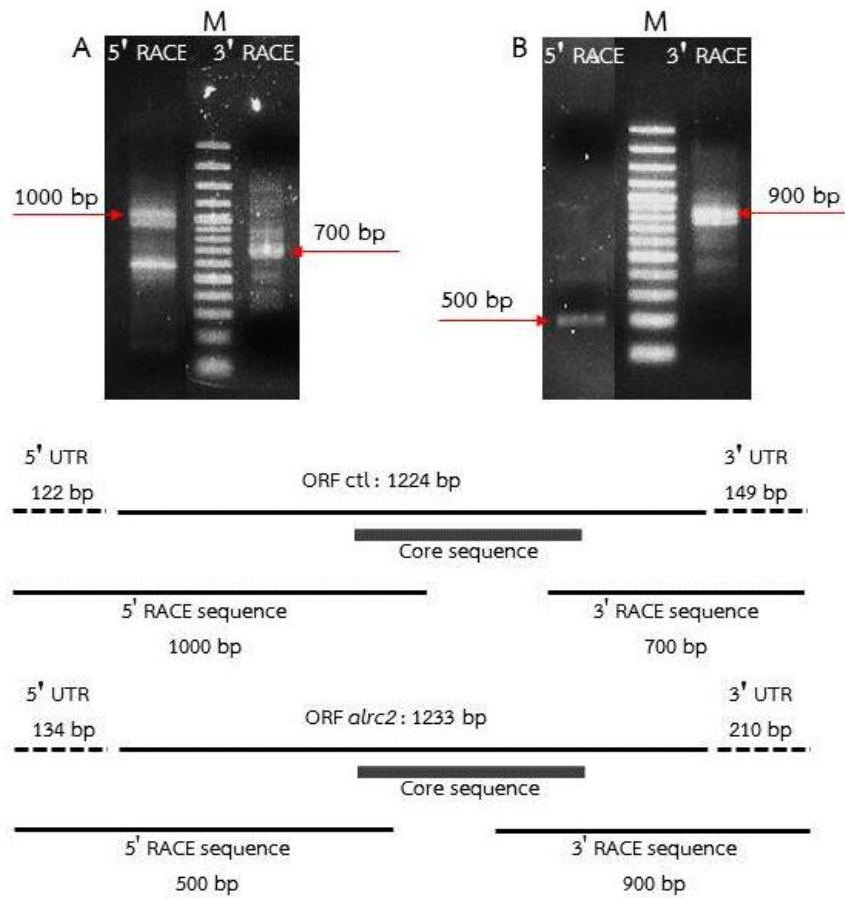


Figure 16 Isolation of full length cDNA of *ctl* and *alrc2* by RACE PCR. The nested RACE-PCR products (5' and 3' fragments) from *C. ternatea* (A) and *A. lakoocha* (B) are shown on 1% agarose gel, M: 1 kb DNA marker. The contigs from RACE-PCR products and core sequences were aligned to obtain the full-length sequence of *ctl* and *alrc2* (C).

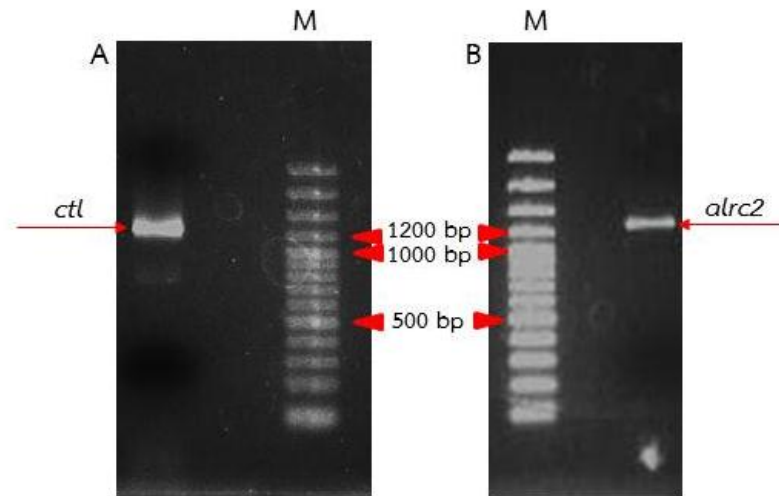
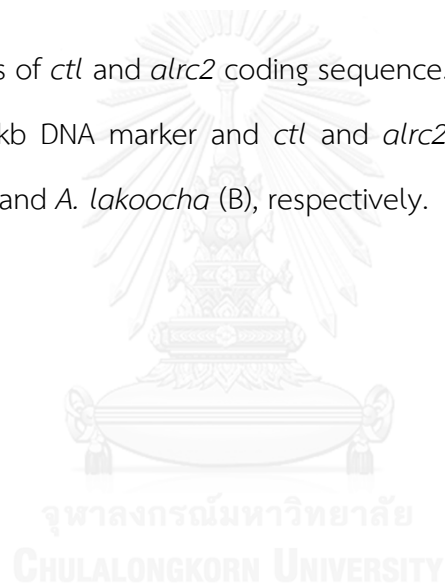


Figure 17 Agarose gels of *ctl* and *alrc2* coding sequence. The bands are shown on 1% agarose gel, M: 100 kb DNA marker and *ctl* and *alrc2* coding sequences amplified from *C. ternatea* (A) and *A. lakoocha* (B), respectively.



```

1 GACAGTGTGG TTCTCAAATA TCTGTGTTTC AGTGAATCGG CGGCGGAGGC GAGGCGGAAG GTTTAGGGAA AGAAAGAGTG
81 ATGTGTTGTTG TGAGCTTTTG AGTAGCAGTT TACAGTAGTC ACATGGATTG GGTGCTCTAT GGATCTTTGC CTAAGGCCTC
>>.....CTL.....>
1 M D S V L Y G S L P K A
161 TTCACTAACC ACTGGTGCCA ATTTCTGGAC TACTAAATGT CGTGCCACACA ATTACCATGC AAGCTCTTAT GCACCAAAAAG
>.....CTL.....>
13 S S L T T G A N F W T T K C R A H N Y H A S S Y A P K
241 CCICATGGCA CAAATGGAAG TTCCATAAAG AATACAGTGT TTTAAGGTTT AGACAATCAA GCTTGAGCCA ICATTACAAA
>.....CTL.....>
40 A S W H K W K F H K E Y S V L R F R Q S S L S H H Y K
321 GGCATTGGCG GAGGGTCTAC ACATCAAGAA AGTAACAGGA GATAIGTTGT GAAAGCGGCC ICTGGACAAT CTTTITGAATC
>.....CTL.....>
67 G I G G G S T H Q E S N R R Y V V K A A S G Q S F E
401 TGAACCCCAA GCTTTTGATC AGAAAAGCAT TTTGGACTCT GTCAAAAATT CCTTGGATGC TTTCTACAGG TTTCTAGGC
>.....CTL.....>
93 S E P Q A F D Q K S I L D S V K N S L D A F Y R F S R
481 CACACACAGT TATTGGCACA GCATTAAGCA TAATTTCTGT ATCTCTCCTT GCATTGGAGA AATTATCTGA TATATCTCCA
>.....CTL.....>
120 P H T V I G T A L S I I S V S L L A L E K L S D I S P
561 ATGTTTTTTA CTGGTGTGTT GGAGGCTGTG GTTGCTGCCC TGTTTATGAA TATTTATATT GTTGGTTTGA ATCAATTATC
>.....CTL.....>
147 M F F T G V L E A V V A A L F M N I Y I V G L N Q L
641 TGATGTTGAA ATAGACAAGA TAAACAAGCC ATATCTTCCA CTGGCATCCG GAGAATACTC CTTTGGAACT GGTGTTACTA
>.....CTL.....>
173 S D V E I D K I N K P Y L P L A S G E Y S F G T G V T
721 TTGTTGCATC ATTTTCAGTT CTGAGTTTTT GGCTTTGCTG GATTGTAGGT ICATGGCCAT IGTTTTGGGC ICITTTTGTC
>.....CTL.....>
200 I V A S F S V L S F W L C W I V G S W P L F W A L F V
801 AGTTTTTGTC TAGGGACTGC TTATTCAATC AATGTGCCCC TTTAAGATG GAAGAGGTTT GCAGTGCTTG CAGCAATGTG
>.....CTL.....>
227 S F V L G T A Y S I N V P L L R W K R F A V L A A M
881 CAITCTAGCT GTTCGTGCGA TAATAGTTCA ACTTGCATTT TTCTGCACA TGCAGACCCA TGTGTACAAG AGGCCAGCTG
>.....CTL.....>
253 C I L A V R A V I V Q L A F F L H M Q T H V Y K R P A
961 TCTTCTCAAG ACCTCTGATT TTTGCTACTG CAITCATGAG CTCTTCTCT GTAGTTATAG CAITGTCAA GGATATACCT
>.....CTL.....>
280 V F S R P L I F A T A F M S F F S V V I A L F K D I P
1041 GACATTGAAG GGGATAAAAT ATTTGGCATC CAATCCTTTT CAGTACGTTT AGGTCAGAAG CGGGTATTCT GGATCTGTGT
>.....CTL.....>
307 D I E G D K I F G I Q S F S V R L G Q K R V F W I C
1121 TTCCCTTCTT GAAATAGCTT ATGGAGTCGC CCICATGGTG GGAGCAGCAT CTCCTGTCT CTGGAGTAAA GCTATCACGG
>.....CTL.....>
333 V S L L E I A Y G V A L M V G A A S P C L W S K A I T
1201 GTGCGGGACA TGCTGTTCTG GCTTCACTTC TCIGGIATCA GGCCAAATCT GTAGATTTGA ATACCAAAGC TTCGATAACA
>.....CTL.....>
360 G A G H A V L A S L L W Y Q A K S V D L N T K A S I T
1281 TCGTCTACA TGTTTATCTG GAAGCTAATT TACGCAGAAT ACCTGCTCCT CCCTTATGTT AGATGAGGAT GCAGGGGCTT
>.....CTL.....>
387 S F Y M F I W K L F Y A E Y L L L P Y V R -
1361 TGTTGACTTT AGATATACTT GTGTCCAAA GGATGCTGCC TGTCACAGGC CGGGCCTGGT GTCTGCACAA GTTTTAAGTT
1441 TTTCACAGCA ATGTAAATG AAGAATTACT TTTGGGATTA AAAAAAAAAA AAAAA

```

Figure 18 The full length cDNA of *ctl* gene and its translated protein. The translated amino acids were decoded from ORF of *ctl* and indicated below their corresponding nucleotide codon.

```

1 AAAACCCCR A AACAGAAGT ATATTGAGAA ACCAGTCTCG CTCCTTTTGC AAGTACAAGA GTGGGCAAGA GTGTGAATT
81 TCCCTTTTGC TTTTTTTTT TTTTTTCTT TTTGCTGTT CTAATACATT GCCAATGGAT TCTTTTCTC TGGGTTCATT
>>.....ALRC2.....>
M D S F L L G S
161 GAAAGGTCCT TCCTACTAG CAAATGGAGT GAATCAITGG AAGAGGACA ATCTCAAGA GGTTCGCTTI TCAGGTTCAI
>.....ALRC2.....>
L K G P S L L A N G V N H W K K D N L K K V R F S G S
241 ATGTATCACA TAGTCCTCG AGCTTCAGTG AGTGGAACTG CATAGAAAGA CGATGCATG CTAGGTTTCA ACATGCTCTT
>.....ALRC2.....>
Y V S H S P S S F S E W N V I E R R C T A R F Q H A L
321 CCAAAGCATT GCACGAAGGG TACTAGAGAA GCTTCTACAT TTTACCAATG ACAAACAAA AGACTCTGG TAAATGCCAC
>.....ALRC2.....>
P K H C T K G T R E A S I F Y H G Q N K R L L V N A
401 TGTGGACAC CCGCTCGAGT CGGAACCTGG AGCCACTAGT TCAAAAATG CTTGGAACTC TACTAAAGGI GOCCTAGGTG
>.....ALRC2.....>
T A G H P L E S E P G A T S S K N A W N S T K G A L G
481 TTTTTACAG GTTTTCTGG CCACACACAG TCAATGGAC AGCAATGAGC ATAGTCTCAG TTTCCCTCCT TGCAGTACAG
>.....ALRC2.....>
V F Y R F S R P H T V I G T A L S I V S V S L L A V Q
561 AGACTTTCAG ATATTTCTCC ATATTTTTC ACTGGGGTGC TGGAGGCTGT GGTTCGTGCC CTCTTAIGA ATATATATAI
>.....ALRC2.....>
R L S D I S P L F F T G V L E A V V A A L F M N I Y
641 TGTGGTITG AATCAATGT ATGACATGA TATAGACAAG GTTACAAGC CATCTCTTCC ATTGGCTTCA GGGGAATATT
>.....ALRC2.....>
I V G L N Q L Y D I D I D K V N R P S L P L A S G E Y
721 CCGTTTCAAC TGGCACCTTG ATTGTACAI CTTTGGCTGT TGTAGCTTT TGCCTCTCAI GGATGGITGG TTCATGGCCC
>.....ALRC2.....>
S V S T G T L I V T S F A V L S F C L S W I V G S W P
801 TTGTTTTGGG CGCTCTTCAI AAGTTTCTGA CTTGAAGCTG CTAATCAAT CAATATGCCO CTTTTAGAI GGAAGAGATT
>.....ALRC2.....>
L F W A L F I S F V L G T A Y S I N M P L L R W K R
881 TGTGTAGTT GCTGCGATGT GCACTCTTGC GGTCCGTGCA GIGATTGTC AACTAGCATI TTTCTGCAC ATGCAGACCC
>.....ALRC2.....>
F A V V A A M C I L A V R A V I V Q L A F F L H M Q T
961 ATGTATCAA AAGACCTGCC ATCTTCTCAA GGCCCTGAT TTATGCTACT GCAITTAIGA GCTTCTTCTC AGITGITAIT
>.....ALRC2.....>
H V Y K R P A I F S R P L I Y A T A F M S F F S V V I
1041 GCATTTTITA AGGATATACC TGATATCGAC GGAGATAGGA TATATGGIAT TCGAICTTTI ACAGTGGGTI TAGGTCAAAA
>.....ALRC2.....>
A L F K D I P D I D G D R I Y S I R S F I V R L G Q
1121 GAAGTIATC TGGATCTGCA TTTCACTTCT TGAATGGCT TATAGCGTTC CTCITTTAGI GGGGGCTCA TCTGGTICT
>.....ALRC2.....>
K K V F W I C I S L L E M A Y S V A L L V G A S S G F
1201 TATGGAGCAA AGTTGCTAG GTTTTGGAC ACACAATCIT GCTTTCATTA CTTTGGGGTC GTGCCAAGTC CGTTGATTG
>.....ALRC2.....>
L W S R V A T V L G H T I L A S L L W G R A K S V D L
1281 TCCAGCAAAG CTGCAATAAC ATCCTTTTAC ATGTTTATAT GGAAGCTCTT TTATGCCGAG TATCTACTTA TACCCTCGT
>.....ALRC2.....>
S S K A A I T S F Y M F I W K L F Y A E Y L L I P L
1361 TAGGTGAAAG AATAGAGAC AGAATGTTGT ATAAAGGGTA TTTATAGGIT TGAGTTTATI TGACGGATAA TCTAAGAAGG
>.....>> ALRC2
V R -
1441 GATAGAAAAA GTTTATTTGG GAAGTGATTI AGTGTGGAT GTTCAAAGTA GGGATTTAAG TTCATTTGGG AAGTGCAAAA
1521 TGTATCGTAT TGCCAAAGTC CTGAAAATGT GCTAATGTTG TACGTAAGAA GCAGCCITGC TAAATGAGGA GTTGAAGAAC
1601 TAATTTGGGA AAAAAAAAAA AAAAA

```

Figure 19 The full length cDNA of *alrc2* gene and its translated protein. The translated amino acids were decoded from ORF of *alrc2* and indicated below their corresponding nucleotide codon.

4.4 Cloning of full length genes

The full length genes obtained from RACE-PCR were cloned into pGem-T easy vector and subjected to sequence verification. To confirm the insertion to the vector, the pGem-T vectors carrying the genes were cut by *EcoRI* restriction enzyme. After enzyme digestion, the band of full length *ctl* and *alrc2* genes along with the bands of pGemT easy backbone at 3 kb were clearly seen on the agarose gel (Figure 20). The full length gene sequences were confirmed by sequencing.

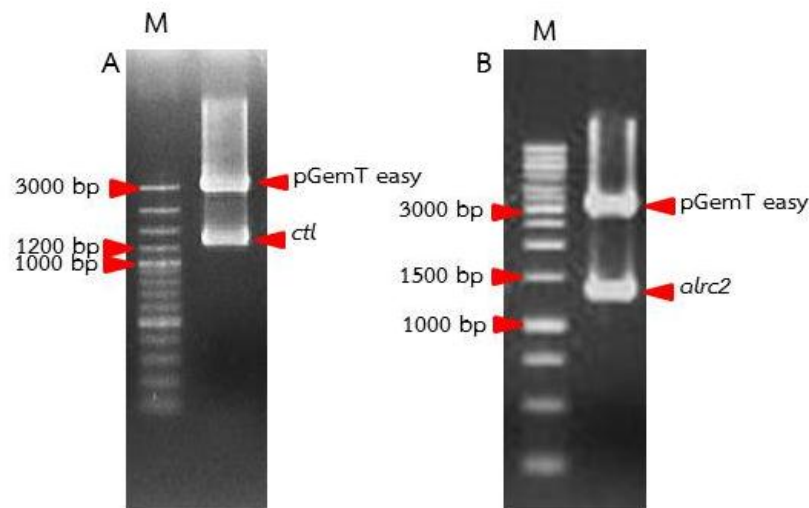


Figure 20 Verification of gene insertion to pGemT vector by restriction enzyme digestion are shown on 1% agarose gel against 1 kb DNA marker (M). The *EcoRI* restriction enzyme was used to digest recombinant pGem-T easy vector of *ctl* (A) and *alrc2* (B).

4.5 *In silico* protein identification and characterization

All deduced proteins from ORF of *ctl* and *alrc2* were predicted for their functional domain group by PSI-blast search (<http://www.ebi.ac.uk/Tools/sss/psiblast/>) against the UniProtKB/Swiss-Prot database.

The deduced proteins showed their significant E-value with UbiA prenyltransferase family of homogentisate prenyltransferase (Figure 21). Then the sequences were predicted for their molecular weights and theoretical pI values by the Compute pI/Mw Tool from ExPASy (http://web.expasy.org/compute_pi/). The predicted sizes were 45.58 and 45.59 kDa and pI values were 9.53 and 9.87 of CTL and ALRC2, respectively (Table 12). The results indicated that *ctl* and *alrc2* are in the group of UbiA prenyltransferase gene family and possibly encoded putative proteins functioning as homogentisate prenyltransferase.

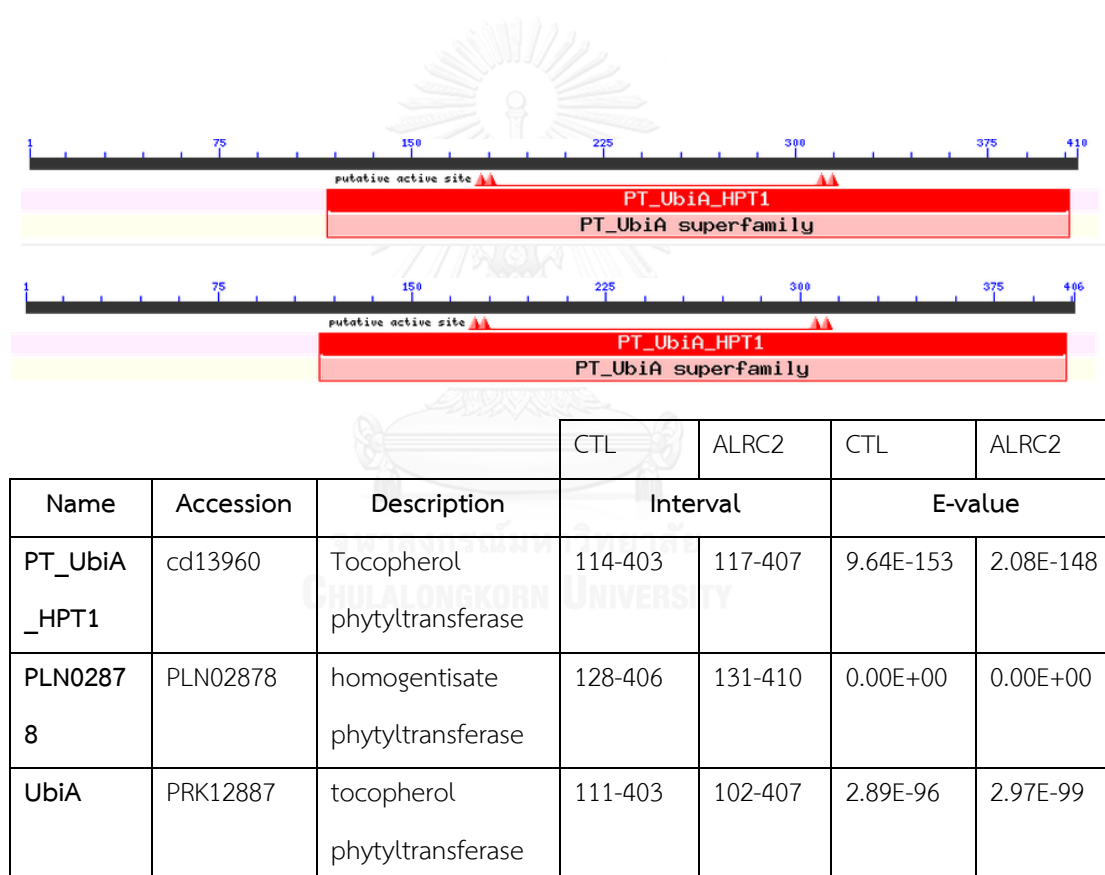


Figure 21 PSI-blast search of the putative proteins CTL and ALRC2.

Table 12 Summary of computed pI and MW of the deduced proteins.

	ORF (bp)	Amino acid (residues)	pI	MW (kDa)
<i>alrc2</i>	1233	410	9.87	45.59
<i>ctl</i>	1224	407	9.53	45.58

The transmembrane (TM) domains of CTL and ALRC2 were predicted by TMHMM program (<http://www.cbs.dtu.dk>). These genes contained nine putative TM domains (Table 13 and Figure 22) and possessed a conserved prenyltransferase motif (NQXXDXXXD) and an aspartate rich motif (KD(I/L)XDX(E/D)GD) between TM domain 2 and 3 and TM domain 6 and 7, respectively (Figure 23). Subcellular localization of all amino acid sequences were predicted on their N-terminal peptide by TargetP 1.1. The result showed that this program was failed to assign the organelle localization with low reliable prediction (RC=5) as showed in Table 14. Therefore, the proteins were predicted localization and signal peptide position by other programs e.g. SignalP 4.1 (<http://www.cbs.dtu.dk/services/SignalP/>), WoLF PSORT (http://www.genscript.com/psort/wolf_psort.html) and Protcomp 9.0 (<http://www.softberry.com/berry.phtml?topic=protcomppl>). Using the SignalP, it was found that the amino acid sequences showed low signal peptide (S- score ≤ 0.2) as shown in Figure 24 while CTL and ALR were chloroplast protein containing transit peptide 15 and 17 amino acid residues when prediction by WoLF PSORT and Protcomp (Table 15).

Table 13 List of transmembrane domains of ALRC2 and CTL.

	ALRC2	CTL
Transmembrane alpha helix regions		
TM1	VIGTALSIVSVSLLAVQRL	VIGTALSIVSVSLLALEKL
TM2	FFTGVLEAVVAALFMNIYIVG	FFTGVLEAVVAALFMNIYIVG
TM3	GEYSVSTGTLIVTSFAVLSFCLS	GEYSFGTGVTIVASFVLSFWLC
TM4	SWPLFWALFISFVLGTAYSINMP	SWPLFWALFVSVFVLGTAYSINV
TM5	VAAMCILAVRAVIVQLAFFLHMQ	LAAMCILAVRAVIVQLAFFLHMQ
TM6	RPAIFSRPLIFATAFMSFFSVIALF	RPLIFATAFMSFFSVIALF
TM7	ICISLLEMAYSVALLVGASS	ICVSLLEIAYGVALMVGAAAS
TM8	KVATVLGHTILASLLWGRAKSV	KAITGAGHAVLASLLWYQAKSV
TM9	SFYMFIWKLFYAEYLLIPFVR	SFYMFIWKLFYAEYLLLPYVR

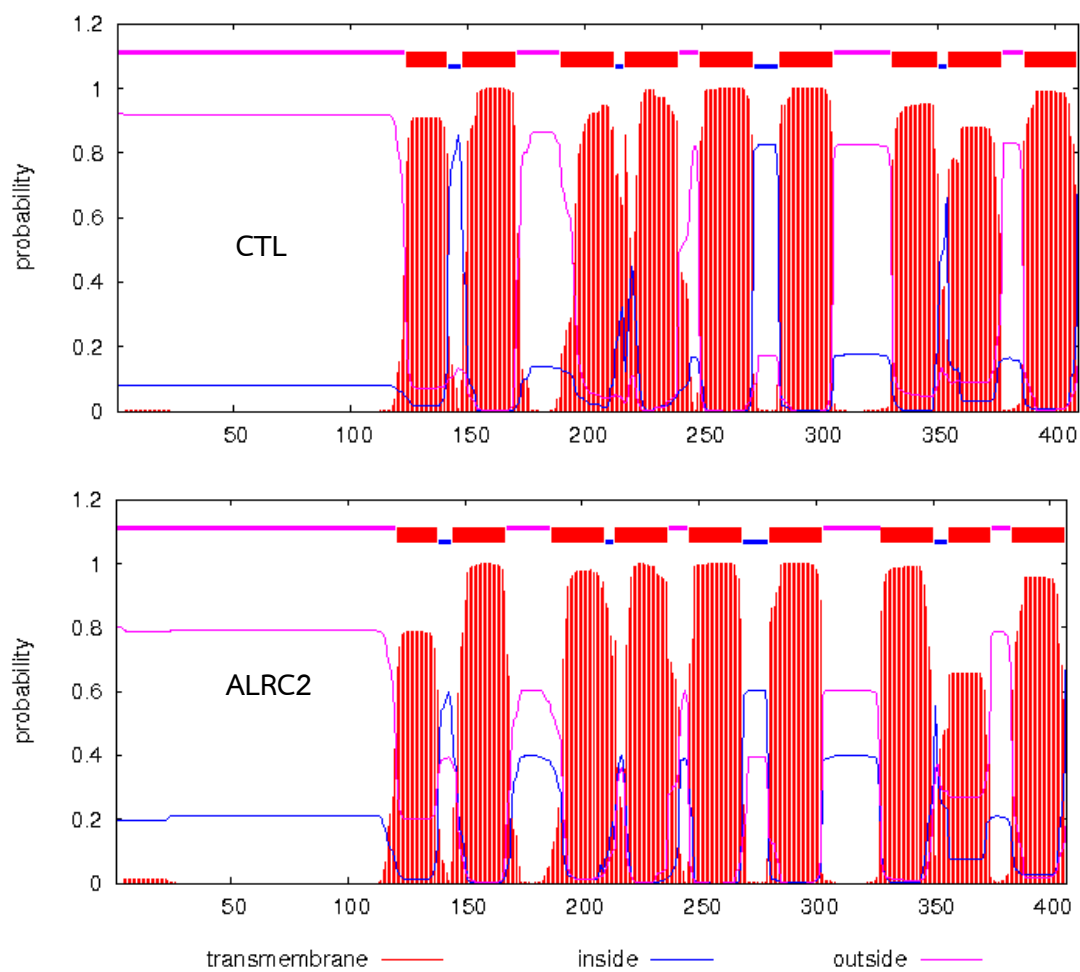


Figure 22 TMHMM analysis of ALRC2 and CTL protein sequences. The colors showed the probabilities for transmembrane regions (red), inside region of an organelle (blue) and outside of an organelle (pink).

Table 14 Sequence data analysis by TargetP.

Name	Len	cTP	mTP	SP	other	Loc	RC
ALRC2	410	0.422	0.073	0.030	0.460	*	5
CTL	407	0.074	0.444	0.023	0.626	*	5

Table 15 Sequence data analysis by WoLF PSORT and Protcomp.

	Amino acid sequence	Similarity in location DB	Extracellula r score	Intigral score	chloroplast transit peptide
CTL	407	chloroplast	0.9	9.3	15
ALRC2	410	chloroplast	0.9	9.5	17



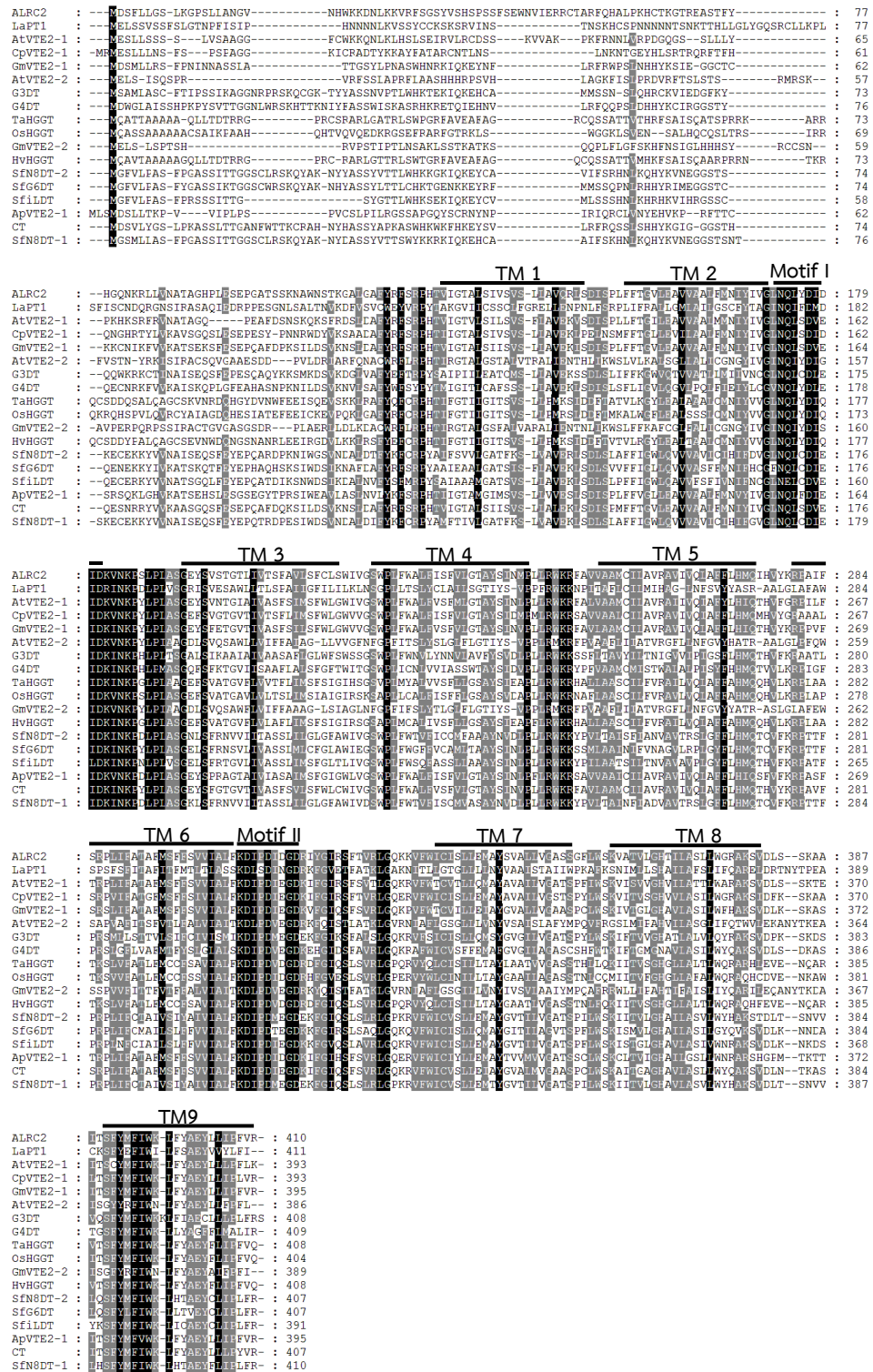


Figure 23 Multiple alignment of prenyltransferases family in plants. Motif I (NQxxDxxxD) and Motif II (KD(I/L)xDx(E/D)GD) indicated with black arrows are

conserved amino acid sequences among prenyltransferases and transmembrane domain (TM) are indicated with black lines.

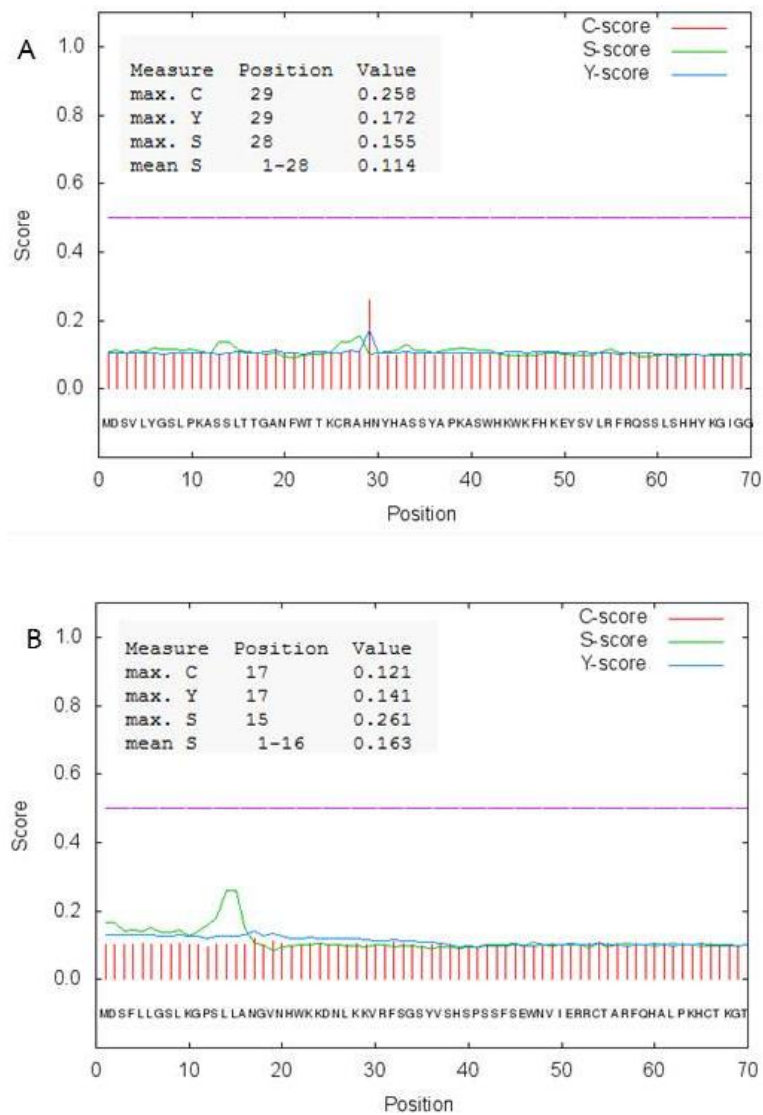


Figure 24 The graphical image of transmembrane prediction by SignalP, C-, S-, and Y-score cleavage site were predicted to be at position of maximal Y score (A) CTL and (B) ALRC2. C-score: raw signal peptide cleavage sites, S-score: positions within signal peptides from positions in the mature part of the proteins and Y-score: combined cleavage site score (C and S).

4.6 Phylogenetic analysis

Amino acid sequences of CTL and ALRC2 from candidate genes were compared to their homologs by using BLASTX algorithm in the NCBI database. The CTL and ALRC2 showed high sequence homology to homogentisate phytyltransferase of *Glycine max* and *Morus notabilis* with 84% and 88%, respectively. The phylogenetic tree of prenyltransferase families was constructed including homogentisate phytyltransferase (HPT), flavonoid prenyltransferase (flavonoid PTase), homogentisate geranylgeranyltransferase (HGGT), and homogentisate solanesyl transferase (HST) and shown in Figure 25. The analysis revealed that the proteins CTL and ALRC2 are closely related to the group of HPTs. The CTL and ALRC2 were highly similar to VTE2-1 involved in vitamin E biosynthesis in plants. Further sequence examination, the conserved aspartate rich regions (motif I and motif II) of various prenyltransferases were compared (Figure 26). In motif I, the CTL showed high similarity with the HPT of *G. max* (GmVTE2-1) and *Arabidopsis thaliana* (AtVTE2-1) while the ALRC2 were closest to the HPT of *Cuphea avigera* var. *pulcherrima* (CpVTE2-1) and *M. notabilis* (MnVTE2-1). In motif II, the CTL showed similarity with a group of HPTs of AtVTE2-1, GmVTE2-1, CpVTE2-1, *Triticum aestivum* (TaVTE2-1), and flavonoid prenyltransferase of *Sophora flavescens* (SfiLDT). The ALRC2 showed similarity with a group of HPTs of *Allium ampeloprasum* (ApVTE2-1), MdVTE2-1 and homogentisate geranylgeranyltransferase of *Oryza sativa Japonica* (OsHGGT). These results suggested that CTL and ALRC2 were likely to be HPT/VTE2 enzymes.

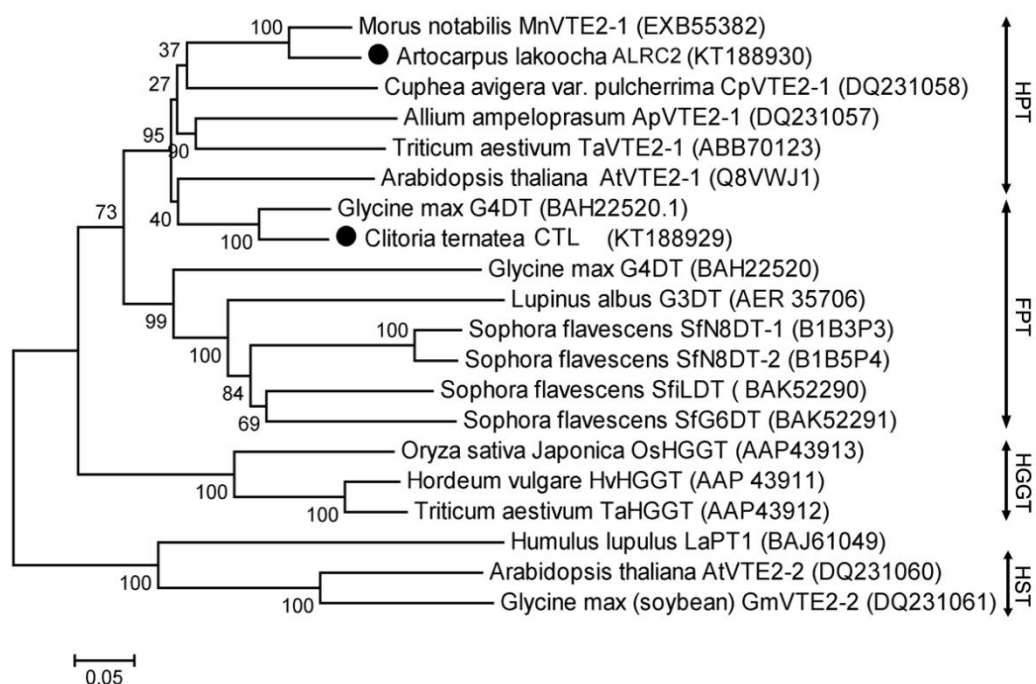
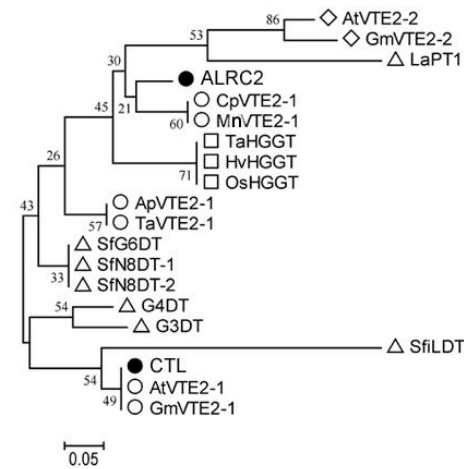


Figure 25 The phylogenetic tree of putative protein sequences of CTL and ALRC2 and related prenyltransferase proteins in plants. Protein sequences from various plant species were retrieved from NCBI database and their accession numbers were shown in parenthesis. The neighbor-joining was drawn using MEGA4. The optimal tree with the sum of branch length = 5.75502538 was shown. Bootstrap values 1000 replicate are shown, and the branch lengths represented relative genetic distances. The evolutionary distances were measured by JTT matrix-base method. The abbreviations were following: FPT, Flavonoid prenyltransferase; HPT, homogentisate phytyltransferase; prenyltransferase and HGGT, homogentisate geranylgeranyltransferase.

Motif I

AtVTE2-2 : NQLYDIDGID
 GmVTE2-2 : NQLYDISID
 LaPT1 : NQLIDMDID
 ALRC2 : NQLYDIDID
 CpVTE2-1 : NQLSDIDID
 MnVTE2-1 : NQLSDIDID
 TaHGGT : NQLYDIDGID
 HvHGGT : NQLYDIDGID
 OsHGGT : NQLYDIDGID
 ApVTE2-1 : NQLSDIEID
 TaVTE2-1 : NQLSDIEID
 SfG6DT : NQLSDIEID
 SfN8DT-1 : NQLSDIEID
 SfN8DT-2 : NQLSDIEID
 G4DT : NQLYDIEID
 G3DT : NQLSDIEID
 SfiLDT : NELSDVEID
 CTL : NQLSDVEID
 AtVTE2-1 : NQLSDVEID
 GmVTE2-1 : NQLSDVEID



Motif II

GmVTE2-2 : KDLPDVEGD
 AtVTE2-2 : KDLPDVEGD
 ApVTE2-1 : KDIPDIEGD
 MnVTE2-1 : KDIPDIEGD
 OsHGGT : KDIPDIEGD
 ALRC2 : KDIPDIEGD
 HvHGGT : KDIPDIEGD
 TaHGGT : KDIPDIEGD
 SfG6DT : KDIPDIEGD
 G3DT : KDIPDIEGD
 SfN8DT-1 : KDIPDIEGD
 SfN8DT-2 : KDIPDIEGD
 CpVTE2-1 : KDIPDIEGD
 SfiLDT : KDIPDIEGD
 CTL : KDIPDIEGD
 TaVTE2-1 : KDIPDIEGD
 AtVTE2-1 : KDIPDIEGD
 GmVTE2-1 : KDIPDIEGD
 G4DT : KDIPDIEGD
 LaPT1 : KDLSIDIEGD

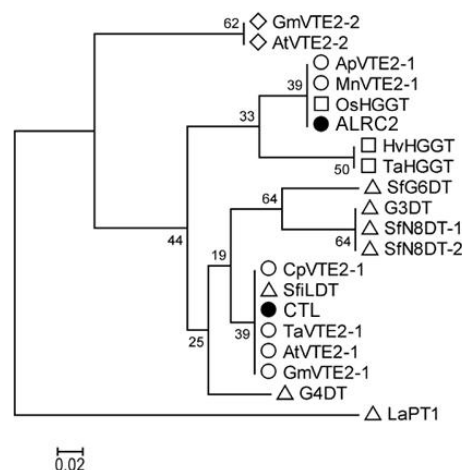


Figure 26 Phylogenetic trees for conserved amino acid sequences (the aspartate rich regions) of prenyltransferase family. The alignment of motif I (A) and motif II (B) from prenyltransferase family. Trees were generated by MEGA6 with neighbor-joining method. The available protein sequences from VTE, GDT, HGGT, and PT groups were retrieved from various species including *Arabidopsis thaliana* (At), *Allium ampeloprasum* (Ap), *Cuphea avigera* var. *pulcherrima* (Cp), *Glycine max* (Gm), *Hordeum vulgare* (Hv), *Humulus lupulus* (La), *Morus notabilis* (Mn), *Oryza sativa Japonica* (Os), *Triticum aestivum* (Ta) and *Sophora flavescens* (Sf).

4.7 Construction of plant expression vectors

The ORF genes were amplified with sets of primers in 3.15.1. The PCR products were overhanging at start codon and blunt end at stop codon. Then the gel-purified PCR products were cloned into pENTR™/D-TOPO® vector by Topoisomerase I to produce the entry clone and transformed into *E. coli*. The obtained recombinants were checked for their insertional direction by *NotI* restriction digestion, PCR, and sequencing. The correct orientation pattern of recombinants showed 3.8 kb but empty vector showed 2.5 kb when cut with *NotI* restriction enzyme (Figure 27A and 27B). Amplification of *ctl* and *alrc2* from the recombinant vectors by PCR showed the expected bands at about 1.2 kb (Figure 27C and 27D). The gene sequences were confirmed again by sequencing. Hence, the correct entry vectors were subcloned separately into a destination clone (pGWB6) by Gateway® LR clonase® II to produce the plant expression clones. The pGWB6::*ctl*, and pGWB6::*alrc2* were finally obtained and confirmed the recombinant vectors by PCR showed the expected bands at about 1.2 kb (Figure 28A and 28B), respectively. Each construct was subsequently transformed into *E. coli*. and *Agrobacterium tumefaciens* for further used in plant transformation.

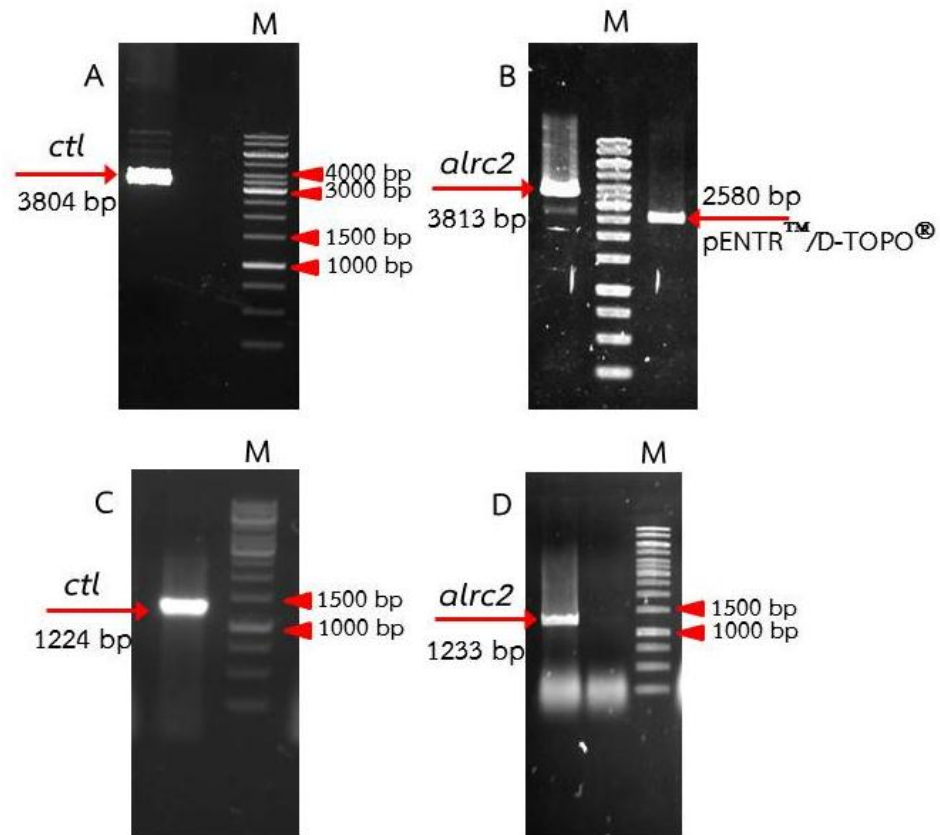


Figure 27 The construction of the entry vector (pENTRTM/D-TOPO[®]) harboring the *ctl* and *alrc2* genes were analyzed on 1% agarose gel against 1 kb DNA marker (M). The recombinant pENTRTM/D-TOPO[®]:*ctl* digested with *NotI* restriction enzyme (A) and the recombinant pENTRTM/D-TOPO[®]:*alrc2* digested with *NotI* restriction enzyme and the empty pENTRTM/D-TOPO[®] vector (B). PCR products from recombinant *ctl* and *alrc2* in pENTRTM/D-TOPO[®] vector (C and D).

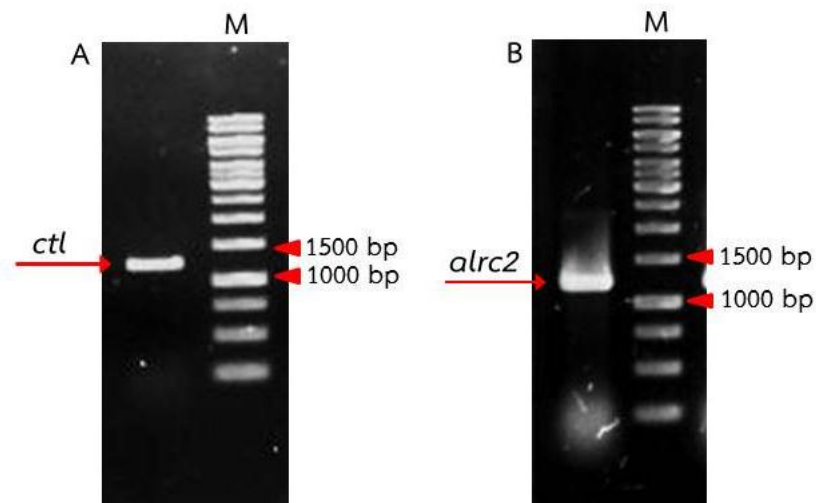


Figure 28 The construction of the destination vector. The PCR products amplified from recombinant *ctl* (A) and *alrc2* (B) in pGWB6 vector and shown on 1% agarose gel against 1 kb DNA marker (M).

4.8 Gene expression of *ctl* and *alrc2* overexpressed in tomato leaves

The *ctl* and *alrc2* genes were transiently expressed in tomato leaves via *Agrobacterium*-mediated transformation. After infiltration of the recombinant expression vectors, leaves were harvested at 1, 3, 6 and 9 day post agroinfiltration; dpa and their total RNA were extracted for cDNA synthesis. During 1 – 6 dpa the visible phenotypes of infiltrated tomato leaf of empty vector and pGWB6::*ctl* not different when compare with control but these transient expressions were slightly induce cell death at 9 dpa that found light yellow around of brown spot. In transient of pGWB6::*alrc2* leaf showed visible phenotype same as control during 1 – 3 dpa but the leaf was induced cell death at 6 dpa that seem little yellow and increasing at 9 dpa. (Figure 29)

Expressions of *ctl* and *alrc2* were under the control of CaMV 35 promoter and the gene expression profile was performed by RT-PCR was performed on tomato

leaves overexpressed the genes as showed in Figure 30. The recombinant pGWB6::*ctl* showed highest expression at 1 dpa and sharply decreasing after 3 dpa according to RT-PCR (Figure 30A). The RT-PCR results showed that the recombinant pGWB6::*alrc2* showed expression between 1 and 6 dpa and very low at 9 dpa (Figure 30B).



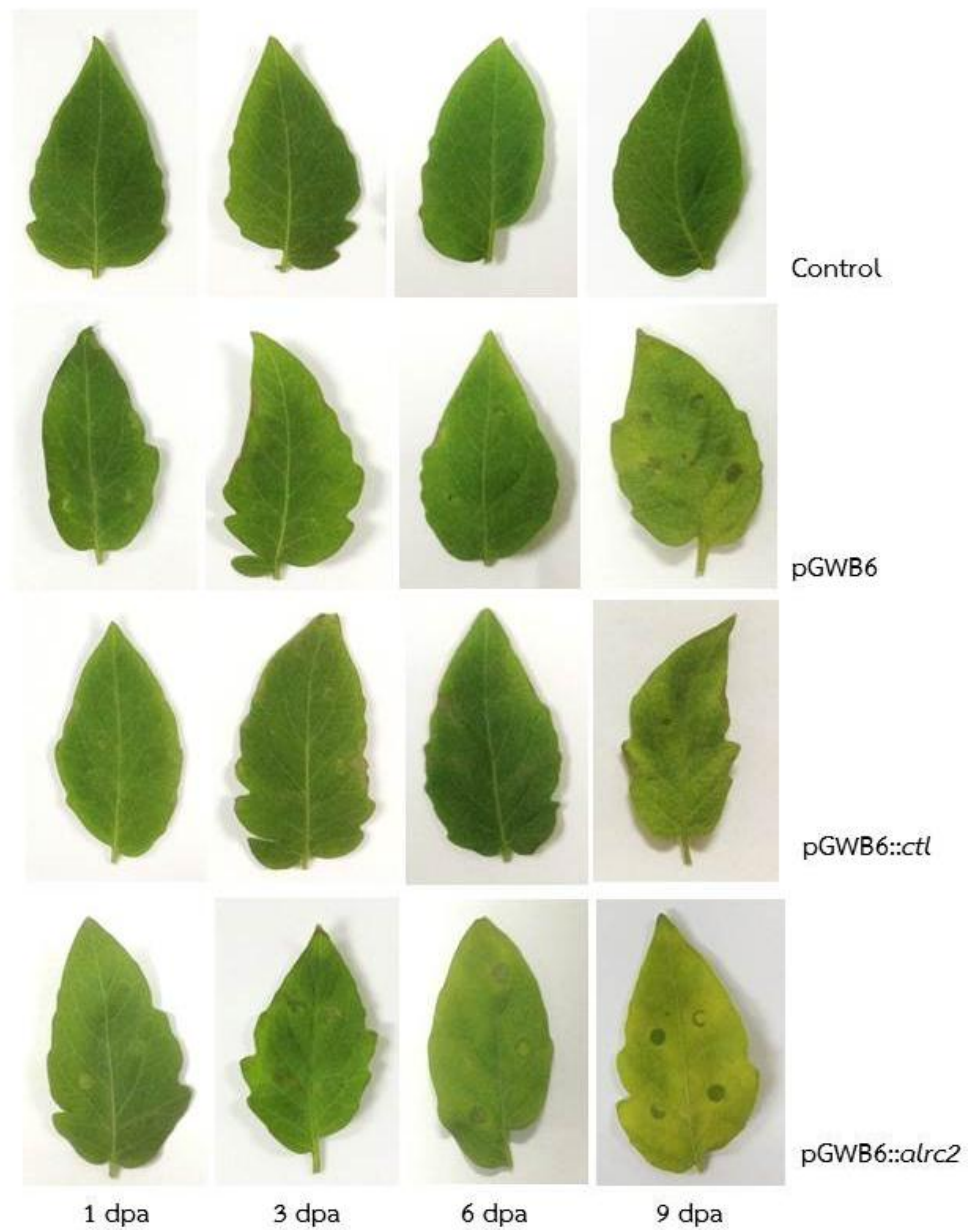


Figure 29 Tomato leaves after infiltration of the recombinant expression vectors via *A. tumefaciens*-mediated transformation. Leaves were harvested at 1, 3, 6 and 9 day post agroinfiltration (dpa). Leaves were harvested at 1, 3, 6 and 9 day post agroinfiltration (dpa).

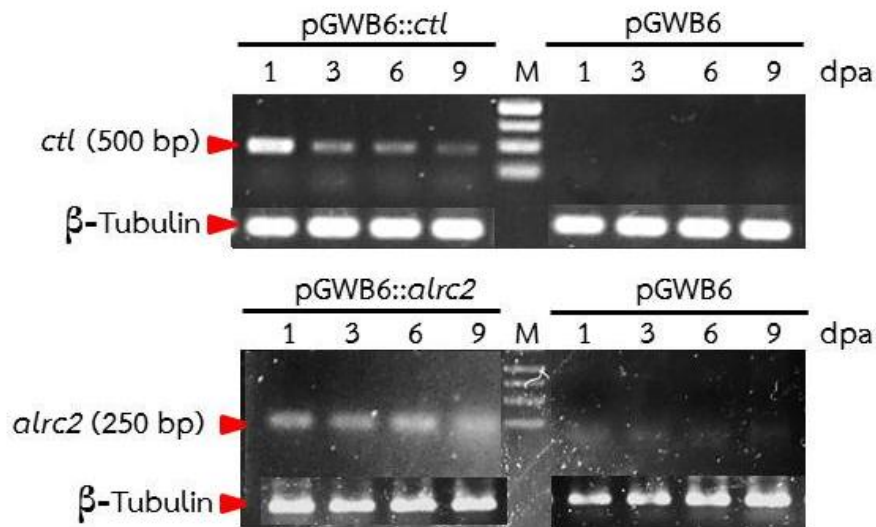


Figure 30 RT-PCR expression analysis of *ctl* and *alrc2* in the agroinfiltrated tomato leaves at 1 – 9 dpa. β -Tubulin was served as an internal reference gene and the empty vectors were served as negative control. Gene Ruler 1 kb DNA ladder (M) was used to indicate the product size. The gene expression of the recombinant pGWB6::*ctl* (A) and pGWB6::*alrc2* (B) were detected on the 1 % agarose gel.

4.9 Recombinant protein expression in tomato leaves

All proteins (CTL and ALRC2) in the pGWB6 vector expressed in transformed tomato leaves were fused with GFP protein (26.8 kDa) at the N-terminal of the proteins. Total proteins were extracted from the leaves and determined the protein concentration by Bradford's method. One hundred micrograms of total protein were loaded and separated on 10% SDS-PAGE gel. The proteins were detected by blotting with anti-GFP antibody conjugated with HRP on PVDF membrane and visualized using chemiluminescent HRP substrate (Figure 31). The CTL was slightly expressed at 1 dpa and gradually increased at 3 dpa. In contrary, the ALRC2 could not be detected at 1 dpa. However, it was gradually expressed at 3 and 6 dpa.

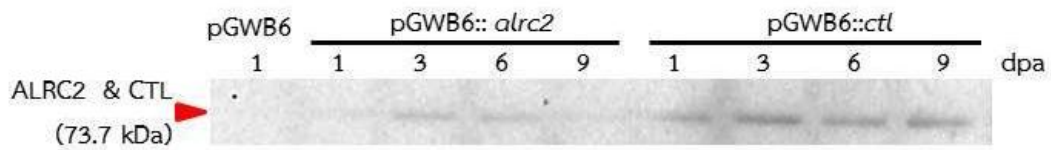


Figure 31 Detection of the recombinant proteins by western blots analysis. Expression of ALRC2 and CTL proteins from agroinfiltration tomato leaves using antibody against GFP protein in different dpa compared with the empty vector (pGWB6).

4.10 Determination of tocopherol content in agroinfiltrated tomato leaves

Transformed tomato leaves at 1, 3, 6 and 9 days were extracted and analyzed for the accumulation of α -tocopherol against control by TLC technique. The amount of α -tocopherol was determined against the α -tocopherol standard curve as shown in Figure 32. The recombinant protein from pGWB6::*ctl* showed high effectiveness in enhancing the production of α -tocopherol content at 3 dpa. The results showed 2.4 ± 0.38 fold increment of α -tocopherol content compared with the control (Figure 33) and the intensity of α -tocopherol band on TLC clearly showed the difference after 3 dpa (Figure 34A). Moreover, the transformation of pGWB6::*alrc2* could induce the accumulation of α -tocopherol in infiltrated tomato leaves at 3 dpa (Figure 34B). The α -tocopherol content was increased 1.4 ± 0.05 fold higher than the control (empty vector; pGWB6) (Figure 33).

4.11 Determination of total chlorophyll content in agroinfiltrated tomato leaves

When *ctl* and *alrc2* were introduced to tomato leaves mediate agrobacterium, the resulting transient plants showed the decreased total chlorophyll when compare with the control. The total chlorophyll of transient plants *ctl* and

alrc2 dropped from 31.2 ± 0.34 to $28.2 \pm 0.09 \mu\text{g ml}^{-1}$ and 32.1 ± 0.07 to $30.8 \pm 0.06 \mu\text{g ml}^{-1}$, respectively in order of day after agroinfiltration (1 – 9 dpa) that correlated with α -tocopherol accumulation (Figure 33).

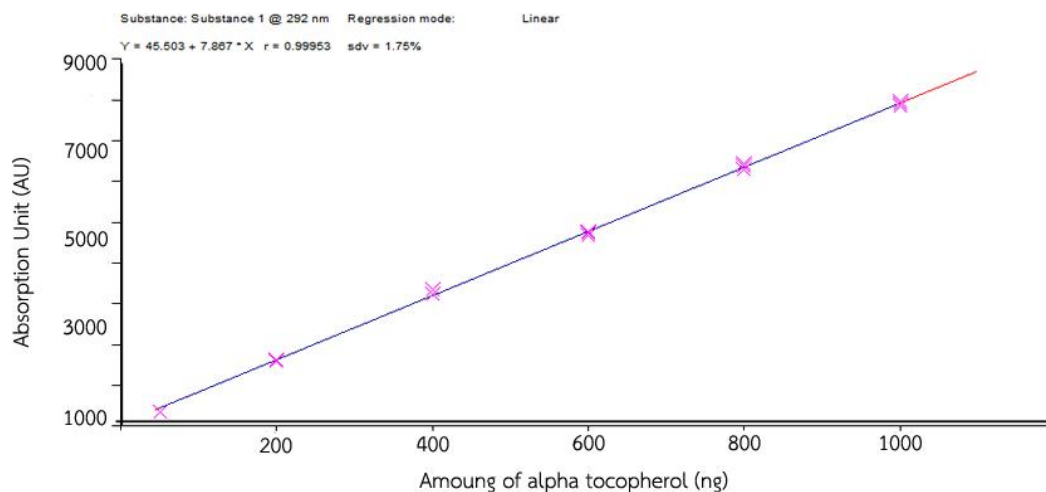


Figure 32 The standard curve of α -tocopherol. The amount of α -tocopherol was plotted against absorption unit (AU) measured on TLC plate developed with chloroform:cyclohexane (11:9 v/v) and scanned under 292 nm (n=3).

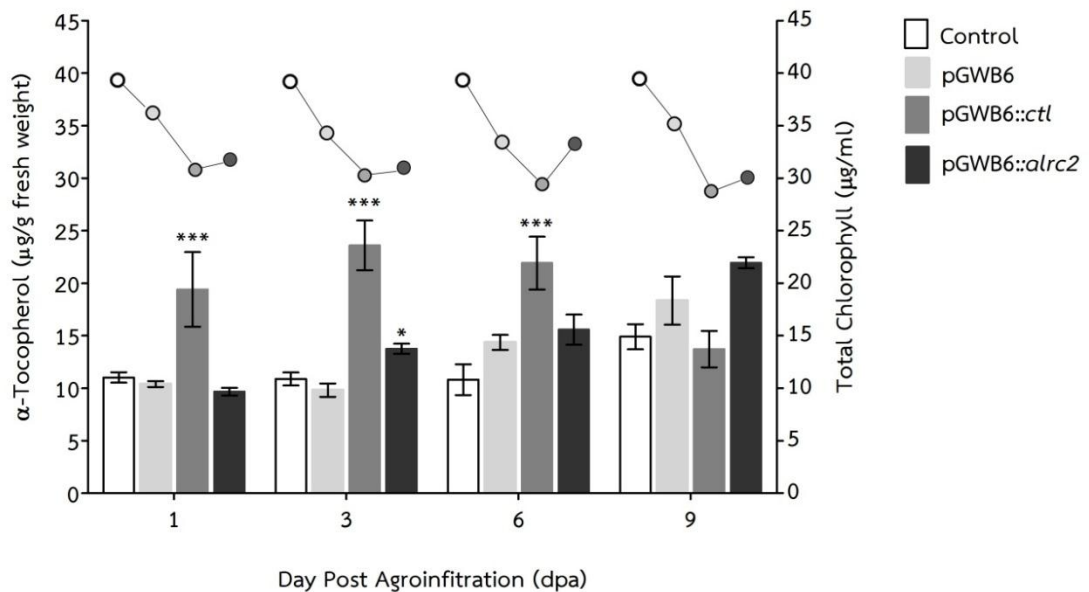
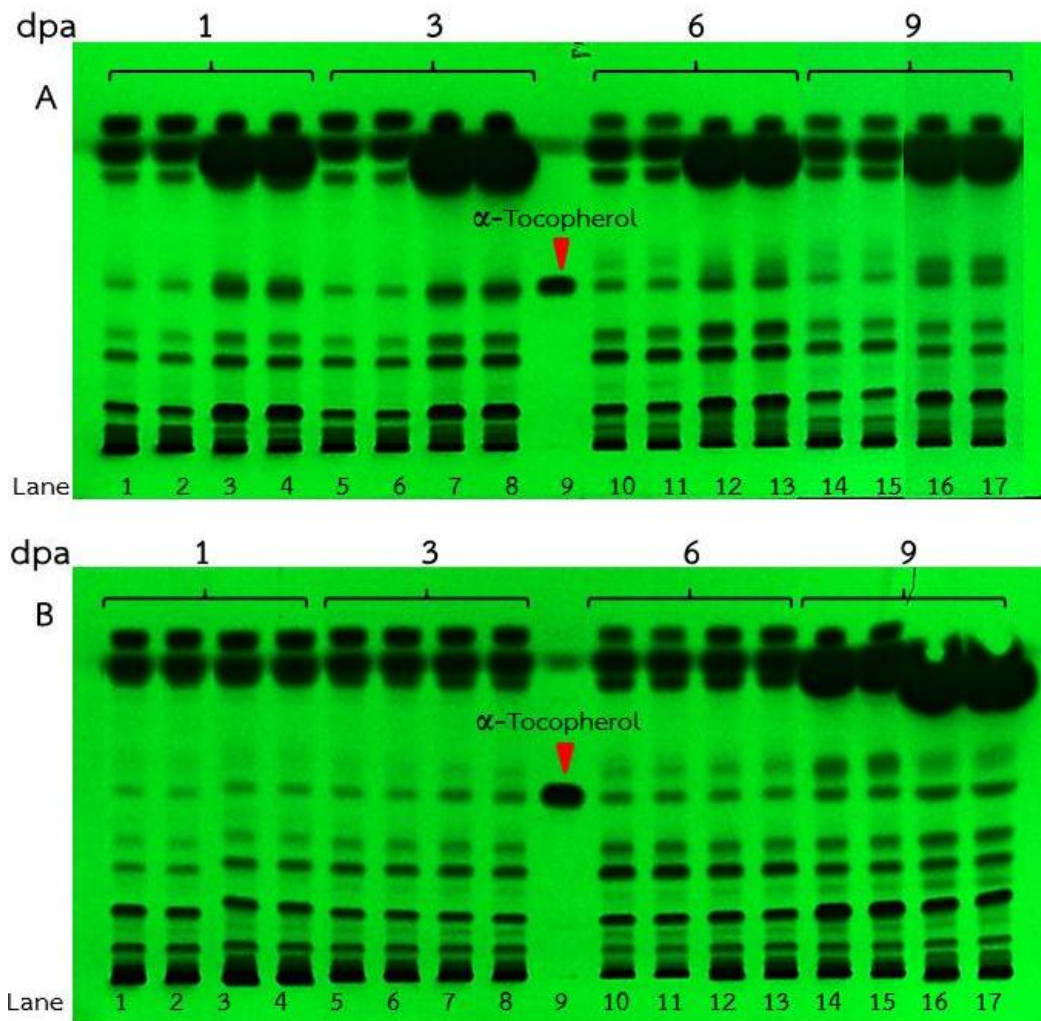


Figure 33 The α -tocopherol and total chlorophyll contents in pGWB6::*alrc2* and pGWB6::*ctl* agroinfiltrated leaves. Determination of α -tocopherol content (bar graph) was from the band intensity on TLC plate. The α -tocopherol content from agroinfiltrated leaves overexpressing *ctl* and *alrc2* genes were compared with empty vector (pGWB6) in 1 – 9 dpa. Data represent the mean and SD (n=3). The different between samples measurement by two way ANOVA test (*: p < 0.05, **: p < 0.01 and ***: p < 0.001). The total chlorophyll content (line graph) was measured by absorption at 663 and 645 nm.



CHULALONGKORN UNIVERSITY

Figure 34 TLC patterns of tomato leaves expressing *alrc2* and *ctl* extracts. The agroinfiltrated leaves at 1, 3, 6 and 9 dpa expressing *ctl* (A) and *alrc2* (B) were extracted and separated on the TLC plate. Standard α -tocopherol was used to compare with α -tocopherol from the samples. Each sample was spotted in duplicate. Lane 1 – 2: empty vector (pGWB6) at 1 dpa, Lane 3 – 4: recombinant at 1 dpa, Lane 5 – 6: empty vector (pGWB6) at 3 dpa, Lane 7 – 8: recombinant at 3 dpa, Lane 9: α -Tocopherol standard, Lane 10 – 11: empty vector (pGWB6) at 6 dpa, Lane 12 – 13: recombinant at 6 dpa, Lane 14 – 15: empty vector (pGWB6) at 9 dpa and Lane 16 – 17: recombinant at 9 dpa.

In order to confirm the α -tocopherol synthesis as a result of the overexpression of the recombinant protein, the α -tocopherol extracted from the infiltrated leaves was detected by GC-MS method. The GC-MS chromatogram showed the increase of α -tocopherol, fatty acids, and lipids from the transformed leaves when compared with the control (Figure 35). In addition, during transient overexpression of both genes showed high level of phytol (6.074 min), a precursor of phytyldiphosphate (PDP) which is the substrate of enzyme HPT and also palmitic acid (5.534 min), linoleic acid (6.248 min), α -linoleic acid (6.281 min) and stearic acid (6.359 min) (Figure 36A and 36B), was detected at 3 and 6 dpa corresponding to the increase of α -tocopherol content at retention time of 12.953 min and its intermediate accumulation MPBQ and DMPBQ have retention time of 7.923 and 8.023 min, respectively (Figure 36C and 36D) From GC-MS spectra, it is possible to identify α -tocopherol, MPBQ and DMPBQ, intermediates which are not commercially available, as shown in Figure 37A, B and C, respectively. The MS spectrum of MPBQ revealed quinol head group fragment at m/z 281 and 321 combined with phytyl group fragment at m/z 265 while, the DMPBQ MS spectrum showed quinol head group fragment at m/z 281 and 335 combined with phytyl group fragment at m/z 265 and 155.

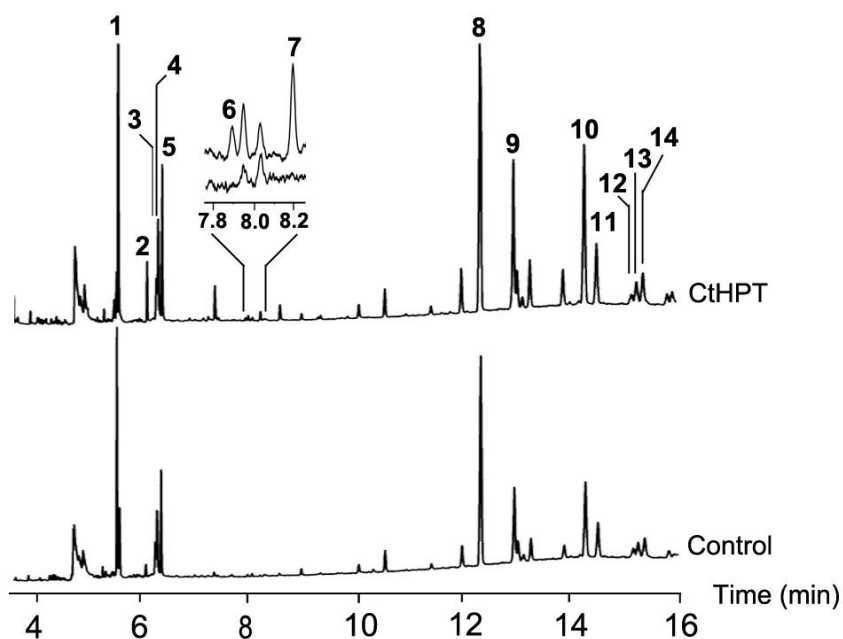


Figure 35 GC-MS chromatogram of infiltrated leaves in 3 dpa of pGWB6::*ctl* showed the increase of metabolites. The numbers on the GC-MS chromatograms are the compounds: 1: palmitic acid (5.534 min), 2: phytol (6.074 min), 3: linoleic acid (6.248 min), 4: α -linoleic acid (6.281 min), 5: stearic acid (6.359 min), 6: MPBQ (7.923 min), 7: DMPBQ (8.203 min), 8: pentacosane (12.321 min), 9: α -tocopherol (12.953 min), 10: nanocosane (14.279 min), 11: α -stigmasterol (14.511 min) 12: β -Sitosterol (15.171 min), 13: Monolinoelaidin (15.258) and 14: β -Amyrin (15.387 min).

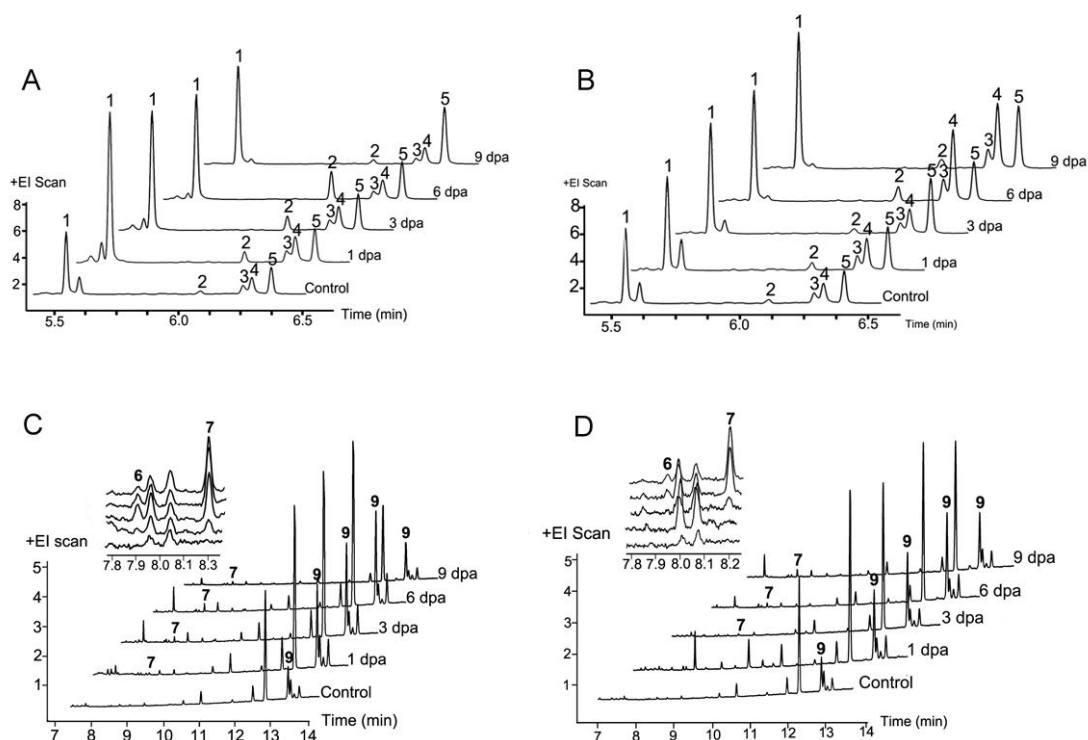


Figure 36 GC-MS analysis of the chemical profiles of phytol and fatty acids comparing between the transient expression of *ctl* (A) and *alrc2* (B) and α -tocopherol together with intermediates (MPBQ, DMPBQ) involved in the biosynthetic pathway of *ctl* (C) and *alrc2* (D) in tomato leaves at 1, 3, 6 and 9 dpa compare with control (empty vector: pGWB6). The labeled numbers: 1: palmitic acid (5.534 min), 2: phytol (6.074 min), 3: linoleic acid (6.248 min), 4: α - linoleic acid (6.281 min), 5: stearic acid (6.359 min), 6:MPBQ (7.923 min), 7: DMPBQ (8.203 min), 8: pentacosane (12.321 min), 9: α -tocopherol (12.953 min).

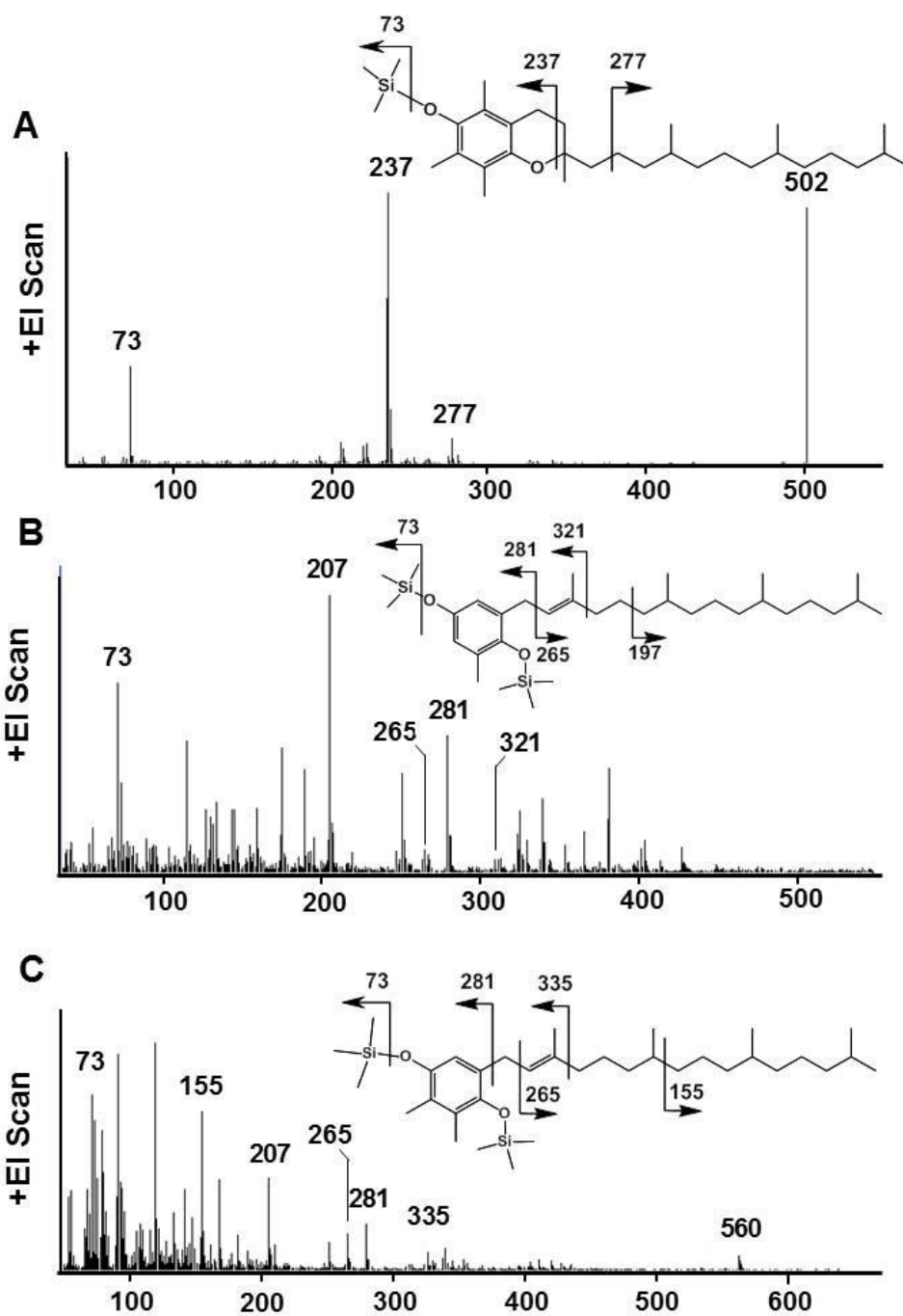


Figure 37 Mass spectra of silylated (A) α -tocopherol (12.955 min), (B) MPBQ (7.923 min) and (C) DMPBQ (8.203 min) from infiltrated leaves.

CHAPTER V

Discussion

Plant aromatic PTases are divided into three groups based on their aromatic substrates: (I) the enzymes involved in shikonin and ubiquinone biosynthesis in which their substrate is *p*-hydroxybenzoate (PHB) (Ohara, et al., 2009; Ohara, et al., 2006; Yazaki, et al., 2002) (II) the enzymes in the plastoquinone, tocopherol and tocotrienol biosynthesis with the substrate homogentisate (HGA) (Matsuzuka, et al., 2013; Sadre, et al., 2010; Schledz, et al., 2001), and (III) the enzymes in the prenylated flavonoid biosynthesis with flavonoids as the substrates (Akashi, et al., 2009b). Mostly, plant aromatic PTases are membrane bound proteins consisting of 6 – 9 transmembrane α -helices. The homogentisate phytyltransferase (HPT or VTE2) is thought to be the rate-limiting step enzyme that catalyzes the prenylation reaction in the initial step of tocopherol biosynthetic pathway. HPT catalyzes the reaction by condensation of the aromatic head group precursor, homogentisate (HGA) and the phytyl tail precursor, phytyl diphosphate (PDP) to produce the first intermediate, 2-methyl-6-phytylbenzoquinol (MPBQ) for the production of tocopherol. According to the phylogenetic tree analysis, the flavonoid PTases showed similarity with HPT indicating that the flavonoid PTases are evolved from HPT in tocopherol biosynthesis.

In this study, we isolated *ctl* and *alrc2* cDNA from *C. ternatea* L. and *A. lakoocha* Rox. Construction of the phylogenetic tree showed that *ctl* and *alrc2* are the member of HPT family, in which HGA is their aromatic substrate (prenyl acceptor) and phytyl diphosphate (PDP) is their prenyl substrate (prenyl donor). Both appeared to be most closely related to HPT of *Glycine max* and *Morus notabilis*. Their amino acid sequences display two aspartate (Asp) rich conserved motifs which are particularly found in UbiA prenyltransferase family. The motif I: NQXXDXXXD is

corresponding to prenyl diphosphate binding and catalytic reaction by chelation of Mg^{2+} and the motif II: KDXDXD helps stabilizing the substrate binding (Huang, et al., 2014; Melzer and Heide, 1994). The activity of these enzyme required Mg^{2+} or related ion. The Asp rich motif is important for substrate binding affinity. It has been reported that point mutation at Asp rich motif resulted in the declination of substrate binding affinity (Ohara, et al., 2009). From our results, the motif I of CTL and ALRC2 showed high similarity with a group of the enzymes in tocopherol and tocotrienol biosynthesis that can bind to PDP or GGPP, while their motif II showed high similarity between flavonoid PTase and HPT or HGGT group. Like the identified aromatic PTases, CTL and ALRC2 are located in the same clan with HPT group in phylogenetic analysis and they have an N-terminal signal peptide which destines these translated proteins to localize in chloroplast membrane, as were the results predicted by WoLF PSORT and Protcomp. Both proteins were predicted to be transmembrane proteins with nine transmembrane α -helices. Altogether, the results suggested that CTL and ALRC2 are likely to be the group of HPT enzymes.

To characterize the *ctl* and *alrc2* functions, overexpression of these genes in tomato leaves were conducted by agroinfiltration. In recent years, transient gene expression mediated by agroinfiltration has been used as a tool to demonstrate transcription and protein expression analysis. It is rapid, simple, and effective procedure to generate the recombinant protein within a few days by injection of *A. tumefaciens* into leaves or fruits of plants (Leckie and Neal Stewart, 2011; Zottini, et al., 2008). In this study, agroinfiltration technique was used to follow the expression of the recombinant genes in tomato leaves. The *ctl* and *alrc2* genes were constructed into binary vector pGWB6 carrying GFP at the N-terminus and under control of 35S CaMV promoter. *A. tumefaciens* strain GV3101 containing pJL3:p19 that expressing RNA silencing suppressor protein (p19) was used to improve agroinfection

efficiency (Kanagarajan, et al., 2012; Wydro, et al., 2006). The mRNA expression of these genes showed the highest level on the first day postinfiltration (dpa) and decreased afterward. The recombinant protein expression were detected by western blot analysis and it has been found that the expression of CTL showed the highest level at 3 dpa and slightly decrease until 9 dpa while ALRC2 showed little expression at 3 and 6 dpa. It was common that the genes must be expressed first in order to encode their proteins later. The results clearly demonstrated that the genes and their corresponding proteins were expressed oppositely during the days after infiltration. Similarly the level of protein expression via agrobacterium infiltration followed by GFP protein or GUS activity showed high expression after 3 dpa and decrease after that (Kim, et al 2009, Orzaez, et al. 2006, Yasmin and Debener, 2010). In addition, these results suggested that the CTL had higher expression than ALRC2 in this system and the protein expression can increase to the maximum level at 3 dpa as well as slightly CTL expression showed high activity to induced α -tocopherol accumulation at first day after agroinfiltration. It may be influenced by the presence of 5'-UTRs and 3'-UTRs of mRNA that form complexes with protein in post-transcription process for control transcription mRNA stability and translation in chloroplast (Choquet. and Wollman, 2002, Cohen and Mayfield, 1997, Del Campo, 2009, Gao, et al. 2012, Monde, 2000 and Robida, 2002.). Furthermore, overexpression of these genes clearly led to the increase of α -tocopherol accumulation in tomato leaves. The successful detection of increased α -tocopherol content from agroinfiltration tomato leaves in this study was analyzed by TLC. The *ctl* and *alrc2* genes isolated from *C. ternatea* and *A. lakoocha*. could enhance the α -tocopherol content up to 2.4 fold and 1.4 fold, respectively within 3 dpa when compared with the control. The increase of the α -tocopherol content was parallel with the increase of the protein expression level. Similar results have been reported in overexpression of HPT (also called VTE2) genes isolated from other species. The overexpression of A.

thaliana VTE2 (*At-VTE2*) in *Arabidopsis* have been reported to increase the total tocopherol level up to 4.4 fold in leaves and 40% in seeds (Collakova and DellaPenna, 2003a). Moreover, *At-VTE2* has also been found to enhance α -tocopherol level up to 5.5 and 2 fold in tobacco and lettuce transgenic leaves, respectively (Harish, et al., 2013a; Harish, et al., 2013b; Koeun, et al., 2007) and also 106 % increasing of α -tocopherol level in potato tuber (Crowell, et al., 2008). The α -tocopherol levels from transgenic expression of lettuce HPT (*LsHPT*) and apple HPT (*MdHPT*) have been reported to raise to 18 and 3.6 fold in lettuce and tomato leaves, respectively (Ren, et al., 2011; Seo, et al., 2011). It was obvious that the overexpression of HPT led to the high accumulation of α -tocopherol; however, the levels of increment appear to be varied and seem to be depending on the species whose HPT genes are isolated from.

Our results also indicated that the accumulation of α -tocopherol was affected by the activity of the *ctl* and *alrc2* genes. However, the limitation of transient expression method should be taken into account when monitoring the phenotype after infiltration. In this case, the genes and their proteins could be detected up until 6 dpa while it was observed that at 9 dpa the accumulation of α -tocopherol of control was higher than both recombinant gene infiltration samples because the infiltrated area may be damaged due to the stress of agroinfiltration. Therefore, this result suggested that the phenotype of these genes transiently expressed in tomato leaves should be monitored within a week of post-infiltration.

According to the biosynthetic pathways of tocopherol and chlorophyll, tocopherol production is somewhat related to chlorophyll degradation. It has been known that HGA and PDP are the substrates of HPT and HGA is derived from shikimate pathway but PDP can be derived from de novo synthesis of MVA or MEP pathway and chlorophyll degradation. During the stress conditions, chlorophyll is

degraded by chlorophyllase to produce chlorophyllide and free phytol. Phytol is then stepwise phosphorylated by phytyl kinase (VTE5) and unknown phytylphosphate kinase to produce PDP as a precursor for chlorophyll, tocopherol, phylloquinone and fatty acid alcohol ester biosynthesis (Ischebeck, et al., 2006; Valentin, et al., 2006). The correlation between chlorophyll degradation and tocopherol accumulation is still not clear although it is possible that phytol involved in tocopherol biosynthesis may derive from chlorophyll degradation. It has been reported that phytol is incorporated to tocopherol in seedling *Arabidopsis* by feeding experiment and affected increasing of tocopherol in overexpressed HPT and TC tobacco cell suspensions (Harish, et al., 2013b; Rise, et al., 1989). In addition, it has been found that chlorophyll content was declined about 20% while the tocopherol content was increased in overexpressed HPT plant (Lee, et al., 2007). To demonstrate the effect of the recombinant protein (CTL and ALRC2) on tocopherol accumulation and chlorophyll degradation in plant, the transformed plant extracts were analyzed by spectrophotometry method. The result showed that CTL and ALRC2 transiently expressed leaves were related with the chlorophyll decline. Total chlorophylls slightly continuous decreased after agroinfiltration when compare with control at 1 – 6 dpa. At 9 dpa, the α -tocopherol accumulation dropped while the total chlorophyll degradation slightly increased that could be effect of senescence during stress. GC-MS after silylation. At 3 and 6 dpa, the CTL and ALRC2 transiently expressed leaves contained pools of phytol, fatty acid e.g. palmitic acid (16:0), stearic acid (18:0) and linolenic acid (18:3), and together with α -tocopherol accumulation. These results suggested that overexpression of the recombinant CTL and ALRC2 proteins might induce chlorophyll hydrolysis to release free phytol as a precursor of tocopherol. However, the expression of genes related in chlorophyll degradation should be further investigated to reveal the correlation between α -tocopherol and chlorophyll accumulation. In addition, the pools of those fatty acids highly

accumulated in the transgenic leaves were likely the result of free phytol increment since it serves as a precursor of fatty acid biosynthesis (Ischebeck, et al., 2006). Although fatty acid can be derived from the degradation of the chloroplast envelope membrane where they are its major components (Poincelot, 1976; Whitaker, 1986) or from chloroplast lipid in response to pathogen attack (Upchurch, R.G. 2008, Walley, J.W., et al. 2013), these causes were unlikely to affect the increase of fatty acid accumulation in transgenic CTL and ALRC2 tomato leaves because if these processes occurred, they would lead to plant cell death but the sign of cell death was not detected at that moment.

Overexpression of CTL and ALRC2 increased the amounts of MPBQ and DMPBQ in transgenic tomato leaves. MPBQ, DMPBQ and γ -tocopherol are stepwise intermediates in α -tocopherol biosynthesis pathway. These compounds are synthesized by HPT, tocopherol cyclase (TC), and γ -tocopherol methyltransferase (γ TMT), respectively. In this study, GC-MS could detect MPBQ and DMPBQ but could not detect γ -tocopherol. It is possible that γ TMT activity may rapidly convert γ -tocopherol to α -tocopherol under stress condition (Collakova and DellaPenna, 2003b). To identify MPBQ and DMPBQ, their fragmentation patterns were compared with the patterns from previous reports (Kobayashi and DellaPenna, 2008; Porfirova, et al., 2002; Sussmann, et al., 2011) instead of standard compounds because MPBQ and DMPBQ are not commercially available. The mass spectrum of derivatized α -tocopherol showed molecular ion signal at m/z 502 and heterocyclic chromanol ring at m/z 237 (Liebler, et al., 1996; Mottier, et al., 2002). The suspected peaks of MPBQ and DMPBQ were at retention time of 7.923 and 8.203 minute and their expected m/z were 546 and 560, respectively. However, the expected molecular ions of derivative compounds was only detected for DMPBQ but not detected for MPBQ. This would be due to its low amount or instability of MPBQ. Considering

fragmentation patterns of these compounds, MPBQ showed major fragment of quinol head group at m/z 281 and 321 and DMPBQ showed the major fragment of quinol head group at m/z 281 and 335. Moreover, the quinol head group of these compounds showed fragment ion at m/z 207 which was calculated from m/z 281 deleted by m/z 73 of TMS (trimethylsilane) derivative. The phetyl tail fragment of MPBQ and DMPBQ displayed at m/z 265 and m/z 265 and 155, respectively. These patterns of MPBQ and DMPBQ were in agreement with previous reports; therefore, GC-MS is a suitable detection method for MPBQ and DMPBQ and these results confirmed the presence of MPBQ and DMPBQ in the transgenic tomato leaves expressing CTL and ALRC2. Overexpression of CTL increased the accumulation of MPBQ and DMPBQ since 1 dpa while overexpression of ALRC2 increased little accumulation of intermediates after 3 dpa. This result indicated that CT has higher potential to catalyze reaction than ALRC2.

CHAPTER VI

Conclusion

Altogether, this study revealed that *ctl* and *alrc2* genes isolated from *Clitoria ternatea* L. and *Artocarpus lakoocha* Rox., respectively, encoded HPT enzyme which is an important enzyme in α -tocopherol biosynthesis. Both genes were identified and characterized based on their protein structure which appeared to consist of 9 transmembrane α -helixes, N-signal transit peptide at N-terminal and Asp rich regions as substrate binding site. Both genes were highly expressed at 1 dpa and their proteins were highly expressed at 3 dpa in transient tomato. These overexpression genes in tomato leaves resulted in the increase of MPBQ (the product of HPT activity) and DMPBQ and consequently enhance α -tocopherol accumulation. The MPBQ and DMPBQ that are the intermediates in pathway were also detected to be increased by GC-MS chromatogram. Furthermore, the overexpression of *CTL* and *ALRC2* induced chlorophyll degradation and released free phytol that is the precursor of α -tocopherol.

REFERENCES

- Akashi, T., *et al.* (2009a) Molecular Cloning and Characterization of a cDNA for Pterocarpan 4-Dimethylallyltransferase Catalyzing the Key Prenylation Step in the Biosynthesis of Glyceollin, a Soybean Phytoalexin, *Plant Physiology*, **149**, 683-693.
- Akashi, T., *et al.* (2009b) Molecular cloning and characterization of a cDNA for pterocarpan 4-dimethylallyltransferase catalyzing the key prenylation step in the biosynthesis of glyceollin, a soybean phytoalexin, *Plant Physiol*, **149**, 683-693.
- Alkadi K. A. A, *et al.* (2013) Prenylated xanthone and rubraxanthone with Antiplatelet aggregation activity in human whole blood isolated from *Garcinia griffithii*., *Orient J Chem*, **23**, 5.
- Arung, E.T., Shimizu, K. and Kondo, R. (2006) Inhibitory effect of isoprenoid-substituted flavonoids isolated from *Artocarpus heterophyllus* on melanin biosynthesis, *Planta Med*, **72**, 847-850.
- Asensi-Fabado, M.A. and Munné-Bosch, S. (2010) Vitamins in plants: occurrence, biosynthesis and antioxidant function, *Trends in plant science*, **15**, 582-592.
- Ashby, M.N., *et al.* (1992) COQ2 is a candidate for the structural gene encoding para-hydroxybenzoate:polyprenyltransferase, *J Biol Chem*, **267**, 4128-4136.
- Biggins, J. and Mathis, P. (1988) Functional role of vitamin K1 in photosystem I of the cyanobacterium *Synechocystis* 6803, *Biochemistry*, **27**, 1494-1500.
- Block, A., *et al.* (2013) Functional modeling identifies paralogous solanesyl-diphosphate synthases that assemble the side chain of plastoquinone-9 in plastids, *J Biol Chem*, **288**, 27594-27606.
- Botta, B., *et al.* (2009) Prenylated isoflavonoids: Botanical distribution, structures, biological activities and biotechnological studies. An update (1995-2006), *Curr Med Chem*, **16**, 3414-3468.
- Botta, B., *et al.* (2005) Prenylated flavonoids: pharmacology and biotechnology, *Curr Med Chem*, **12**, 717-739.

- Cerqueira, F., *et al.* (2008) The natural prenylated flavone artelastin is an inhibitor of ROS and NO production, *Int Immunopharmacol*, **8**, 597-602.
- Cerqueira, F., *et al.* (2003) Inhibition of lymphocyte proliferation by prenylated flavones: artelastin as a potent inhibitor, *Life Sci*, **73**, 2321-2334.
- Cha, J.D., *et al.* (2007) Antibacterial activity of sophoraflavanone G isolated from the roots of *Sophora flavescens*, *J Microbiol Biotechnol*, **17**, 858-864.
- Chen, C.-C. (2002) Garcinone E, a xanthone derivative, has potent cytotoxic effect against hepatocellular carcinoma cell lines, *Planta Med*, **68**, 975-979.
- Chenna, R., *et al.* (2003) Multiple sequence alignment with the Clustal series of programs, *Nucleic Acids Res*, **31**, 3497-3500.
- Cheon, B.S., *et al.* (2000) Effects of prenylated flavonoids and biflavonoids on lipopolysaccharide-induced nitric oxide production from the mouse macrophage cell line RAW 264.7, *Planta Med*, **66**, 596-600.
- Collakova, E. and DellaPenna, D. (2003a) Homogentisate phytyltransferase activity is limiting for tocopherol biosynthesis in *Arabidopsis*, *Plant Physiol*, **131**, 632-642.
- Collakova, E. and DellaPenna, D. (2003b) The role of homogentisate phytyltransferase and other tocopherol pathway enzymes in the regulation of tocopherol synthesis during abiotic stress, *Plant Physiol*, **133**, 930-940.
- Crowell, E.F., McGrath, J.M. and Douches, D.S. (2008) Accumulation of vitamin E in potato (*Solanum tuberosum*) tubers, *Transgenic Res*, **17**, 205-217.
- Dej-adisai, S., *et al.* (2014) Antityrosinase and antimicrobial activities from Thai medicinal plants, *Arch Pharm Res*, **37**, 473-483.
- DellaPenna, D. and Mène-Saffrané, L. (2011) Chapter 5 - Vitamin E. In Fabrice, R. and Roland, D. (eds), *Advances in Botanical Research*. Academic Press, pp. 179-227.
- DellaPenna, D. and Pogson, B.J. (2006) Vitamin synthesis in plants: tocopherols and carotenoids, *Annu Rev Plant Biol*, **57**, 711-738.
- Devi, B.P., Boominathan, R. and Mandal, S.C. (2003) Anti-inflammatory, analgesic and antipyretic properties of *Clitoria ternatea* root, *Fitoterapia*, **74**, 345-349.

- Epifano, F., *et al.* (2007) Chemistry and pharmacology of oxyprenylated secondary plant metabolites, *Phytochemistry*, **68**, 939-953.
- Falk, J. and Munne-Bosch, S. (2010) Tocochromanol functions in plants: antioxidation and beyond, *J Exp Bot*, **61**, 1549-1566.
- Harish, M.C., *et al.* (2013a) Enhancement of α -tocopherol content through transgenic and cell suspension culture systems in tobacco, *Acta Physiologiae Plantarum*, **35**, 1121-1130.
- Harish, M.C., *et al.* (2013b) Overexpression of homogentisate phytyltransferase (HPT) and tocopherol cyclase (TC) enhances α -tocopherol content in transgenic tobacco, *Biologia Plantarum*, **57**, 395-400.
- Huang, H., *et al.* (2014) Structure of a membrane-embedded prenyltransferase homologous to UBIAD1, *PLoS Biol*, **12**, e1001911.
- Hunter, S.C. and Cahoon, E.B. (2007) Enhancing vitamin E in oilseeds: unraveling tocopherol and tocotrienol biosynthesis, *Lipids*, **42**, 97-108.
- Ischebeck, T., *et al.* (2006) A salvage pathway for phytol metabolism in Arabidopsis, *J Biol Chem*, **281**, 2470-2477.
- Jacob, L. and Latha, M. (2012) Anticancer Activity of Clitoria ternatea Linn. Against Dalton's Lymphoma, *Int J Pharmacog Phyto Res*, **4**, 207-212.
- Jain, N.N., *et al.* (2003) Clitoria ternatea and the CNS, *Pharmacology Biochemistry and Behavior*, **75**, 529-536.
- Jantan, I., *et al.* (2002) In vitro inhibitory effect of rubraxanthone isolated from *Garcinia parvifolia* on platelet-activating factor receptor binding, *Planta Med*, **68**, 1133-1134.
- Kanagarajan, S., *et al.* (2012) Functional expression and characterization of sesquiterpene synthases from *Artemisia annua* L. using transient expression system in *Nicotiana benthamiana*, *Plant Cell Rep*, **31**, 1309-1319.
- Kelemu, S., Cardona, C. and Segura, G. (2004) Antimicrobial and insecticidal protein isolated from seeds of *Clitoria ternatea*, a tropical forage legume, *Plant Physiology and Biochemistry*, **42**, 867-873.

- Kim, D.W., *et al.* (2002) Effects of sophoraflavanone G, a prenylated flavonoid from *Sophora flavescens*, on cyclooxygenase-2 and in vivo inflammatory response, *Arch Pharm Res*, **25**, 329-335.
- Kobayashi, N. and DellaPenna, D. (2008) Tocopherol metabolism, oxidation and recycling under high light stress in *Arabidopsis*, *Plant J*, **55**, 607-618.
- Koeun, L., *et al.* (2007) Overexpression of *Arabidopsis* Homogentisate Phytlyltransferase or Tocopherol Cyclase Elevates Vitamin E Content by Increasing γ -tocopherol Level in Lettuce (*Lactuca sativa* L.), *Mol. Cells*, **24**, 301-306.
- Kuete, V., *et al.* (2011) Cytotoxicity and mode of action of four naturally occurring flavonoids from the genus *Dorstenia*: gancaonin Q, 4-hydroxyonchocarpin, 6-prenylapigenin, and 6,8-diprenyleriodictyol, *Planta Med*, **77**, 1984-1989.
- Larkin, M.A., *et al.* (2007) Clustal W and Clustal X version 2.0, *Bioinformatics*, **23**, 2947-2948.
- Leckie, B.M. and Neal Stewart, C., Jr. (2011) Agroinfiltration as a technique for rapid assays for evaluating candidate insect resistance transgenes in plants, *Plant Cell Rep*, **30**, 325-334.
- Lee, K., *et al.* (2007) Overexpression of *Arabidopsis* homogentisate phytlyltransferase or tocopherol cyclase elevates vitamin E content by increasing γ -tocopherol level in lettuce (*Lactuca sativa* L.), *Mol Cells*, **24**, 301-306.
- Lee, N.K., *et al.* (2004) Prenylated flavonoids as tyrosinase inhibitors, *Arch Pharm Res*, **27**, 1132-1135.
- Li, H., *et al.* (2015) A heteromeric membrane-bound prenyltransferase complex from hop catalyzes three sequential aromatic prenylations in the bitter acid pathway, *Plant Physiol*, **167**, 650-659.
- Liebler, D.C., *et al.* (1996) Gas chromatography-mass spectrometry analysis of vitamin E and its oxidation products, *Anal Biochem*, **236**, 27-34.
- Likhitwitayawuid, K., *et al.* (2005) Phenolics with antiviral activity from *Millettia erythrocalyx* and *Artocarpus lakoocha*, *Natural product research*, **19**, 177-182.

- Lima, G.P.P., *et al.* (2014) Ozonated water and chlorine effects on the antioxidant properties of organic and conventional broccoli during postharvest, *Scientia Agricola*, **71**, 151-156.
- Lin, J.-J. (1995) Electrotransformation of *Agrobacterium*. In, *Electroporation Protocols for Microorganisms*. Springer, pp. 171-178.
- Liu, X., *et al.* (2007) AG protein-coupled receptor is a plasma membrane receptor for the plant hormone abscisic acid, *Science*, **315**, 1712-1716.
- Maneechai, S., *et al.* (2012) Flavonoid and stilbenoid production in callus cultures of *Artocarpus lakoocha*, *Phytochemistry*, **81**, 42-49.
- Mangano, S., Gonzalez, C.D. and Petruccelli, S. (2014) *Agrobacterium tumefaciens*-Mediated Transient Transformation of *Arabidopsis thaliana* Leaves. In, *Arabidopsis Protocols*. Springer, pp. 165-173.
- Matsuzuka, K., *et al.* (2013) Investigation of tocotrienol biosynthesis in rice (*Oryza sativa* L.), *Food Chem*, **140**, 91-98.
- Melzer, M. and Heide, L. (1994) Characterization of polyprenyldiphosphate: 4-hydroxybenzoate polyprenyltransferase from *Escherichia coli*, *Biochim Biophys Acta*, **1212**, 93-102.
- Mene-Saffrane, L., Jones, A.D. and DellaPenna, D. (2010) Plastochromanol-8 and tocopherols are essential lipid-soluble antioxidants during seed desiccation and quiescence in *Arabidopsis*, *Proc Natl Acad Sci U S A*, **107**, 17815-17820.
- Mottier, P., *et al.* (2002) Comparison of gas chromatography-mass spectrometry and liquid chromatography-tandem mass spectrometry methods to quantify alpha-tocopherol and alpha-tocopherolquinone levels in human plasma, *Anal Biochem*, **301**, 128-135.
- Mukherjee, P.K., *et al.* (2008) The Ayurvedic medicine *Clitoria ternatea*--from traditional use to scientific assessment, *J Ethnopharmacol*, **120**, 291-301.
- Nakata, Y., Tang, X. and Yokoyama, K.K. (1997) Preparation of competent cells for high-efficiency plasmid transformation of *Escherichia coli*, *Methods Mol Biol*, **69**, 129-137.

- Nesa, M.L., *et al.* (2015) Cytotoxic, anti-inflammatory, analgesic, CNS depressant, antidiarrhoeal activities of the methanolic extract of the *Artocarpus Lakoocha* leaves, *World J Pharm Sci*, **3**, 167-174.
- Nithianantham, K., *et al.* (2011) Hepatoprotective potential of *Clitoria ternatea* leaf extract against paracetamol induced damage in mice, *Molecules*, **16**, 10134-10145.
- Nowicka, B. and Kruk, J. (2010) Occurrence, biosynthesis and function of isoprenoid quinones, *Biochimica et Biophysica Acta (BBA) - Bioenergetics*, **1797**, 1587-1605.
- Ohara, K., *et al.* (2009) Functional characterization of LePGT1, a membrane-bound prenyltransferase involved in the geranylation of p-hydroxybenzoic acid, *Biochem J*, **421**, 231-241.
- Ohara, K., Sasaki, K. and Yazaki, K. (2010) Two solanesyl diphosphate synthases with different subcellular localizations and their respective physiological roles in *Oryza sativa*, *J Exp Bot*, **61**, 2683-2692.
- Ohara, K., *et al.* (2006) Functional characterization of OsPPT1, which encodes p-hydroxybenzoate polyprenyltransferase involved in ubiquinone biosynthesis in *Oryza sativa*, *Plant Cell Physiol*, **47**, 581-590.
- Okada, K., *et al.* (2004) The AtPPT1 gene encoding 4-hydroxybenzoate polyprenyl diphosphate transferase in ubiquinone biosynthesis is required for embryo development in *Arabidopsis thaliana*, *Plant Mol Biol*, **55**, 567-577.
- Park, K.M., *et al.* (2003) Kuwanon G: an antibacterial agent from the root bark of *Morus alba* against oral pathogens, *J Ethnopharmacol*, **84**, 181-185.
- Pedro, M., *et al.* (2005) Artelastin is a cytotoxic prenylated flavone that disturbs microtubules and interferes with DNA replication in MCF-7 human breast cancer cells, *Life Sciences*, **77**, 293-311.
- Poincelot, R.P. (1976) Lipid and Fatty Acid composition of chloroplast envelope membranes from species with differing net photosynthesis, *Plant Physiol*, **58**, 595-598.

- Porfirova, S., *et al.* (2002) Isolation of an Arabidopsis mutant lacking vitamin E and identification of a cyclase essential for all tocopherol biosynthesis, *Proc Natl Acad Sci U S A*, **99**, 12495-12500.
- Pshybytko, N.L., *et al.* (2008) Function of plastoquinone in heat stress reactions of plants, *Biochimica et Biophysica Acta (BBA) - Bioenergetics*, **1777**, 1393-1399.
- Puntumchai, A., *et al.* (2004) Lakoochins A and B, New Antimycobacterial Stilbene Derivatives from *Artocarpus lakoocha*, *J Nat Prod*, **67**, 485-486.
- Pyka, A., *et al.* (2011) Comparison of NP-TLC and RP-TLC with densitometry to quantitative analysis of tocopherol acetate in pharmaceutical preparation, *J Liq Chromatogr Relat Technol*, **34**, 2548-2564.
- Rai, K., *et al.* (2002) Clitoria ternatea root extract enhances acetylcholine content in rat hippocampus, *Fitoterapia*, **73**, 685-689.
- Ren, W., *et al.* (2011) Molecular analysis of a homogentisate phytyltransferase gene from *Lactuca sativa* L, *Mol Biol Rep*, **38**, 1813-1819.
- Rise, M., *et al.* (1989) Accumulation of α -Tocopherol in Senescing Organs as Related to Chlorophyll Degradation, *Plant Physiology*, **89**, 1028-1030.
- Sadre, R., *et al.* (2010) Catalytic reactions of the homogentisate prenyl transferase involved in plastoquinone-9 biosynthesis, *J Biol Chem*, **285**, 18191-18198.
- Sambrook, J., Fritsch, E.F. and Maniatis, T. (1989) *Molecular cloning*. Cold spring harbor laboratory press New York.
- Sasaki, K., *et al.* (2008) Cloning and characterization of naringenin 8-prenyltransferase, a flavonoid-specific prenyltransferase of *Sophora flavescens*, *Plant Physiol*, **146**, 1075-1084.
- Sasaki, K., *et al.* (2011) Molecular characterization of a membrane-bound prenyltransferase specific for isoflavone from *Sophora flavescens*, *J Biol Chem*, **286**, 24125-24134.
- Sasaki, K., Tsurumaru, Y. and Yazaki, K. (2009) Prenylation of flavonoids by biotransformation of yeast expressing plant membrane-bound prenyltransferase SfN8DT-1, *Biosci Biotechnol Biochem*, **73**, 759-761.

- Savidge, B., *et al.* (2002) Isolation and characterization of homogentisate phytyltransferase genes from *Synechocystis* sp. PCC 6803 and *Arabidopsis*, *Plant Physiol*, **129**, 321-332.
- Schledz, M., *et al.* (2001) A novel phytyltransferase from *Synechocystis* sp. PCC 6803 involved in tocopherol biosynthesis, *FEBS Lett*, **499**, 15-20.
- Seo, Y.S., *et al.* (2011) Ectopic expression of apple fruit homogentisate phytyltransferase gene (MdHPT1) increases tocopherol in transgenic tomato (*Solanum lycopersicum* cv. Micro-Tom) leaves and fruits, *Phytochemistry*, **72**, 321-329.
- Sharma, P., *et al.* (2012) Reactive Oxygen Species, Oxidative Damage, and Antioxidative Defense Mechanism in Plants under Stressful Conditions, *Journal of Botany*, **2012**, 26.
- Shen, G., *et al.* (2012) Characterization of an isoflavonoid-specific prenyltransferase from *Lupinus albus*, *Plant Physiol*, **159**, 70-80.
- Shimizu, K., *et al.* (2002) The skin-lightening effects of artocarpin on UVB-induced pigmentation, *Planta Med*, **68**, 79-81.
- Smolarek, A.K., *et al.* (2013) Dietary tocopherols inhibit cell proliferation, regulate expression of ER α , PPAR γ , and Nrf2, and decrease serum inflammatory markers during the development of mammary hyperplasia, *Molecular carcinogenesis*, **52**, 514-525.
- Son, J.K., *et al.* (2003) Prenylated flavonoids from the roots of *Sophora flavescens* with tyrosinase inhibitory activity, *Planta Med*, **69**, 559-561.
- Son, K.H., *et al.* (2001) Papyriflavonol A, a new prenylated flavonol from *Broussonetia papyrifera*, *Fitoterapia*, **72**, 456-458.
- Soo, C.C.-Y., *et al.* (2004) Dose-dependent effects of dietary α - and γ -tocopherols on genetic instability in mouse mutator tumors, *Journal of the National Cancer Institute*, **96**, 796-800.
- Sritularak, B., *et al.* (2010) New 2-arylbenzofurans from the root bark of *Artocarpus lakoocha*, *Molecules*, **15**, 6548-6558.

- Stone, W.L., *et al.* (2004) Tocopherols and the treatment of colon cancer, *Annals of the New York Academy of Sciences*, **1031**, 223-233.
- Sussmann, R.A., *et al.* (2011) Intraerythrocytic stages of *Plasmodium falciparum* biosynthesize vitamin E, *FEBS Lett*, **585**, 3985-3991.
- Swain, S.S., Rout, K.K. and Chand, P.K. (2012a) Production of triterpenoid anti-cancer compound taraxerol in *Agrobacterium*-transformed root cultures of butterfly pea (*Clitoria ternatea* L.), *Appl Biochem Biotechnol*, **168**, 487-503.
- Swain, S.S., Rout, K.K. and Chand, P.K. (2012b) Production of triterpenoid anti-cancer compound taraxerol in *Agrobacterium*-transformed root cultures of butterfly pea (*Clitoria ternatea* L.), *Applied biochemistry and biotechnology*, **168**, 487-503.
- Tamura, K., *et al.* (2013) MEGA6: molecular evolutionary genetics analysis version 6.0, *Molecular biology and evolution*, **30**, 2725-2729.
- Tashiro, M., *et al.* (2001) Effects of prenylflavanones from *Sophora* species on growth and activation of mouse macrophage-like cell line, *Anticancer research*, **22**, 53-58.
- Tunsaringkarn, C.P.S.I.T., *et al.* (2007) Pharmacognostic study of *Artocarpus lakoocha* heartwood, *J Health Res*, **21**, 257-262.
- Valentin, H.E., *et al.* (2006) The *Arabidopsis* vitamin E pathway gene5-1 mutant reveals a critical role for phytol kinase in seed tocopherol biosynthesis, *Plant Cell*, **18**, 212-224.
- Vranová, E., Coman, D. and Grisse, W. (2013) Network Analysis of the MVA and MEP Pathways for Isoprenoid Synthesis, *Annu Rev Plant Biol*, **64**, 665-700.
- Wang, R., *et al.* (2014) Molecular characterization and phylogenetic analysis of two novel regio-specific flavonoid prenyltransferases from *Morus alba* and *Cudrania tricuspidata*, *J Biol Chem*, **289**, 35815-35825.
- Wang, Y., *et al.* (2006) Bioassay-guided isolation of antiatherosclerotic phytochemicals from *Artocarpus altilis*, *Phytother Res*, **20**, 1052-1055.
- Wei, X., Kuhn, D.N. and Narasimhan, G. (2003) Degenerate primer design via clustering, *Proc IEEE Comput Soc Bioinform Conf*, **2**, 75-83.

- Whitaker, B.D. (1986) Fatty-acid composition of polar lipids in fruit and leaf chloroplasts of "16:3"- and "18:3"-plant species, *Planta*, **169**, 313-319.
- Wilmoth, G.C. (2002) Tocopherol (vitamin E) content in invasive browse species on underutilized Appalachian farmland. Virginia Tech.
- Wydro, M., Kozubek, E. and Lehmann, P. (2006) Optimization of transient Agrobacterium-mediated gene expression system in leaves of *Nicotiana benthamiana*, *Acta Biochim Pol*, **53**, 289-298.
- Xu, Z., *et al.* (2014) Cytotoxic prenylated xanthenes from the pericarps of *Garcinia mangostana*, *Molecules*, **19**, 1820-1827.
- Yazaki, K., *et al.* (2002) Geranyl diphosphate:4-hydroxybenzoate geranyltransferase from *Lithospermum erythrorhizon*. Cloning and characterization of a ket enzyme in shikonin biosynthesis, *J Biol Chem*, **277**, 6240-6246.
- Zheng, Z.-P., *et al.* (2008) Tyrosinase inhibitors from paper mulberry (*Broussonetia papyrifera*), *Food Chem*, **106**, 529-535.
- Zingg, J.-M., *et al.* (2013) In vivo regulation of gene transcription by alpha-and gamma-tocopherol in murine T lymphocytes, *Archives of Biochemistry and Biophysics*, **538**, 111-119.
- Zottini, M., *et al.* (2008) Agroinfiltration of grapevine leaves for fast transient assays of gene expression and for long-term production of stable transformed cells, *Plant Cell Rep*, **27**, 845-853.

VITA

Miss Thaniya Wunnakup received Bachelor's degree of in General Science, Faculty of Liberal Arts and Science, Kasetsart University, Thailand in 2004. She graduated Master of Science in Biochemistry, Faculty of Science, Chulalongkorn University, Thailand in 2008. After that she entered in Ph.D. program in Biomedical Chemistry during 2009 – 2015.

SCIENTIFIC PUBLICATION

Chanama, M., Wunnakup, T., De-Eknamkul, W. and Chanama, S. 2009. Improvement of thin-layer chromatography for enzyme assay of geranylgeraniol 18-hydroxylase from *Croton stellatopilosus* Ohba, *J. Planar Chromatogr*, 22(1) 49 – 53.

POSTER PRESENTATION

Chanama, M., Wunnakup, T., De-Eknamkul, W. and Chanama, S. Improvement of thin-layer chromatography for enzyme assay of geranylgeraniol 18-hydroxylase from *Croton stellatopilosus* Ohba. International Symposium of Thin Layer Chromatography, Helsinki, Finland, 11 – 13 June 2008.

Chanama, M., Wunnakup, T., De-Eknamkul, W. and Chanama, S. Kinetic characterization of geranylgeraniol-18-hydroxylase from *Croton stellatopilosus* Ohba. The 8th Joint Innovative Research in Natural Products for Sustainable Development NRCT-JSPS, Faculties of Pharmaceutical Sciences, Chulalongkorn University, 3 - 4 February, 2009.

Wunnakup, T., Promden, W. and De-Eknamkul, W. Cloning and Characterization of Flavonoid Prenyltransferase Genes from Thai Medicinal Plants. Phytochemical Society of North America, Hawai'i, 10 – 15 December, 2011.